MAC Design and Analysis for MU-MIMO and Full-duplex Enabled Wireless Networks

Ruizhi Liao

UPF DOCTORAL THESIS / JULY 2014

DIRECTOR OF THE THESIS

Boris Bellalta and Miquel Oliver

Department of Information and Communication Technologies

To my family.

Acknowledgements

I am sincerely grateful to many people who helped me.

First, I would like to thank my supervisors-Boris Bellalta for his broad expertise, complete dedication and continuous encouragement; Miquel Oliver for his continuous support and inspiring guidance. Their professional guidance has made this work not only possible but also valuable. Thank them for creating a great research environment that allows me to pursue interesting topics in wireless networks.

Secondly, I want to thank my colleagues and collaborators, Cristina Cano, Anna Sfairopoulou, Trang Cao Minh, Jaume Barcelo, Alex Bikfalvi, Victor Valls and Luis Sanabria-Russo. Thank them for their help and insightful comments to either my research or teaching activities. Also, I want to thank my dear friends in the department: Sougata Pal, Jelena Skulic, Lydia Garcia, Vanessa Jimenez, Jana Safrankova, Javier Gonzalez, Albert Domingo, Manuel Palacin, Gabriel Martins Dias, Simon Oechsner, Albert Bel, Toni Adame and Pol Cirujeda. With them, life in Barcelona becomes fun and vivid.

In addition, I am grateful to the Spanish Government, the Catalan Government and Universitat Pompeu Fabra for the financial supports under the CISNETS project, the SGR project, and the DTIC PhD programme.

Lastly, I want to thank my family for their warm and unconditional supports. The spirits that I inherited from them have inspired me through-

out my study and life.

Abstract

IEEE 802.11 based wireless networks, especially the infrastructure based Wireless Local Area Networks (WLANs) or Wi-Fi networks, are hugely successful, and have become an indispensable part of our life at homes and working places. However, the rapid growth of wireless devices, and a shift of users' habit from web browsing to a wide variety of bandwidth-hungry applications (e.g., high-definition video, social network and cloud uploading), have made today's WLANs not only crowded, but also low at throughput.

The latest IEEE WLAN amendment-802.11ac responds to these challenges by introducing a set of novel physical (PHY) and medium access control (MAC) features, including downlink multi-user Multiple-Input and Multiple-Output (MU-MIMO), higher modulation and coding scheme, channel bonding, frame aggregation, etc. Among them, downlink MU-MIMO is one of the most important features due to its potential to significantly improve the performance. It allows the access point (AP) to transmit frames to multiple stations (STAs) in parallel, which can substantially increase the network throughput, as well as to mitigate high collision rates.

On the other side, recent research advances on the full-duplex (FD) transmission open another line to improve the performance of wireless network in dense areas. FD transmissions in wireless networks break the long-hold assumption that nodes can not transmit and receive simultaneously using the same frequency. This exciting progress not only promises a twofold capacity increase by allowing concurrent transmission and reception, but could also bring revolutionary changes to the MAC design

by shaking the foundation of IEEE 802.11 medium access mechanism-Carrier Sense Multiple Access with Collision Avoidance (CSMA/CA). As CSMA/CA can become obsolete, and be replaced by the on-the-fly collision detection thanks to the FD's capability of simultaneous transmission and reception.

However, these two lines of PHY advances (i.e., MU-MIMO and FD) do not directly translate to the useful performance gains at the MAC layer (e.g., the throughput increase). In order to take full benefits of MU-MIMO and FD, adaptations of the current IEEE 802.11 MAC protocols are needed. In this thesis, we first investigate the prominent MAC proposals in the literature, and then propose the required MAC adaptations to support MU-MIMO downlink and uplink transmissions separately. After that, we combine the downlink and uplink adaptations into a unified MU-MIMO MAC protocol to look into what influence would bring to the uplink or the downlink when both up/down-link traffic are present. We extensively evaluate the performance of the proposed protocol in saturated and non-saturated conditions to emulate the highly-densed scenario and the lightly-increased traffic scenario. Next, we model and evaluate the new IEEE 802.11ac standard MAC operations, and compare them with our proposals in a wireless mesh backhaul network. Afterwards, we utilize full-duplex technique and propose a full-duplex MAC (FD+) scheme to improve the performance of a wireless system. We analytically model FD transmissions and investigate what gains can be achieved at the MAC layer. Finally, we conclude our work and look into the future directions. Results from simulations and analytic models show that the significant performance gain can be achieved by extending traditional IEEE 802.11 MAC schemes to support MU-MIMO and FD transmissions.

Resum

Les xarxes sense fils basades en l'estàndard IEEE 802.11, sobretot aquelles que funcionen en mode infraestructura, conegudes com a xarxes WLAN o Wi-Fi, han tingut molt d'èxit i s'han convertit en una part indispensable de la nostra vida tant a les llars com als llocs de treball. No obstant això, el ràpid creixement dels dispositius sense fils, i un canvi d'hàbits dels usuaris des de la navegació web cap a una àmplia varietat d'aplicacions que requereixen un gran ample de banda (per exemple, vídeo d'alta definició, les xarxes socials o la càrrega de continguts al núvol), han fet que les WLAN d'avui en dia tinguin un baix rendiment. La pròxima generació de WLANs, basades en el nou estàndard IEEE 802.11ac, respon a aquests reptes mitjançant la introducció d'una sèrie de novetats a nivell físic (PHY) i a nivell d'accés al medi (MAC), incloent l'enllaç de baixada Multi-user Multiple-Input Multiple-Output (MU-MIMO), un nou esquema de modulació i codificació, canals amb major amplada de banda i l'agregació de trames. Entre ells, l'enllaç de baixada MU-MIMO és una de les novetats més importants per a millorar significativament el rendiment de les xarxes WLAN, ja que permet que el punt d'accés (AP) pugui transmetre trames a múltiples estacions (STA) en paral·lel, cosa que pot augmentar substancialment el rendiment de la xarxa, així com mitigar les altes taxes de col·lisió.

D'altra banda, els avenços recents en investigació sobre la transmissió full-duplex (FD) obren una altra línia per millorar el rendiment de les xarxes WLAN amb molts usuaris. Transmissions full-duplex en xarxes sense fils trenquen la suposició que diu que els nodes no poden transmetre i rebre simultàniament usant la mateixa freqüència. Aquest emo-

cionant avenç no només promet un augment de capacitat en permetre la transmissió i recepció simultània, sinó que també podria portar canvis revolucionaris en el disseny MAC sacsejant els fonaments del mecanisme Carrier Sense Multiple Access amb prevenció de col·lisions (CSMA/CA). Així, el CSMA/CA pot arribar a ser obsolet i ser reemplaçat per un sistema de detecció de col·lisions gràcies a la capacitat de transmissió i recepció simultània dels nodes que suportin full-duplex.

No obstant això, aquestes dues línies d'avenços PHY (és a dir, MU-MIMO i FD) no es tradueixen directament en guanys de rendiment útils a la capa MAC (per exemple, l'augment de rendiment). Per tal de tenir beneficis per fer servir MU-MIMO i FD, es necessita adaptar els actuals protocols MAC. En aquesta tesi, primer examinem les propostes de protocols MAC existents a la literatura i, a continuació, mostrem els nostres esforços en la introducció de les adaptacions necessàries per donar suport MAC MU-MIMO a l'enllaç descendent i a l'enllaç ascendent per separat. Després d'això, combinem les adaptacions per a l'enllaç descendent i ascendent en un protocol MU-MIMO MAC unificat i avaluem el seu rendiment tant en condicions saturades com no saturades. A continuació, anem a modelar i avaluar el funcionament del nou IEEE 802.11ac MAC, i els comparem amb les nostres propostes en una xarxa mallada sense fils (xarxa back-haul). A continuació, es proposa un MAC que suporta full-duplex (FD+) per millorar les prestacions dels sistemes sense fils, on analíticament modelem transmissions FD i investiguem quins guanys es poden aconseguir a la capa MAC. Finalment, presentem les conclusions del nostre treball i plantegem les direccions futures en aquest camp de recerca.

Contents

List of Figures

List of Acronyms

AC (Access Category)
ACK (Acknowledgement)
AIFS (Arbitration Inter Frame Space)
A-MPDU (Aggregated MAC Protocol Data Unit)
A-MSDU (Aggregated MAC Service Data Unit)
AP (Access Point)
AWGN (Additive White Gaussian Noise)
BO (Backoff)
CDMA (Code Division Multiple Access)
COST (Component Oriented Simulation Toolkit)
CSI (Channel State Information)
CSMA/CA (Carrier Sense Multiple Access/Collision Avoidance)
CTS (Clear to Send)
CW (Contention Window)
DCF (Distributed Coordination Function)
DIFS (DCF Inter Frame Space)
DPC (Dirty Paper Coding)
DSSS (Direct Sequence Spread Spectrum)
ECFB (Explicit Compressed Feedback)
EDCA (Enhanced Distribution Channel Access)
EIFS (Extended Inter frame space)
FD (Full duplex)
FIFO (First-in First-out)
GI (Guard Interval)
Group-ID (Group Identifier)

HCCA (Hybrid Coordination Function Controlled Access)
HD (High Definition)
HEW (High Efficiency WLAN)
IP (Internet Protocol)
LTF (Long Training Fields)
MAC (Medium Access Control)
MCS (Modulation and Coding Scheme)
MIMO (Multiple-Input Multiple-Output)
MMSE (Minimum Mean Square Error)
MN (Mobile Nodes)
MPR (Multi-Packet Reception)
MPT (Multi-Packet Transmission)
MUD (Multi-user Detection)
MUIC (Multi-user Interference Cancellation)
MU-MIMO (Multi-user MIMO)
NAV (Network Allocation Vector)
NDP (Null Data Packet)
NDPA (Null Data Packet Announcement)
OFDM (Orthogonal Frequency Division Multiplexing)
OSI (Open System Interconnection)
P2P (Peer-to-Peer)
PCF (Point Coordination Function)
PHY (Physical)
PLCP (PHY Layer Convergence Procedure)
QAM (Quadrature Amplitude Modulation)
QoS (Quality of Service)
RTS (Request to Send)
SDMA (Space Division Multiple Access)
SDR (Software Defined Radio)
SIC (Successive Interference Cancellation)
SIFS (Short Inter Frame Space)
SINR (Signal-to-Interference-plus-Noise Ratio)
SNR (Signal-to-Noise Ratio)
STA (Station)

STF (Short Training Field)
SU-MIMO (Single-user MIMO)
TXOP (Transmit Opportunity)
USRP (Universal Software Radio Peripheral)
VHT (Very High Throughput)
WARP (Wireless Open-Access Research Platform)
WLANs (Wireless Local Networks)
ZF (Zero Forcing)

Chapter 1

INTRODUCTION

1.1 Background

IEEE 802.11 is a set of Physical Layer (PHY) and Medium Access Control (MAC) specifications for the prevalent Wireless Local Area Networks (WLANs). Current IEEE 802.11 WLANs contribute to approximate 40% of overall Internet Protocol (IP) traffic [1]. However, as smart devices boom and bandwidth-hungry applications (e.g., HD videos, telepresence and cloud storage services) get popular, today's WLANs become not only crowded, but also low at throughput. The employment of recent advances at the PHY layer, such as Multiple-Input and Multiple-Output (MIMO) and Full-duplex (FD), has huge potentials to substantially improve the performance of wireless networks in dense areas.

Multi-user MIMO (MU-MIMO), introduced by IEEE 802.11ac [2], is one of the most crucial techniques that lead WLANs towards the gigabit era. Compared to Single-user MIMO (SU-MIMO), which focuses on transmitting to a single destination, MU-MIMO holds the following three advantages: (1) The increased capacity. By employing SU-MIMO, the theoretical capacity gain can be manifested by a multiplicative factor of $min\{N_{\mathrm{t}}, N_{\mathrm{r}}\}$, where N_{t} and N_{r} are the number of transmitting and receiving antennas [3] [4]; while in the case of MU-MIMO, the multiplicative factor can be further extended to $min\{aN_{\mathrm{t}}, bN_{\mathrm{r}}\}$, where a and

b are the number of simultaneous transmitters and receivers; (2) The increased diversity gain. The spatially distributed stations (STAs) make the MU-MIMO system more immune to the channel rank loss and the antenna correlation, which may severely affect the SU-MIMO system performance [5]; (3) The reduced terminal cost. The MU-MIMO system supports multiple spatially separated STAs (even only equipped with a single antenna) to simultaneously communicate with the Access Point (AP), which makes the development of compact and low-cost user terminals possible.

On the other side, FD transmissions have attracted much attention due to its promise of doubling the channel capacity. Traditional wireless systems are not able to transmit and receive frames using the same frequency simultaneously. The reason of that is the strong signal presented at the receiving antenna from the same node's transmitting end, i.e., the self interference. Recent developments in the antenna design and the analog/digital interference cancellation [6–9] have lifted this limitation, and pave the way for FD transmissions in wireless networks.

1.2 Motivation

In the context of the rapid increase of wireless devices, and the evolution of users' habit from mainly web browsing and file transfers to a wide variety of applications (including considerable amount of content-rich files generated by users), most environments of future wireless networks will be characterized by high density of STAs and decreased per-STA throughput [10].

The thesis is motivated to utilize the above-mentioned two PHY advances (i.e., MU-MIMO and FD) to improve the performance of crowded IEEE 802.11 networks in the wake of surged wireless devices and the changed IP traffic pattern. Although MU-MIMO and FD have potentials to significantly increase the channel capacity, there are several fundamental IEEE 802.11 mechanisms and features that prevent the translation of PHY data rate to the useful MAC throughput. The reasons are as follows.

First, the traditional IEEE 802.11 MAC schemes only support single-user transmissions at a time, which underutilize the full promise of the MU-MIMO and FD transmissions. Secondly, the overheads at the MAC layer also lead to the throughput loss. They include the management frames (e.g., association requests/responses), control frames (e.g., RTS, CTS and ACK), frame headers (e.g., PHY preambles, PHY/MAC headers) and the compulsory idle duration (e.g., random backoff, DIFS/SIFS). Thirdly, other non-overhead factors, such as frame collisions and the airtime unfairness caused by low-rate STAs that monopolize the channel, further contribute to the MAC throughput decrease. In the current IEEE 802.11 communication architecture, these overhead and non-overhead factors are either predetermined to facilitate the correct transmission and reception of data or difficult to be eliminated.

Therefore, traditional MAC protocols, used among multiple STAs to share a common wireless channel, have to be redesigned or adapted to improve efficiency, and to support multi-STA simultaneous transmissions/receptions.

There are two main MAC categories: (1) the fixed-assignment one, where the channel frequencies, the access time or the mutually orthogonal codes are predefined for each STA, e.g., FDMA, TDMA and CDMA, namely, Frequency Division, Time Division and Code Division Multiple Access; and (2) the random access one, where each STA independently determines when to compete for the channel, e.g., CSMA/CA, namely, Carrier Sense Multiple Access with Collision Avoidance. Due to nomadic STAs (i.e., STAs join or leave WLANs at any time), asymmetrical up/down-link traffic, and the implementation simplicity, the random access based CSMA/CA has dominated the MAC mechanism of WLANs. The thesis will focus on the random access MAC schemes.

1.3 Objectives and Contributions

The objectives of this thesis are to study, design and evaluate random access based MAC mechanisms for MU-MIMO and FD enabled wireless

networks. To this end, the objectives are separated by six sub-objectives.

O1. *To know what is the state of art of MAC schemes for MU-MIMO enabled wireless networks.*

We thoroughly investigate MAC schemes in the literature and overview IEEE 802.11 standards and amendments, which not only provides us with an aerial view of IEEE 802.11 evolution, but also enables us to summarize key components towards building efficient MAC proposals. A survey paper [11] based on the work is submitted for publication.

O2. *To explore what is the performance gain of using multiple antennas in WLANs, and how the MAC scheme should be adapted to support simultaneous transmissions to multiple STAs in the downlink.*

We propose a MAC protocol for downlink MU-MIMO transmissions, where frames are scheduled to each STA according to the First-in First-out (FIFO) policy. The Channel State Information (CSI) needed for multi-STA transmissions is obtained through estimating the training sequence included in the CTS preamble. We evaluate the proposed MAC with different queue length, number of antennas and nodes by simulation. The results show that a significant throughput gain is obtained by exploiting the spatial domain of the channel. The results also show that the achieved gain is neither linear with the number of antennas nor the frame length due to the extra overheads of the protocol. A conference paper [12] based on the work is produced.

O3. *To explore how the MAC scheme should be modified to accommodate multi-STAs' parallel transmissions in the uplink.*

We extend the IEEE standard one-round channel contention to two rounds to coordinate multiple STAs for the concurrent uplink access. We place a special focus on 2-nd round Contention Window (CW_{2nd}), a parameter making the length of the second contention round elastic. By evaluating the proposal in simulations, a set of optimal CW_{2nd} values that can obtain the highest system performance are identified. A conference paper [13] based on the findings is produced.

O4. *To explore how to design a unified downlink and uplink MU-MIMO MAC protocols, and evaluate what effect could be on either downlink or uplink when both down/up-link traffic are in presence.*

We propose a unified MU-MIMO MAC protocol (Uni-MUMAC) to integrate the two separated downlink and uplink MAC proposals. Compared to [12] and [13], where only one-way traffic is considered (i.e., the downlink or the uplink), the presence of simultaneous downlink and uplink transmissions have been taken into account. By analyzing the simulation results, we observe that the 2-nd round Contention Window $CW_{2\text{nd}}$, which is tuned to optimize the uplink transmission, is however not bringing the same benefit to the downlink one. An adaptive frame aggregation scheme and queue scheme is applied at the AP to offset this disadvantage. With the optimized $CW_{2\text{nd}}$ and other properly configured parameters (e.g., the number of aggregated frames and the queue length of the AP), the results show that a WLAN implementing Uni-MUMAC is able to avoid the AP bottle-neck problem and performs very well in both the traditional downlink-dominant and emerging down/up-link balanced traffic scenarios. A journal paper [14] based on the work is submitted for publication.

O5. *To evaluate how the novel features of the latest IEEE amendment-802.11ac will affect the system performance, and what is the best transmitting strategy when the node is equipped with multiple antennas.*

We first briefly survey the main features of IEEE 802.11ac; and then, we evaluate these new features in a fully-connected wireless mesh network using an analytic model and simulations. More specifically, the performance of the MAC scheme defined by the IEEE 802.11ac, which employs the Explicit Compressed Feedback (ECFB) mechanism for the channel sounding, is evaluated. In addition, we propose an extended RTS/CTS scheme that integrates the ECFB operation to compare with the IEEE 802.11ac defined one in saturated conditions. Three spatial-stream allocation algorithms are proposed to find out the best transmitting mode. By analyzing the results, we conclude that MU-RTS/CTS is more efficient than MU-Basic as the number of nodes and the size of A-MPDU increase. Regarding the spatial-stream allocation algorithms, the Beam-greedy algorithm outperforms the Stream-greedy one, but the ideal Stream-independent algorithm is the one that provides the best performance. A journal paper [15] is produced based on the work.

O6. *To explore what are the benefits of FD transmissions, and what MAC modifications should be done to support FD transmissions.*

We analytically model FD transmissions and investigate what gains can be achieved at the access layer by considering MAC operations and overheads. We propose an enhanced full-duplex MAC (FD+) scheme to further improve the performance of FD transmissions. The IEEE 802.11 Distributed Coordination Function (DCF) scheme is utilized as a benchmark to compare with FD and FD+ schemes. Both analytic and simulation results show that FD+ is able to provide an average factor of 2.3 throughput increase against DCF and FD. A journal paper [16] based on the work is submitted for publication.

1.4 Methodology

The research methodology utilized to achieve the objectives consists of two steps: 1) study and evaluate IEEE 802.11 standard MAC schemes or prominent MAC proposals in the literature, and 2) design, implement and analyze our proposals using simulations and analytic models. The first step helps me to understand the existing schemes' characteristics and limitations, while the second one enables me to explore and validate improvements of new protocols.

1.5 Thesis Organization

The remainder of this thesis is organized as follows. Chapter 2 identifies key requirements for designing MU-MIMO MAC protocols, and surveys the prominent MAC schemes in the literature. Chapter 3 presents MAC enhancements for downlink transmissions, and Chapter 4 introduces MAC adaptations for uplink transmissions in MU-MIMO based WLANs. Chapter 5 proposes a unified MU-MIMO MAC protocol that supports both uplink and downlink transmissions. Chapter 6 evaluates IEEE 802.11ac MAC protocol in wireless mesh networks, and proposes an extended MAC protocol to compare with the standard one. Chapter

7 models and extends FD MAC operations in generalized wireless networks. Chapter 8 summarizes the thesis and looks into the future directions.

Chapter 2

MAC DESIGNING REQUIREMENTS AND STATE OF THE ART

2.1 Evolution of IEEE 802.11 Standards and Amendments

2.1.1 Standards

Loosely speaking, both standards and amendments can be interchangeably used to refer to different variants of IEEE releases. However, a more strict nomenclature designates standards as documents with mandatory requirements (denoted as IEEE 802.11 followed by the published year, e.g., IEEE 802.11-2012), and amendments as documents that add to, remove from, or alter material in a portion of existing standards [17] (denoted as IEEE 802.11 followed by a non-capitalized letter or letters, e.g., IEEE 802.11n or 802.11ac). In this thesis, we will follow the original IEEE nomenclature.

Since 1997, IEEE has released four standards: 802.11-1997, 802.11-1999, 802.11-2007 and 802.11-2012. IEEE 802.11-2012 [18] is the latest

and the only version that is currently in publication. Standards are continuously updated by amendments, e.g., 802.11-2012 is created by integrating ten amendments such as 802.11n and 802.11p with the base standard 802.11-2007, which was replaced since the release of 802.11-2012. In other words, each standard will be superseded by its successor in its entirety.

2.1.2 Amendments

In 1999, two amendments were first introduced: (1) IEEE 802.11a, which operates in the 5 GHz band using the Orthogonal Frequency Division Multiplexing (OFDM) modulation with a maximum data rate of 54 Mbps; (2) IEEE 802.11b, which operates in the 2.4 GHz band using the Direct Sequence Spread Spectrum (DSSS) modulation with a maximum data rate of 11 Mbps. Compared to 802.11-1997, 802.11b substantially increases the data rate (from 2 Mbps to 11 Mbps) using the same modulation technique and the frequency band, which made 802.11b the then-definitive WLAN technology. In 2003, IEEE 802.11g, a new amendment working in the 2.4 GHz band was ratified, which extends 802.11b to reach a maximum data rate of 54 Mbps. IEEE 802.11n [19], ratified in 2009, operates in either 2.4 GHz or 5 GHz band, boosting the data rate to 150 Mbps (600 Mbps by 4 streams) by utilizing MIMO.

802.11ac [2] is the latest IEEE amendment. It is operating exclusively in the 5 GHz band. Driven by the need for higher speeds, 802.11ac aims to provide an aggregated multi-station throughput of at least 1 gigabit per second, namely, Very High Throughput (VHT) WLANs. Compared to 802.11n, this significant improvement is achieved by introducing novel PHY and MAC features, such as wider bandwidths (80 and 160 MHz), a denser modulation scheme (256-QAM: Quadrature Amplitude Modulation), a compulsory frame format (A-MPDU: Aggregated MAC Protocol Data Unit), and most importantly, downlink MU-MIMO transmissions (supporting simultaneous transmissions of up to 4 STAs with the maximum number of 8 streams).

Although each amendment is revoked as it is merged into the latest

Table 2.1: **Features of Related IEEE 802.11 Standards/Amendments**

Version	Description	Incorporated Baselines	Frequency	Max. Data Rate	Modulation
802.11-1997	WLAN MAC and PHY Specifications	–	20 (MHz) @ 2.4 (GHz)	2 (Mbps)	DSSS, FHSS
802.11-1999	Part II WLAN MAC and PHY Specifications	–	20 @ 2.4	2	DSSS, FHSS
a	Higher Speed PHY Extension	802.11-1999	20 @ 5	54	OFDM
b	Higher Speed PHY Extension	802.11-1999, a, c	20 @ 2.4	11	DSSS
g	Further Higher Data Rate Extension	802.11-1999, a-d	20 @ 2.4	54	OFDM, DSSS
802.11-2007	Standard Maintenance Revision	802.11-1999, a-e, g-j	–	–	–
n	High Throughput	802.11-2007, k, r, y, w	20, 40 @ 2.4, 5	150 x 4	OFDM
802.11-2012	Accumulated Maintenance Changes	802.11-2007, k, n, p-s, u-w, y, z	–	–	–
ac	Very High Throughput	802.11-2012, aa, ad, ae	20, 40, 80, 160 @ 5	866.7 x 8	OFDM

standard, the sign of IEEE 802.11a/b/g/n/ac is often employed by the industry to denote the capability and compatibility of products.

The key features of the above mentioned IEEE 802.11 Standards and Amendments are given in Table 2.1, where FHSS stands for Frequency Hopping Spread Spectrum.

2.1.3 Next Amendment-802.11ax

In March 2014, IEEE approved a new task group-802.11ax [20], which will operate in frequency bands between 1 and 6 GHz. The focus of the amendment has shifted from the peak aggregated throughput to the throughput of each STA. It aims at at least four-time per STA throughput increase comparing to the existing standards and amendments operating in the same band (e.g., 802.11n in 2.4 GHz and 802.11ac in 5 GHz) in both indoor and outdoor dense areas. The ongoing amendment is in its early stage, so some technical parameters are still in discussion. For more details about 802.11ax usage models and functional requirements, please refer to [10] and [21].

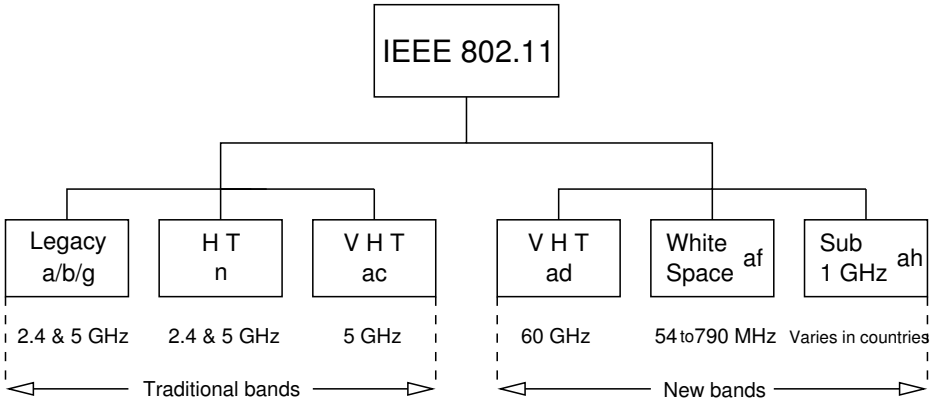

Figure 2.1: IEEE 802.11 frequency bands

2.1.4 New Frequency Bands for IEEE 802.11

Besides the traditional frequency bands (2.4 and 5 GHz), IEEE 802.11 has extended to support other bands (Figure 2.1).

IEEE 802.11ad [22], another VHT WLAN amendment, will operate in the 60 GHz band and focus on multi-gigabits per second data transmissions in a short range point-to-point links (around 10 meters). A typical application scenario of 802.11ad is the wireless transmission of lightly compressed or uncompressed high-definition videos for home entertainment systems. Due to 60 GHz band's characteristics of high propagation loss and high attenuation, directional transmissions and receptions are required.

IEEE 802.11af [23] allows devices to operate in the TV white space spectrum between 54 and 790 MHz. The bands are ideal for long-range transmissions, e.g., broadband services for the rural area. A geographic database is employed by 802.11af to let devices to check and register the available channels.

IEEE 802.11ah [24] will operate in the sub-GHz band. The main purposes of the amendment are to introduce power saving and STA grouping mechanisms. A typical use case is a smart metering network with many sensor nodes, where high collision probability and hidden nodes are ex-

pected. 802.11ah will partition nodes into groups to save power and to reduce the channel contention by assigning the channel to nodes of a given group at a given time [25].

Due to the specific purpose of each amendment and unique features of the employed frequency, the MU-MIMO MAC schemes designed for WLANs of the traditional bands can not be directly applied to these new amendments. For example, 802.11ah relies on the highly centralized medium access scheme, while 802.11ad has to utilize the beam sweeping technique to detect STAs rather than the omnidirectional carrier sensing adopted by IEEE 802.11 DCF. Therefore, this thesis preserves its focus on MAC proposals for the traditional bands, i.e., 2.4 and 5 GHz. However, the potential collaborations at the MAC level between protocols of traditional and new bands will be discussed in Chapter 8-Future Directions.

2.2 IEEE 802.11 MAC Schemes

2.2.1 Distributed Coordination Function

DCF is the fundamental medium access scheme of IEEE 802.11 based WLANs. It relies on CSMA/CA to detect and share the wireless channel among STAs. DCF can either operate in the basic access scheme (Figure 2.2(a)) or the optional RTS/CTS (Figure 2.2(b)) scheme. DCF mandates STAs to keep sensing the channel. If the channel has been idle for DIFS, each STA starts decreasing a backoff (BO) timer chosen from its Contention Window (CW) to compete for the channel. The STA with the lowest BO wins the channel contention and starts to transmit frames. Collisions occur if more than one STA happens to choose the same random BO. When a transmitted frame is successfully received, the receiver waits for a SIFS and then sends back an Acknowledgement (ACK). Note that as soon as the winning STA sends out a frame, other STAs will notice the channel has become busy, therefore immediately freeze their BO timers. These STAs will wait the channel to be idle for another DIFS, and resume decreasing the remaining BO timers. The STA who previously succeeded the channel contention will have a new BO timer at its next transmission

attempt.

Examples of a successful transmission for the basic access and the RTS/CTS schemes are shown in Figure 2.2, where B denotes the channel is initially busy. Please refer to the IEEE standard 802.11-2012 [18] for more details about DCF.

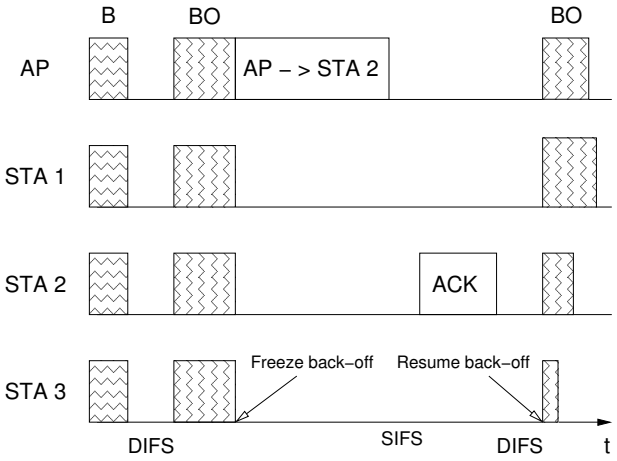

(a) A successful transmission of basic access

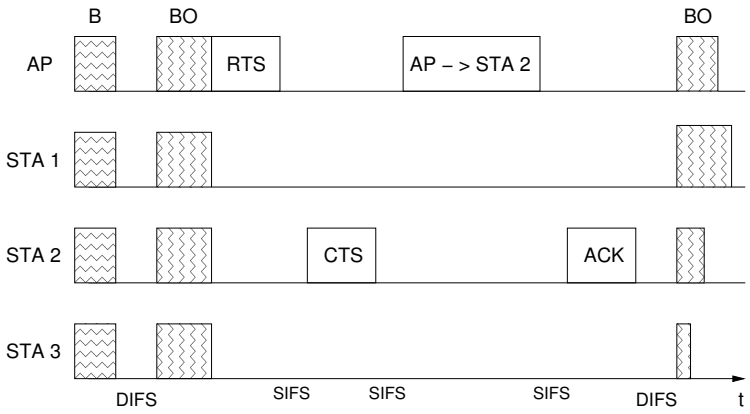

(b) A successful transmission of RTS/CTS

Figure 2.2: DCF transmission procedures

2.2.2 Enhanced Distribution Channel Access

IEEE 802.11e [26] proposes an extension to DCF-Enhanced Distribution Channel Access (EDCA), as a response to the demand of Quality of Service (QoS) for voice and video applications. The main differences between DCF and EDCA are twofold. First, the former does not differentiate traffic from different applications, while the latter classifies traffic into four Access Categories (ACs) with different priorities: Voice (AC_VO), Video (AC_VI), Best Effort (AC_BE) and Background (AC_BK). By doing so, EDCA is able to assign ACs with different parameters. For example, the maximum Transmit Opportunity (TXOP, a contention-free interval, during which a STA can transmit as many frames as possible) for AC_VO and AC_VI are 1.504 ms and 3.008 ms, respectively. Secondly, it is also different that the instant of time at which DCF and EDCA mandate STAs to decrease the BO timer. In DCF, STAs decrease the BO timer at the end of each slot, while in EDCA, the decrement occurs at the beginning of each slot. Please refer to [18] and [27] for detailed comparisons of DCF and EDCA, and [28] for QoS supports in WLANs.

Although IEEE 802.11 has specified other MAC mechanisms such as Point Coordination Function (PCF) and Hybrid Coordination Function Controlled Access (HCCA), this thesis only focuses on the distributed and random access based MAC schemes, because PCF and HCCA (i.e., the centralized schemes) are neither widely adopted by the industry nor the academia.

2.3 Key Components for MU-MIMO and FD MAC

MU-MIMO transmissions in WLANs have two communication paths, the uplink one (i.e., STAs simultaneously transmit frames to the AP, which is also referred as the MIMO-MAC channel) and the downlink one (i.e., the AP sends data to a group of STAs in parallel, which is also referred as the MIMO-broadcast channel). The MU-MIMO uplink and downlink

transmissions face different challenges, and hence, have different requirements in designing MAC protocols.

2.3.1 De/Pre-coding Schemes

In the uplink, the AP needs to separate the simultaneously transmitted signals from STAs, which is the Multi-user Detection (MUD) problem. In the downlink, the AP has to, firstly, select a group of STAs based on a certain criterion such as the queue occupancy, given that the selected STAs have to be spatially non-correlated, which is the scheduling problem, and, secondly, precode the outgoing frames to null the interference among concurrent spatial streams, which is the Multi-user Interference Cancellation (MUIC) problem. An illustration of MU-MIMO uplink and downlink transmissions is given in Figure 2.3.

The design of MUD/MUIC schemes is beyond the topic of the thesis. However, some of the most commonly used MUD/MUIC schemes are sampled.

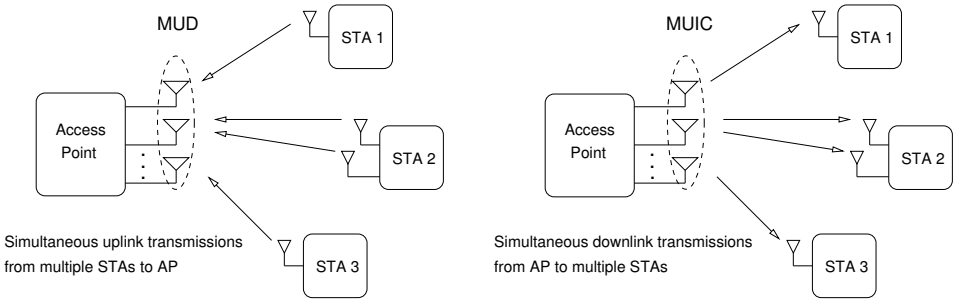

Figure 2.3: Up/Down-link transmissions

MUD Schemes for Simultaneous Uplink Receptions

Minimum Mean Square Error (MMSE) Received signals at each antenna of the AP are multiplied by a complex weight and then summed up. The weight is adjustable through minimizing the difference between the

summation of the output signal and a reference that is known by both the AP and STAs. An example of the weight adjustment is to utilize the steepest descending algorithm. The performance of the MMSE MUD scheme improves as the number of AP's antennas increases, and degrades as the network scales up [29].

Successive Interference Cancellation (SIC) The SIC MUD is an enhancement to MMSE. A detection algorithm is utilized by estimating of the received power at the AP. The signal with the highest power, which is the least interfered by others, is detected. This detected signal is then subtracted from mixed signals, and the next highest signal is singled out using the same process until the lowest STA signal is determined. The SIC MUD tends to be erroneous at the signal classification stage, which leads to the false deduction from composite STA signals and will affect the following calculations [30].

Maximum Likelihood (ML) The ML MUD conducts an exhaustive search to extract the transmitted signals. It provides the best detection performance, but comes with the highest complexity that increases exponentially with the number of STAs, which makes it infeasible in practical systems.

Sphere Decoding (SD) Some SD based MUD algorithms have been proposed to reduce the complexity of the pure ML MUD while to approach the performance of ML MUD. The idea is to decrease the radius of the search scope by focusing on the vicinity of the ML solution.

Other multi-user detection schemes for MU-MIMO uplink transmissions, such as Parallel Interference Cancellation (PIC), Least Squares (LS), Minimum Bit-Error Rate (MBER), QR Decomposition combined with the M-algorithm (QRD-M), Optimized Hierarchy Reduced Search Algorithm (OHRSA), Genetic Algorithm (GA) and Iterative GA (IGA), can be found in [29] [30]. The two categories of MUD algorithms are shown in Figure 2.4.

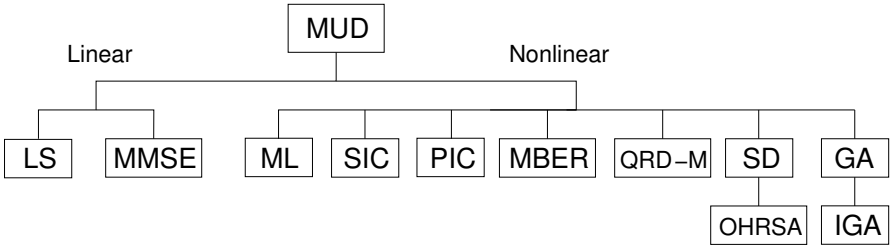

Figure 2.4: MUD schemes

MUIC Schemes for Simultaneous Downlink Transmissions

Although simultaneous downlink transmissions from the AP to multiple STAs can be seen as a combination of several single-user transmissions, STAs' random and independent geolocations make it very challenging to jointly null multi-user interference at the STA side. Therefore, most proposals in the literature precode outgoing signals at the AP to minimize interference among simultaneous streams.

Zero Forcing (ZF) In the ZF scheme, the original signal is multiplied by the pseudo-inverse of the channel matrix to null the MUI. However, the ZF scheme also increases the error rate, because the noise vector is amplified by the pseudo-inverse weight. The amplified noise vector indicates that ZF can only perform well in the high Signal-to-Noise Ratio (SNR) region. In addition, the ZF scheme requires that the number of total receiving antennas is not less than that of transmitting antennas [31].

In comparison, the MMSE scheme can minimize the overall error rate without amplifying the noise. [30] and [31] show that the MMSE scheme performs better than ZF in the low SNR region, and approaches the performance of ZF in the high SNR region.

Dirty Paper Coding (DPC) DPC is a non-linear precoding scheme firstly introduced by Costa [32], which can achieve the optimum performance at the cost of significant computing complexity. The idea is to add an offset (the negative value of the interference that is known at the AP)

to the transmitted signal, which is similar to the concept of writing letters on the dirty paper, where the dirt represents the interference.

Other precoding schemes, such as Block Diagonalization (BD), Successive optimization (SO), Vector Precoding (VP), Tomlinson-Harashima Precoding (THP) and Successive MMSE (SMMSE), can be found in [33] [30] [31]. The two categories of MUIC schemes are shown in Figure 2.5.

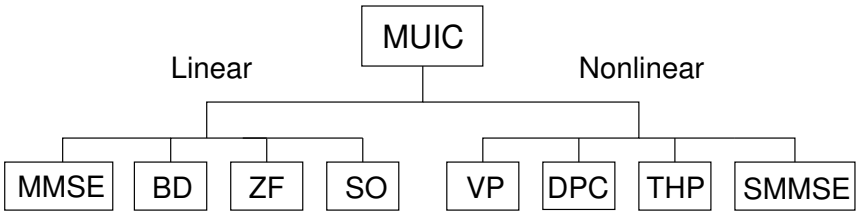

Figure 2.5: MUIC schemes

Remarks on MU-MIMO Up/Down-links

MUD and MUIC schemes allow MU-MIMO systems to separate simultaneously received/transmitted frames, and achieve the spatial multiplexing gain. However, it is important to point out that, in the above discussion, the possession of CSI is assumed at the AP. In the literature, CSI feedback schemes are usually integrated into MAC operations. An exception to obtain the downlink multiplexing gain without needing to feedback CSI is when STAs have more antennas than the AP, where STAs utilize the extra antennas to remove the co-stream interference.

2.3.2 Channel State Information

The CSI is required to fully obtain the multi-user transmission gain. Most proposals in the literature integrate the CSI acquisition into MAC operations. There are generally two types of CSI: the statistical CSI and the instantaneous one. The former employs the statistical characteristics

of the channel (e.g., fading distribution, average channel gain and spatial correlation) to decide the CSI, which performs well in scenarios where the channel has a large mean component (i.e., a large Rician factor) or strong correlation (either in space, time, or frequency) [34].

The instantaneous CSI (or the short-term CSI) means the current channel state is known, which enables the transmitter to adapt its outgoing signal. Because wireless channel varies over time, the instantaneous CSI has to be estimated repeatedly on a short-term basis. The acquisition of CSI can be done by estimating a training sequence known by both transmitters and receivers. In the uplink, the AP can easily extract the uplink CSI from the PHY preambles of received frames. While, for transmissions in the downlink, the acquisition of the CSI is not that straightforward. Depending on who computes the CSI, there are two CSI feedback schemes: (1) the implicit feedback (Figure 2.6(a)), where the AP computes the CSI by estimating training sequences sent from STAs, and (2) the explicit one (Figure 2.6(b)), where STAs calculate the CSI by estimating the training sequence sent from the AP, and then STAs feedback the calculated CSI to the AP.

By assuming the reciprocity of up/down-link channels, the implicit feedback scheme produces less overheads compared to the explicit one. However, in a practical WLAN system, the channel and interference seen by the STAs are generally not the same as those seen by the AP due to their different transmitting/receiving filters and PHY paths. Therefore, the antenna calibration [2] is usually needed to reduce the distortion if implicit feedback is adopted.

The explicit feedback scheme, i.e., STAs feedback the CSI, provides higher CSI resolution, but also higher overhead. MAC control frames are usually extended to support the CSI feedback in the literature, while an explicit compressed Feedback (ECFB) scheme is introduced by IEEE 802.11ac to schedule and compress the volume of CSI feedback.

No matter which CSI feedback scheme is applied, the implicit one or the explicit one, the frequency of CSI feedback would significantly affect the network performance. It is because the frequent CSI feedback increases overheads, while the infrequent one results in the outdated CSI

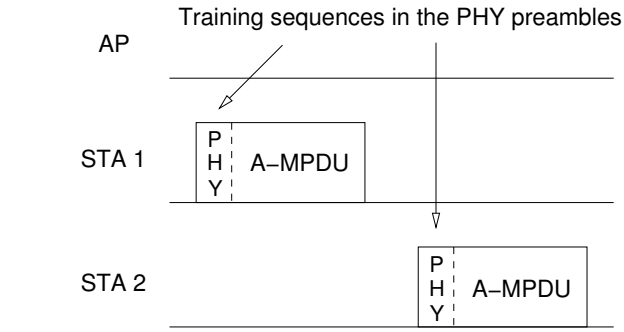

(a) Implicit CSI feedback scheme

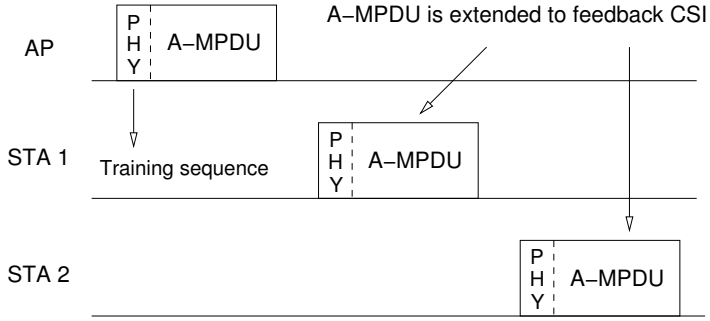

(b) Explicit CSI feedback scheme

Figure 2.6: CSI feedback procedures

that leads to interference among parallel streams. Please refer to [35] and [36] for more details about implicit and explicit CSI feedback schemes.

2.3.3 Scheduling Scheme

Another key point for designing MU-MIMO MAC protocols is the scheduling scheme. It is used to select a group of STAs or frames for transmissions, which can optimize certain aspects of the system performance according to the specific grouping criteria. The design of the scheduling scheme can be divided into two parts: the scheduling in the

uplink and downlink. The latter can be easily categorized by different scheduling algorithms (e.g., the STA based round-robin scheme or the frame based first in-first out scheme), while the characterization of the former is not straightforward.

Scheduling in the Uplink

In the uplink, it is very challenging to make a joint scheduling decision among spatially distributed STAs. Therefore, depending on whether the RTS/CTS exchanging process is employed (i.e., whether the AP has played a coordinating role in exchanging control frames before transmitting data), uplink transmissions can be categorized into the coordinated and the un-coordinated ones, as shown in Figure 2.7.

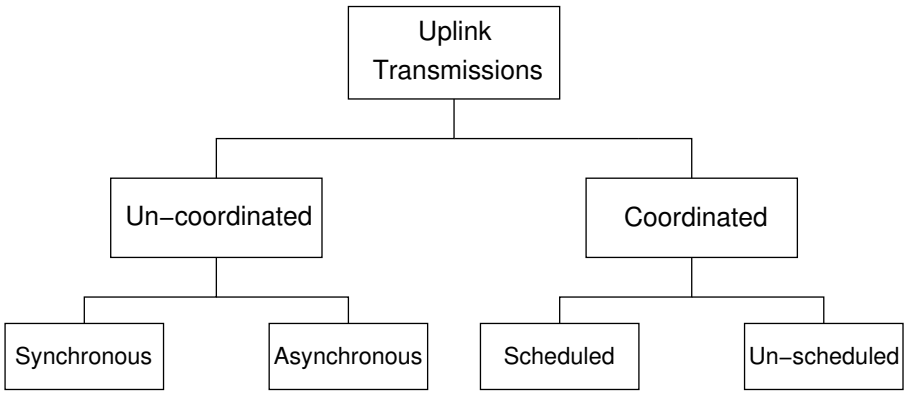

Figure 2.7: Categories of uplink scheduling

In the un-coordinated scenario, STAs utilize the MAC random mechanism to decide who will be allowed for transmissions, which have two cases: synchronous [37] and asynchronous [38] data transmissions, as shown in Figure 2.8. The former lets multiple STAs that coincidently choose the same BO to transmit data frames simultaneously, while the latter allows STAs to transmit frames along with other ongoing transmissions.

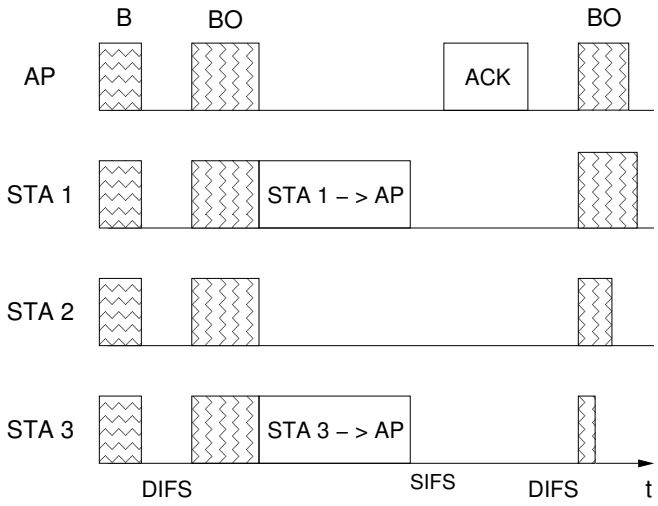

(a) Synchronous data transmissions

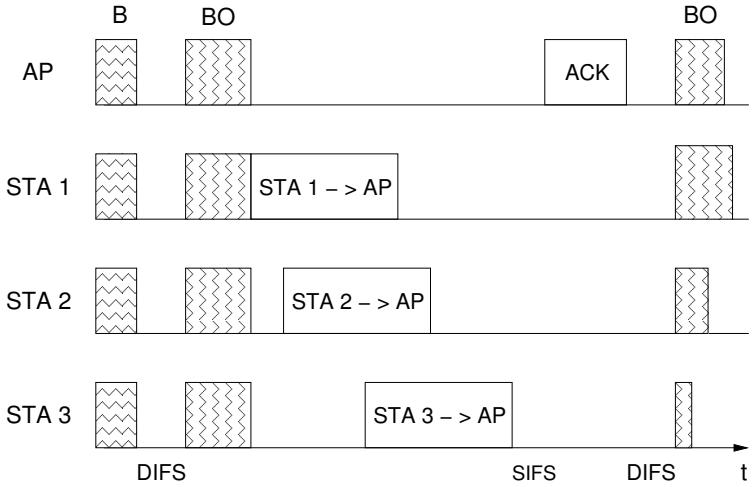

(b) Asynchronous data transmissions

Figure 2.8: Un-coordinated uplink channel access

In the coordinated scenario, STAs utilize the MAC random mechanism to contend for the channel, while let the AP to decide who will

be involved in the followed parallel transmissions. The coordinated uplink access scheme implies the involvement of the AP (as a coordinator) and the employment of RTS/CTS exchanges [39]. The AP extracts the information of interest from RTSs sent by the contending STAs, and then makes scheduling decisions for simultaneous frame transmissions (i.e., the scheduled transmissions), or the AP just responds to the received RTSs to notify who have won the channel contention (i.e., the un-scheduled transmissions). A simple example of the coordinated uplink access is shown in Figure 2.9, which can account for both scheduled and un-scheduled cases depending on whether the CTS is extended to support scheduling.

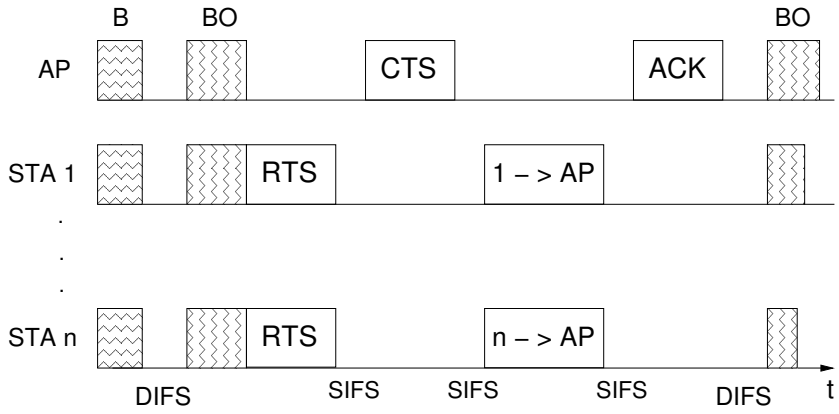

Figure 2.9: Coordinated uplink channel access

Although the un-coordinated uplink channel access requires fewer modifications compared to the coordinated one, it is likely that the spatial domain will be underutilized. The reason is that the concurrent uplink access of the un-coordinated scheme is based on the randomness of the IEEE 802.11 backoff mechanism. In comparison, the coordinated uplink channel access lets the AP to mediate the uplink transmissions by either just notifying a group of STAs that successfully won the channel contention or making a scheduling decision that aims to optimize the system performance. Obviously, the coordinated scheme will introduce over-

heads (e.g., extra fields of RTS/CTS) that are needed for the AP to best exploit the spatial domain.

Scheduling in the Downlink

Compared to the uplink, the AP plays a more direct role in the downlink scheduling, which can be classified into the packet based scheduling and the STA based one.

The packet based scheduling algorithms utilize the packet queueing status at the AP as the scheduling metric to assemble multiple packets for MU-MIMO downlink transmissions. The relevant packet based scheduling algorithms include FIFO, priority-based, delay-based (i.e., the waiting time of packets), queue/packet length-based, etc.

The STA based scheduling employs some specific criteria to identify a set of STAs for simultaneous downlink transmissions. These criteria include the channel state, spatial compatibility, fairness, etc. The channel aware scheduling relies on the channel conditions between the AP and STAs to make a decision, while the spatial compatible one tries to minimize the interference by examining STAs' spatial correlations. Neither of them has taken the fairness into account, which is considered by the round-robin scheduling.

A combination of the above mentioned scheduling schemes is usually considered. For example, [40] and [41] explore the PHY channel condition as well as the packet queueing status; while [42] adopts a three-dimension scheduling scheme that takes the packet length, the packet waiting time and the spatial compatibility into consideration. A typical way to solve the scheduling problem is to formulate it as an optimization problem, e.g., maximizing the throughput with constraints [43] [44].

The combination of several criteria hints that parameters from different layers should be jointly considered [45], which is the concept of cross-layer scheduling as shown in Figure 2.10, where $q(t)$ and $H(t)$ represent the queueing and the channel states at the time t.

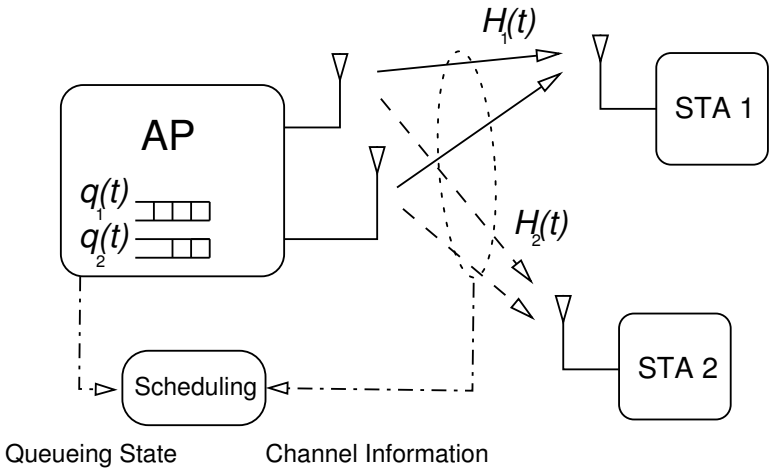

Figure 2.10: Cross-layer scheduling

Cross-layer Scheduling

The cross-layer scheduling has the promise to achieve the optimal system performance by sharing and configuring parameters from different layers, such as the channel information at the PHY layer, the queueing state at the MAC layer and the routing information at the network layer. Unfortunately, the cross-layer scheduling remains far more complex than simply combining these parameters. The reason is that the interaction among the layers breaks the conventional Open System Interconnection (OSI) layered structures and creates tensions between the performance and the stability of systems, which could lead to unexpected consequences as the wireless network scales up [46].

In general, together with the CSI acquisition and other layers' key parameters, these following points should be taken into account for the cross-layer design.

- **System Complexity**: As the cross-layer design breaks the conventional layered structure, the new wireless system could be incompatible with conventional ones. Besides, since the maintenance or upgrade of the cross-layer protocol is no longer isolated within each

layer, any parameter changes must be carefully traced and coordinated [46].

- **Design Constraints**: Various data rates are usually applied to spatially distributed STAs, which may cause interferences from stronger signals to weaker ones in the downlink or the near-far effect in the uplink. Therefore, a power control or a data rate selection scheme needs to be considered with the MAC design. In addition, some QoS metrics, such as the average delay and the jitter, are traditionally not in line with the MAC focus (e.g., decreasing collisions and increasing throughput). Sometimes, maximizing throughput means sacrificing transmission opportunities of some low-rate STAs. Thus, the tradeoff of different performance metrics needs to be jointly considered and given different weights [47] [48].

2.4 MU-MIMO MAC Protocols for WLANs

In this section, we look into prominent MU-MIMO MAC proposals in the literature by focusing on the required features, performance gains, evaluation tools, as well as the key assumptions they made.

2.4.1 MAC Proposals for The Uplink

Un-coordinated Channel Access

Synchronous Data Transmissions Jin et al. in [37] present a simple MU-MIMO MAC scheme that relies on the simultaneous transmissions from STAs. The MAC procedure is the same as illustrated in Figure 2.8(a). The authors assume each STA has an orthogonal preamble so that the AP can estimate the channel coefficients and differentiate STAs. Once the AP knows the channel, it employs the ZF scheme to separate the received signals. The authors extend the Markov chain model proposed by Bianchi in [49] to analyze the performance of the proposed MU-MIMO

scheme in saturated conditions. Compared with SU-MIMO, the numerical results show that the proposed MU-MIMO scheme obtains lower collision probability, shorter delay and higher throughput in the low SNR and small network conditions.

Asynchronous Data Transmissions Babich et al. in [38] develop an analytical model of asynchronous Multi-Packet Reception (MPR), where a STA is allowed to transmit even if other STAs are already transmitting. More specifically, a STA is allowed to decrease its BO counter as long as the channel is empty or the sensed number of ongoing transmissions is below a threshold. A generic error correction code is assumed to protect data frames. The MAC procedure is shown in Figure 2.8(b). Based on the results obtained from the presented theoretical model and simulations, the authors claim that the asynchronous MAC scheme can provide considerable performance gains compared to the synchronous one due to higher utilization of the channel.

Mukhopadhyay et al. in [50] explore the ACK-delay problem that arises in asynchronous MPR. The ACK-delay problem refers to that, due to different transmission durations of asynchronous uplink transmissions, the delayed ACKs sent by the AP to those earlier-finished STAs can trigger STAs' ACK time-out counters, which could interrupt the ACK's transmission and degrade the network performance. Since Babich et al. in [38] did not consider the ACK-delay problem, the authors in [50] propose to change the ACK-waiting STAs' backoff timer to be decreased only when the channel has been idle for DIFS. The simultaneous transmissions are assumed to be decodable by the AP, and a single data rate is also assumed. Comparing to Babich's and IEEE 802.11 standard schemes, the results show that the proposed one not only decreases the frame collision probability and the average delay, but also increases the throughput.

Wu et al. in [51] propose a throughput analytical model for asynchronous uplink transmissions. A beacon sent by the AP will announce the maximum number of STAs that are allowed to transmit in parallel. Each STA maintains a transmission counter by detecting other STAs' frame preambles, and decides whether to contend for the channel. A fixed

data rate is assumed and the network is saturated. By properly configuring the contention window size and other network parameters, the authors obtain the maximized uplink throughput. With those given parameters, the authors derive a threshold of the number of antennas at the AP, which shows no throughput benefit can be achieved by adding more antennas. The reasons for that are: 1) the available transmission time decreases as the number of STAs involved in the parallel transmission increases; and 2) the collision probability increases as more antennas are employed at the AP.

Tan et al. in [52] present a practical Spatial Multiple Access (SAM) scheme for WLANs. SAM relies on a distributed MAC scheme called Carrier Counting Multiple Access (CCMA) to allow asynchronous concurrent transmissions. A chain decoding technique to separate simultaneously received frames is adopted. CCMA follows a MAC procedure similar to the one described above, in [51]. SAM is evaluated in SORA, a Software Defined Radio (SDR) platform developed by Microsoft [53]. Evaluation results show that the proposal can increase the throughput by 70% over the default IEEE 802.11 DCF.

Lin et al. in [54] propose a MIMO concurrent uplink transmission scheme called MIMO/CON, which can support both asynchronous and synchronous data transmissions. A compressive sensing technique [55] is utilized to estimate CSI from multiple concurrently received preambles, and ZF is adopted to separate the data frames. A delayed packet decoding mechanism, namely, using partially retransmitted information to decode the collided frames, is devised to avoid the complete retransmission of all corrupted frames. A fixed frame length is assumed, and the optimal transmission probability is assumed to be known by STAs. Tan's CCMA [52] is implemented to compare with MIMO/CON. The results show that CCMA outperforms MIMO/CON when the AP has fewer antennas, while MIMO/CON scales better as the number of antennas at the AP increases.

Table 2.2 summarizes the main characteristics of the surveyed uncoordinated uplink MU-MIMO MAC protocols.

Table 2.2: **Un-coordinated uplink MU-MIMO MAC protocols**

Remarks	**Evaluation Tool**	**CSI Scheme**	**MUD**	**Key Assumption**	**Scheduling**
Jin [37], compare SU and MU-MIMO, 2008	Analysis	Implicit feedback	Zero forcing	Orthogonal preambles	-
Babich [38], asynchronous MPR, 2010	Analysis	-	-	Code correction scheme	-
Mukhopadhyay [50], ACK-aware MPR, 2012	Simulation + Analysis	-	-	MPR frames decodable	-
Wu [51], throughput model, 2013	Simulation + Analysis	Implicit feedback	-	Fixed data rate	-
Tan [52], carrier counting, 2009	Testbed	Implicit feedback	Chain decoding	-	-
Lin [54], delay packet decoding, 2013	Simulation + Testbed	Compressive sensing	Zero forcing	Fixed frame length	-

Coordinated Channel Access

Scheduled Data Transmissions Huang et al. in [56] present an MPR MAC protocol that utilizes Code Division Multiple Access (CDMA) to separate the compound frames. When the STA's backoff counter reaches zero, a function that considers the number of STAs in the network, the current channel state and the MPR capability of the AP is used to schedule STAs. The MAC procedure is illustrated in Figure 2.9. The CSI is claimed to be obtained from the downlink transmission. Data frames are assumed to have the same length. Results obtained from the analytic model and simulations show that the proposed scheme reduces collisions and avoids considerable transmission errors.

Tandai et al. in [57] propose a synchronized access scheme coordinated by the AP. On receiving applying-RTSs (A-RTSs) from STAs, the AP responds with a pilot-requesting CTS (pR-CTS) to expect pilots. Based on the CSI estimated from the sequential pilots, the AP sends a Notifying-CTS (N-CTS) to inform the selected STAs for parallel transmissions. A unique subcarrier is assumed to be allocated to each STA to differentiate A-RTSs, and the MMSE decoder is adopted to separate the simultaneously received signals. According to the simulation results, the proposed scheme can reduce the overhead and increase the throughput.

Un-scheduled Data Transmissions Zheng et al. in [39] propose a MU-MIMO MAC protocol called MPR-MAC, which extends CTS and ACK to accommodate multiple transmitters. The MPR-MAC procedure is the same as illustrated in Figure 2.9, where the STAs that won the channel contention will transmit RTSs at the same time. The AP then replies with an extended CTS that grants concurrent transmissions to the requesting STAs. A set of orthogonal training sequences are assigned to STAs by the AP to facilitate the channel estimation. A Finite Alphabet (FA) based blind detection scheme is adopted for the frame separation. The network is assumed to be saturated, and all data frames have the same length. Based on the numerical results obtained from the analytic model, the authors claim that the throughput increases nearly linearly with the number of antennas at the AP.

Since the MPR-MAC follows the conventional IEEE 802.11 DCF access scheme, the probability of more than one STA choosing the same random BO is low. In order to increase the number of parallel transmissions, an enhancement called Two-Round RTS Contention (TRRC, Figure 2.11) is also proposed in [39]. Compared to MPR-MAC, TRRC has two RTS contention rounds. Namely, instead of sending a CTS after the first RTS round, the AP waits for an extra round to recruit more RTSs. The results show that TRRC obtains a further 7% throughput increase.

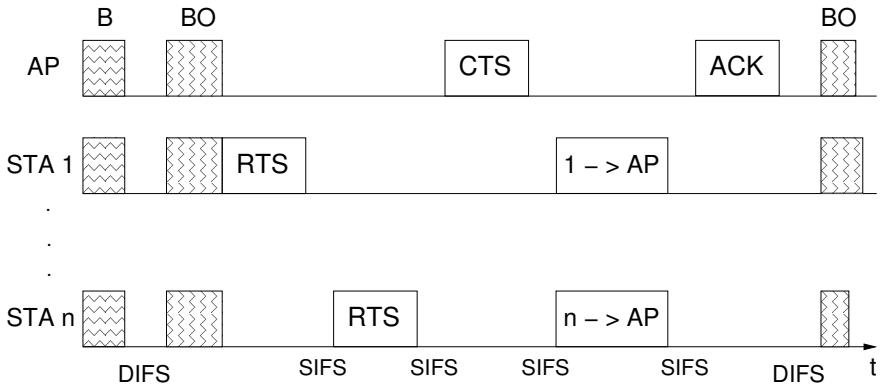

Figure 2.11: TRRC

Jung et al. in [58] present an opportunistic MU-MIMO MAC protocol to coordinate simultaneous transmissions. On receiving several RTSs, the AP sends an adapted CTS to notify the group of STAs that won the channel contention, as well as to announce its still-available channel space. STAs that did not send RTS will compete for the available channel space if their frame transmissions are shorter than the longest ongoing duration (τ_w), which is indicated in the duration field of CTS. Orthogonal preambles are assumed to be included in frames to enable the CSI estimation. The obtained results show that the proposed scheme outperforms other sampled counterparts.

Barghi et al. in [59] present an MPR-aware MAC protocol for receiving two concurrent frames by introducing a waiting time window (t_{w}) at the AP. Specifically, when the AP receives a first RTS, it will wait for a time period of t_{w} to recruit a second RTS for double-frame receptions. CTS and ACK are extended with an extra address field to accommodate two STAs. A space-time code (STC) scheme is adopted to detect multiple frames. The channel is assumed to be error-free and channel coefficients are assumed to be known. Based on the obtained results, the authors claim that, by widening t_{w}, (1) the probability of double-frame transmissions increases, while the probability of collision (i.e., the probability that the number of transmitted RTSs is more than two) increases as well; and (2) the performance of the proposed MPR-aware MAC scheme improves significantly compared to that of the IEEE 802.11 standard one.

Zhou et al. in [60] propose a two-round channel contention mechanism, which divides the MAC procedure into two parts. The two parts, namely, the random access and the data transmission, are illustrated in Figure 2.12. The random access finishes as soon as the AP receives M_{random} (the maximum number of STAs that can transmit simultaneously) successful RTSs, and then the data transmission starts. In the random access part, the AP delivers two types of CTSs: Pending CTS (PCTS) and Final CTS (FCTS). The former responds to RTS and the latter notifies all STAs about the start of data transmissions. Those STAs, who have sent RTSs within a predefined time threshold (T_{timeout}), will transmit simultaneously. If the number of contending users is less than M_{random}, the

T_{timeout} will trigger data transmissions as well. The AP obtains the CSI from RTSs, and utilizes the MMSE detector to separate STAs' signals. Data frames are assumed to be of fixed length. Both simulation and analytic results show that the two-round contention scheme outperforms the IEEE 802.11 single-round one in terms of throughput and delay.

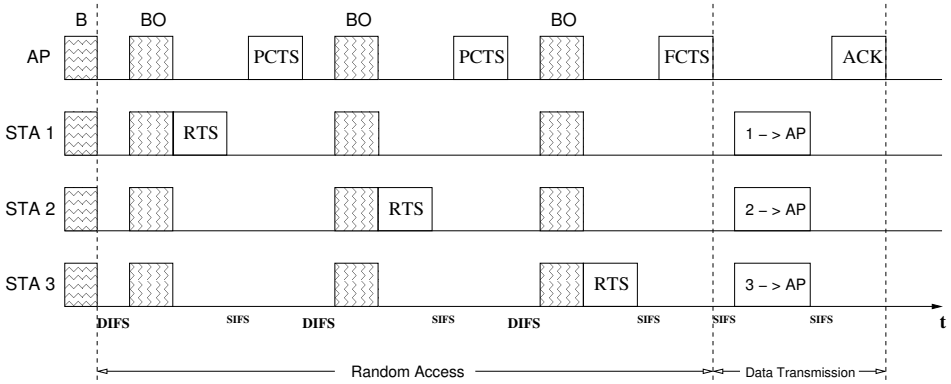

(a) Without timeout

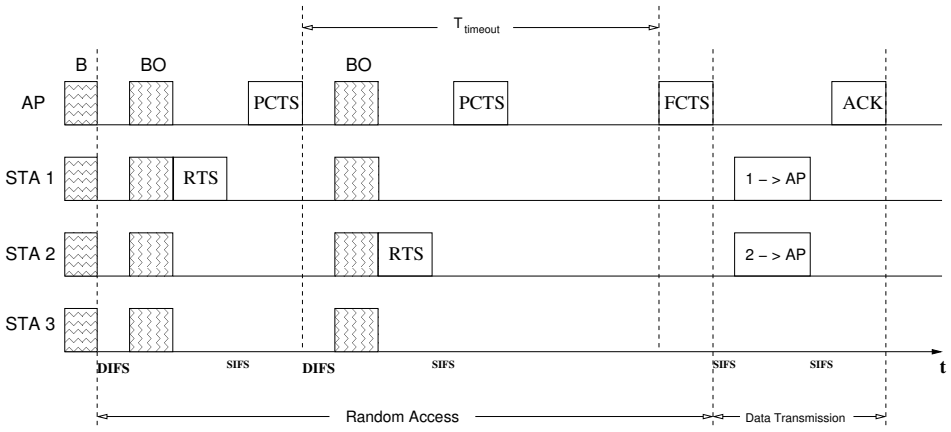

(b) With timeout

Figure 2.12: Two-round MAC procedures with $M_{\text{random}} = 3$

Zhang in [61] further extends two contention rounds to multiple rounds,

which give STAs more opportunities to compete for the channel based on a threshold derived from an optimal stopping algorithm. Meanwhile, an auto fall-back to single-round scheme is also proposed in case the traffic is low and the single-round scheme can provide higher throughput. Frame arrivals are assumed to follow the Poisson distribution. Results obtained from simulations and the analytical model show the multi-round contention can increase the channel utilization rate in a small to moderate network.

Jung et al. in [62] present an asynchronous uplink MPR scheme, where the AP informs STAs about its MPR vacancy through an additional feedback channel. The proposed MAC procedure is shown in Figure 2.13. On receiving an RTS from STA2, the AP replies with a CTS that includes the MPR vacancy (the remaining space for parallel uplink transmissions). STAs who overhear the MPR vacancy will compete for the channel to transmit along with STA2. Once a STA finishes transmitting ahead of the other one, the AP immediately sends an ACK with the updated MPR vacancy information through the additional channel to allow other STAs to compete for the newly available MPR space. The authors assume an orthogonal training sequence is included in the preamble of each frame for estimating the channel. Based on results obtained from the analytic model and simulations, the authors claim that the proposed scheme coordinated by the AP achieves higher channel efficiency in scenarios where the frame size and transmission rates are dynamically varying.

Table 2.3 summarizes the main characteristics of the surveyed coordinated uplink MU-MIMO MAC protocols.

2.4.2 MAC Proposals for The Downlink

A commonly used MAC procedure for MU-MIMO downlink transmissions is illustrated in Figure 2.14. The AP firstly sends out a modified RTS containing a group of targeted STAs. On receiving the RTS, those listed STAs estimate the channel, integrate the CSI into the extended CTS and send it back. As soon as the AP receives all successful CTSs, it precodes the outgoing frames based on the feedback CSI.

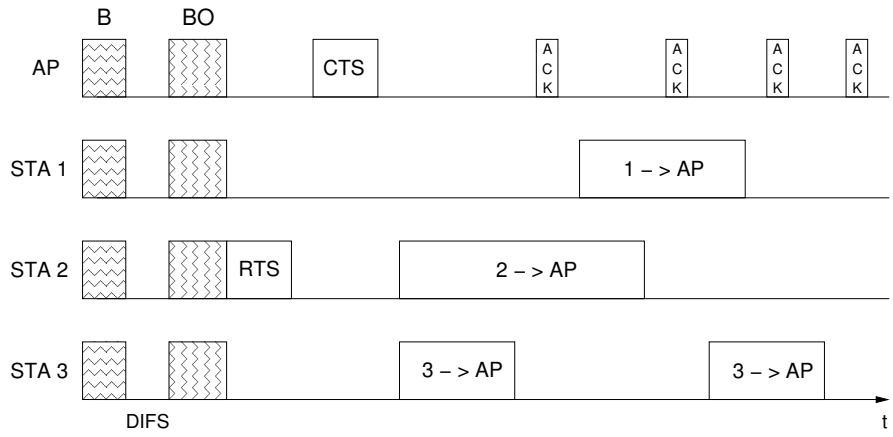

Figure 2.13: Asynchronous data transmissions with 1 MPR vacancy

Table 2.3: **Coordinated Uplink MU-MIMO MAC Protocols**

Remarks	**Evaluation Tool**	**CSI Scheme**	**MUD**	**Key Assumption**	**Scheduling**
Huang [56], SNR based MPR, 2008	Simulation + Analysis	Downlink estimation	CDMA	Fixed data length	Optimal SNR
Tandai [57], TDMA signalling, 2009	Simulation	Implicit feedback	MMSE	Unique subcarrier	Best CSI
Zheng [39], DCF based MPR, 2006	Analysis	Implicit feedback	Blind detection	Fixed data length	-
Jung [58], τ_w based transmission, 2011	Analysis	Implicit feedback	-	Orthogonal preamble	-
Barghi [59], MPR-aware MAC, 2011	Simulation + Analysis	-	STC	Perfect channel	-
Zhou [60], two-round contentions, 2010	Simulation + Analysis	Implicit feedback	MMSE	Fixed data length	-
Zhang [61], multi-round contentions, 2010	Simulation + Analysis	-	-	Poisson arrivals	-
Jung [62], asynchronous MPR, 2012	Simulation + Analysis	Implicit feedback	-	Extra ACK channel	-

Cai et al. in [63] propose a distributed MU-MIMO MAC protocol with extended RTS/CTS frames. The CSI is obtained from the RTS/CTS exchange. An additive white Gaussian noise (AWGN) channel is assumed, and a leakage-based precoding scheme is utilized to cancel interference.

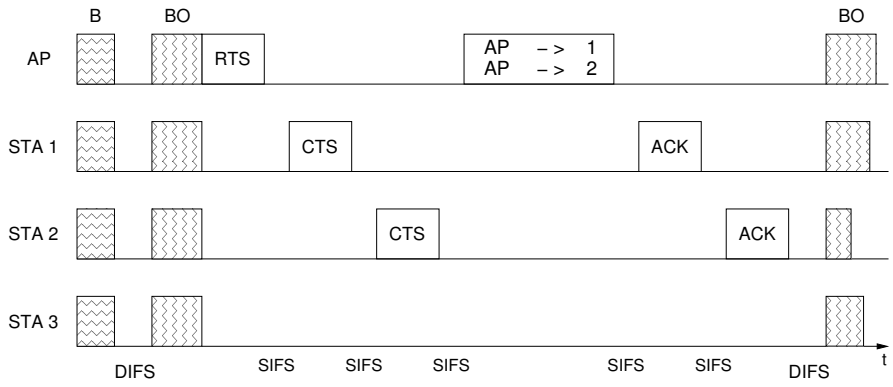

Figure 2.14: Downlink MU-MIMO transmissions

The authors adopt a queue based scheduling scheme, which prioritizes frames with the longer waiting time in the AP buffer. The results derived from the analytic model and simulations show the proposed multi-user MAC substantially outperforms the single-user one.

Li et al. in [64], propose a Multi-user MAC (MU-MAC) protocol, which supports Multi-Packet Transmission (MPT) in the downlink and multiple control packets (e.g., CTSs or ACKs) reception in the uplink. Orthogonal OFDM preambles are utilized to facilitate the CSI extraction from the simultaneously received control frames. The frame errors are assumed to come from collisions only, and all frames are transmitted with the same rate. The scheduling scheme jointly considers the CSI history, the AP's queueing state and the frames' application categories. By observing the results, the authors claim that MU-MAC outperforms MPT-only MAC in terms of the maximum number of supported STAs, and this gain will increase further as the AP employs more transmitting antennas.

Gong et al. in [65] propose a modified CSMA/CA protocol with three different ACK-replying mechanisms, namely, the polled ACK response, the scheduled ACK response and the failed ACK recovery. A weighted queueing mechanism that associates ACs with the value of contention window is also proposed to address the fairness concern. The MMSE precoding scheme is adopted and the CSI is assumed to be known. The

simulation results show that the proposed protocol provides a considerable performance improvement against the IEEE 802.11n beamforming based approach when the SNR is high.

Kartsakli et al. in [66] propose four multi-user scheduling schemes for concurrent frame transmissions, namely, MU-Basic, MU-Deterministic, Mu-Threshold Selective, and MU-Probability. The opportunistic beamforming that selects STAs with the highest signal-to-interference-plus-noise ratio (SINR) for each randomly generated beam is utilized. The CSI is fedback by STAs during the channel contention phase. A block fading channel is assumed, which means the channel remains constant during a frame transmission time. Based on simulation results, the authors argue that the proposed schemes achieve notable gains against the single-user case, although there is still considerable space for improvements compared to the theoretical capacity.

Zhang et al. in [67] present a One-Sender-Multiple-Receiver (OSMR) transmission scheme for WLANs. The authors firstly implement an OSMR prototype using a Universal Software Radio Peripheral (USRP) [68] platform to explore the feasibility of OSMR at the PHY level. Then, based on the study of the OSMR PHY characteristics, they modify the RTS/CTS frames to support the channel estimation. Simulations of the proposed extension are conducted at the MAC level. A greedy scheduling algorithm is proposed to transmit as many frames as possible in a TXOP with the urgent frames being prioritized over the normal ones. The ZF precoding scheme is adopted, while a flat fading channel is assumed. The simulation results show that a significant performance gain is achieved by employing OSMR transmissions.

Redieteab et al. in [69] investigate three different transmission schemes in a PHY and MAC cross-layer platform, which are SU-MIMO, MU-MIMO with multi-user interference and MU-MIMO without multi-user interference. An IEEE 802.11ac channel model [70] is utilized to represent channel variations. The MAC layer is made to be compliant with the 802.11ac specification draft, thus, the amendment defined ECFB protocol is employed to obtain the CSI. The ZF channel-inversion precoding scheme is used to decode frames. Based on the simulation results,

the authors conclude that multi-user interference has important effects on MU-MIMO transmissions, e.g., it results in less throughput and are less stable than SU-MIMO ones. Therefore, an automatic switching algorithm between SU-MIMO and MU-MIMO is suggested by the authors.

Cha et al. in [71] compare the performance of downlink MU-MIMO to Space Time Block Coding. The ZF precoder is utilized, and the CSI is obtained at the AP by receivers' feedback. A Rayeigh fading and error-free channel is assumed. The results show that the downlink MU-MIMO scheme produces a higher throughput than the STBC one if transmitted frames are of similar length, while the results reverse in a fast-varying channel due to high overheads of the CSI feedback .

Balan et al. in [72] implement a distributed MU-MIMO system that consists of several multi-antenna APs, which are connected and assumed to be synchronous by a coordinating server. The authors employ Zero Forcing Beamforming (ZFBF) and THP for the frame separation. The CSI is acquired from uplink pilot symbols. Blind Interference Alignment (BIA) is used when the CSI is unavailable. The system is evaluated in the Wireless Open-Access Research Platform (WARP) platform [73]. The experimental results show that the presented MU-MIMO system can achieve high data rates and approach the theoretical maximum throughput.

Zhu et al. in [74] investigate required modifications for TXOP to support multi-user transmissions. The proposed scheme, called multi-user TXOP (MU-TXOP), enables a STA whose AC won the TXOP to share the transmission period with MPDUs of other ACs. The authors assume all STAs can be grouped for multi-user downlink transmissions. Simulation results show that the proposed scheme not only obtains a higher throughput, but is also more fair compared to the conventional one.

Ji et al. in [75] present a cooperative transmission scheme that addresses the redundant Network Allocation Vector (NAV) setting and the outdated SINR problems. The redundant NAV setting usually occurs at STAs located in the overlapped areas of neighbouring WLANs, while the outdated SINR problem is caused due to the delay between the channel estimation and the data transmission. The authors utilize reserved bits in control frames to announce the last frame of a transmission to synchro-

Table 2.4: **Downlink MU-MIMO MAC Protocols**

Remarks	Evaluation Tool	CSI Scheme	MUIC	Key Assumption	Scheduling
Cai [63], reduce AP-bottleneck effect, 2008	Simulation + Analysis	Explicit feedback	Leakage coding	AWGN channel	Priority queue
Li [64], MU-MAC, 2010	Simulation + Analysis	Explicit feedback	-	Error-free channel	History CSI
Gong [65], ACK-replying schemes, 2010	Simulation	-	MMSE	Assume CSI known	Weighted queue
Kartsakli [66], 4 scheduling schemes, 2009	Simulation	Explicit feedback	Beamforming	Block fading	Highest SINR
Zhang [67], OSMR, 2010	Simulation + Testbed	Explicit feedback	Zero Forcing	Flat fading	Greedy
Redieteab [69], PHY+MAC platform, 2012	Simulation	Explicit feedback	Zero Forcing	-	-
Cha [71], STBC & MU-MIMO, 2012	Analysis	Explicit feedback	Zero Forcing	Error-free channel	-
Balan [72], multi-AP system, 2012	Simulation + Testbed	Implicit feedback	ZFBF, THP, BIA	Phase synchronous	-
Zhu [74], multi-user TXOP, 2012	Simulation	-	-	All STAs groupalbe	-
Ji [75], outdated NAV and SINR, 2014	Simulation + Analysis	Explicit feedback	-	Poisson arrivals	-

nize the NAV setting, and employ STAs’ ACKs to re-estimate and correct the SINR. The analysis model assumes frames that arrive to STAs to follow the Poisson process. The results obtained from the model and simulations show the enhanced scheme can achieve noticeable performance gains compared to the sampled one.

Table 2.4 summarizes the main characteristics of the surveyed downlink MU-MIMO MAC protocols.

2.4.3 Integrated Up-down/link MAC Proposals

Since the unilateral enhancement (e.g., adapted downlink transmissions) may harm the performance of the other side. Integrated up-down/link MAC proposals have to take the effect of downlink enhancements to the uplink traffic (or vice verse) into account. Only a few works have considered both MU-MIMO uplink and downlink transmissions in a single

MAC protocol.

Shen et al. in [76] present a High Throughput MIMO (HT-MIMO) MAC protocol that utilizes frequency signatures to differentiate simultaneously received control frames. HT-MIMO works in the PCF mode, hence both uplink and downlink transmissions can only be initiated by the AP. The CSI is obtained by a channel measurement method. The uplink and downlink channels are assumed to be symmetrical. A greedy scheduling algorithm is adopted with the consideration of fairness and the queue occupancy. The results obtained from the analytical model show that the HT-MIMO MAC outperforms the implemented SU-MIMO and MU-MIMO protocols.

Kim et al. in [77] devise a down/up-link back-to-back transmission scheme to synchronize STAs. The scheme is called Per-flow MAC (PF-MAC, Figure 2.15), where RIFS stands for Reduced Inter Frame Space. The AP first sends a Group-RTS (GRTS) that includes a list of STA addresses to initiate the downlink transmission. As soon as the AP received expected CTSs, it sends data frames to the listed STAs. The STAs who received frames then send back ACKs sequentially. Through the downlink transmission and a Ready to Receive (RTR) frame from the AP, STAs are synchronized for the parallel uplink transmission. The CSI is estimated from uplink frames. The limitation of the proposal is that the uplink transmission can only be started by the downlink one, which may not be desirable in some scenarios where the uplink access is urgent. Note that the proposal is just a conceptual model without any simulation or analytic results.

Yun et al. in [78] present a multi-point to multi-point MIMO system, where the uplink multiplexing is implemented in the SORA platform, while the downlink is implemented in the USRP platform. Multiple APs are coordinated by a controller, and connected via an Ethernet cable. A leader concept is adopted for both the uplink and downlink medium access. A trigger frame that includes co-senders' addresses is sent out by the leader who first won the channel contention. Then, the co-senders transmit preambles sequentially as specified in the trigger frame for the CSI estimation. The downlink scheduling is based on the packet arrival

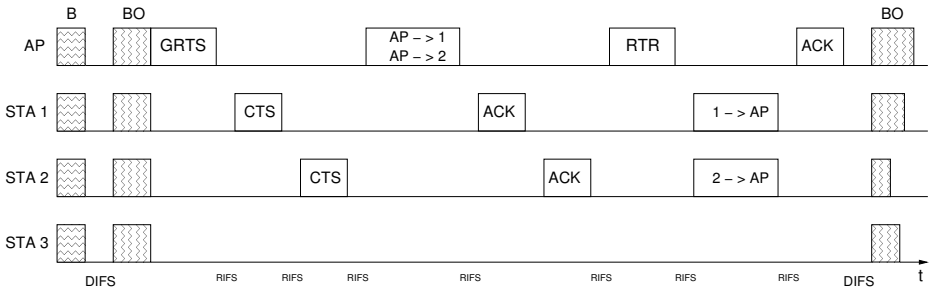

Figure 2.15: PF-MAC

Table 2.5: **Integrated Up-down/link MU-MIMO MAC Protocols**

Remarks	**Evaluation Tool**	**CSI Scheme**	**MUD & MUIC**	**Key Assumption**	**Scheduling**
Shen [76], control frames' encoding, 2012	Analysis	-	-	Symmetrical channel	Greedy
Kim [77], back-to-back transmissions, 2008	Conceptual model	Implicit feedback	-	-	-
Yun [78], multi-APs to multi-STAs, 2013	Testbed	Sequential preambles	Zero Forcing	-	FIFO

time and the length of waiting time in the queue, while the co-senders' selection in the uplink is randomly made. ZF is employed in both the uplink and downlink for frames' de/pre-coding.

Table 2.5 summarizes the main characteristics of the up-down/link MU-MIMO MAC protocols.

Chapter 3

ENHANCED DOWNLINK TRANSMISSIONS IN WLANS

3.1 Introduction

MIMO has two configuration modes, SU-MIMO and MU-MIMO. The former is able to provide a significant improvement when most of the traffic load is directed to only a reduced group of STAs. By introducing SU-MIMO, IEEE 802.11n [19], is able to improve the system throughput compared to the two previous standards (the 802.11a and 802.11g). For instance, the use of four spatial streams with a bandwidth of 40 MHz, increases the maximum data rate from 54 Mbit/s to 600 Mbit/s. On the other hand, MU-MIMO is able to enhance the system performance in scenarios where the number of active STAs is high and the traffic is uniformly distributed.

Both SU-MIMO and MU-MIMO refer to the PHY layer techniques, which take benefits of the spatial dimension of channel. In comparison, Space Division Multiple Access (SDMA) refers to a channel access scheme that uses the MIMO techniques to multiplex different frames (data streams) over that space dimension. There are two challenges that need to be tackled before SDMA is applied to WLANs: firstly, in the downlink, the AP needs the Channel State Information (CSI) feedback from STAs

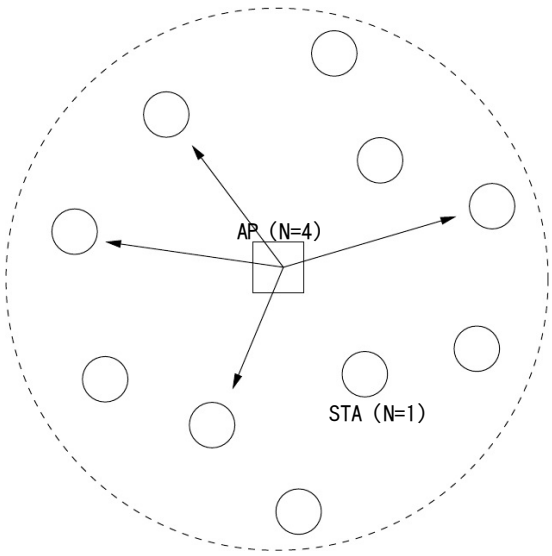

Figure 3.1: Considered WLAN scenario with $N = 4$ antennas at AP and single-antenna at STAs

for the frame/destination selection and precoding scheme, which can be solved by acquiring the CSI embedded in the CTS message or by directly estimating it at the AP from the frames received; secondly, in the uplink, STAs need to be coordinated and synchronized, which are more complicated as STAs access the channel in a distributed and asynchronous way, thus requiring more signalling and message exchanges [60].

In this Chapter, a SDMA-enhanced MAC protocol focusing only on the downlink transmission is proposed. In the uplink, STAs will operate in the standard IEEE 802.11 Distributed Coordination Function (DCF).

3.2 Network Scenarios

A single-hop IEEE 802.11 WLAN consisting of one AP and M STAs is considered. The AP has an array of N antennas, while each STA has

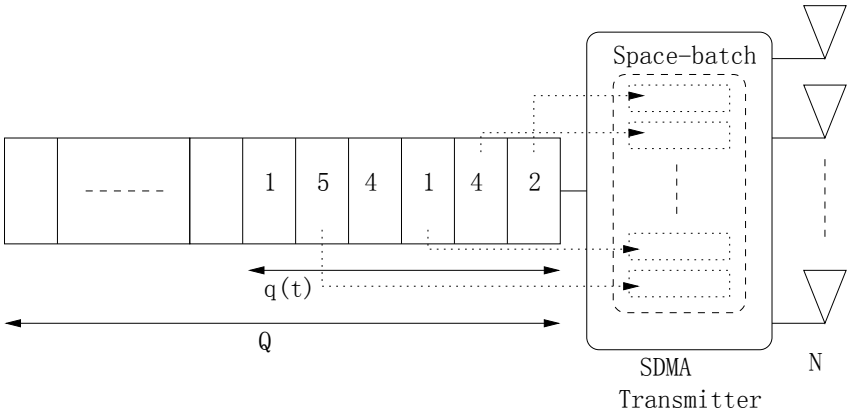

Figure 3.2: The SDMA transmission queue and the Scheduler

a single antenna, which is a reasonable assumption considering STAs' power consumption and cost. A specific scenario for an AP with $N = 4$ antennas is shown in Figure 3.1.

The channel is assumed frame-flat, with the independent fading from frame to frame. Without loss of generality, it is assumed that the instantaneous channel matrix is always ideally conditioned (i.e. the channel realizations are orthogonal), and hence, the beamforming at the AP is able to completely suppress the multi-user interference without any power penalty. Moreover, a single transmission rate is considered. It is assumed that all STAs always can receive error-free frames at that rate. These assumptions lead to N independent downlink channels, which could allow up to N simultaneous transmissions from the AP to the STAs. In the uplink, as no enhancement is considered in this Chapter, only one STA is allowed to access the channel each time.

Frames that arrive to the AP follow the Poisson process with a rate λ. The traffic load of the downlink is ten times higher than that of the uplink, which is reasonable because most of the downlink traffic is a response (i.e. an online video) to the requests (i.e. a http request) from STAs.

Through using the spatial multiplexing provided by the MIMO technology, the AP assembles those frames queued at the MAC layer into a

Table 3.1: System Parameters

Parameters	Values
AP Bandwidth per STA	200 Kbps
STA Bandwidth	20 Kbps
Data Rate	11 Mbps
Phy/Basic Rate	1 Mbps
Queue Length	20 Frames
Frame Length	4000, 8000 bits
Preamble Length	40 bits
MAC Header/RTS/CTS/ACK Length	160 bits
Slot Time (σ)	20 μs
SIFS	10 μs
DIFS	50 μs
CWmin	32
CWmax	1024
Retry Limit	5
AP Antennas	1, 2, 4

Space-batch (a group of frames transmitted simultaneously) according to the destination address, as illustrated in Figure 3.2, where Q is the buffer size and $q(t)$ the instantaneous queue occupation. The AP selects sequentially all frames that satisfy the condition of being directed to different destinations. Note that, the first frame waiting in the queue is always selected, and then, up to N frames. Frames in transmission are not dequeued until they are completely transmitted.

The data rate is fixed at 11 Mbps, while the physical and basic rates are fixed at 1 Mbps. The relevant parameters considered are listed in Table 3.1.

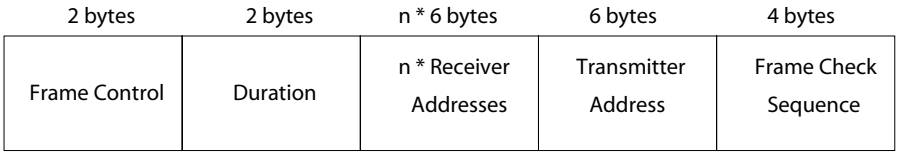

Figure 3.3: MU-RTS Frame Structure

3.3 DCF/DSDMA: the MAC Design

The proposed MAC protocol is called enhanced DCF with SDMA Downlink transmissions (DCF/DSDMA). It extends the DCF mechanism, with the RTS/CTS option enabled, to support multiple simultaneous downlink transmissions.

The RTS/CTS mechanism is adopted for two reasons. Firstly, the RTS/CTS mechanism allows the AP to estimate the CSI via the preamble of the replied CTSs from the STAs. The channel information will be used for the precoding scheme at the AP to cancel the multiuser interference. Secondly, the DCF/DSDMA needs to extend the standard RTS to the Multi-User RTS (MU-RTS) frame, as illustrated in Figure 3.3, as the AP has to specify all receiving addresses of the next Space-batch[1].

For a MU-RTS frame, the type and sub-type fields of the frame are 10 (that denotes a control frame) and 1001 (MU-RTS identifier, one of the non-assigned combinations in the standard), these values allow the receiver to identify the reception of a MU-RTS and process it accordingly.

DCF/DSDMA conducts some minor changes to the conventional MAC operations, as illustrated in Figures 3.4 and 3.5. The description of the protocol is divided into two parts: successful transmissions and recovering from collisions. Note that, initially in all figures the channel is assumed busy (B), and the random Back-Off time is denoted as BO.

[1]Note that if a single frame is included in the Space-batch, the MU-RTS is equivalent to a standard RTS.

3.3.1 Successful Transmissions

First of all, any STA, including the AP, operates like the conventional IEEE 802.11 DCF scheme: when the medium has been idle for a DCF Inter Frame Space (DIFS) time, after a random backoff time it starts to send an RTS or an MU-RTS based on the number of antenna and the frames in the queue, as previously depicted in Figure 3.2. If an RTS is sent out, the DCF/DSDMA operates exactly the same as the conventional one, as shown in Figure 3.4(a). If a MU-RTS is sent out, as illustrated in Figure 3.4(b), the STAs listed in the receiving field will send a CTS back sequentially (following the same order of their addresses included in the MU-RTS) to confirm that they are ready to receive a frame from the AP. Those STAs who are not included in the MU-RTS will set their Network Allocation Vector (NAV) to defer their transmission activities. The NAV is equal to the duration of the whole transmission in order to reserve the medium. On receiving all the CTS messages (if not all, the AP is going to send frames in parallel only to those who successfully replied with a CTS). Lastly, after the transmission of all frames is completed and a Short Inter Frame Space (SIFS) time, STAs start to send back their respective Acknowledgement (ACK) sequentially in the same order of the CTS.

3.3.2 Collision Recovering

If more than one STA pick the same BO from their respective Contention Window (CW), a collision will happen, as illustrated in Figure 3.5, where the dashed lines denote that the frames should be there if the transmission was successful.

In standard DCF, on sending the RTS, the AP and STAs will set a timer equal to Equation (3.1) to receive the expected CTS, where CTS_{tx} denotes the transmission duration of a CTS. If the CTS is not received before the timer expires, the sending STAs assume that collisions or errors have occured, and start to compete for the channel again. For the non-transmitting STAs, none of the RTSs can be received correctly. So after the collision time, the receiving STAs wait for an Extended Inter frame

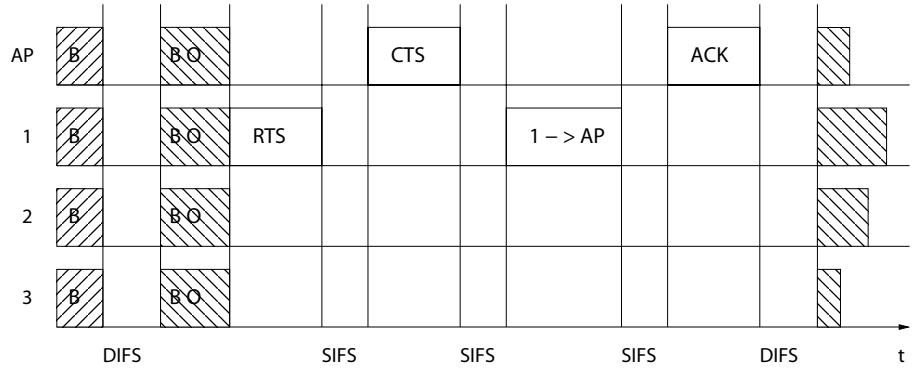

(a) Successful transmission of a STA

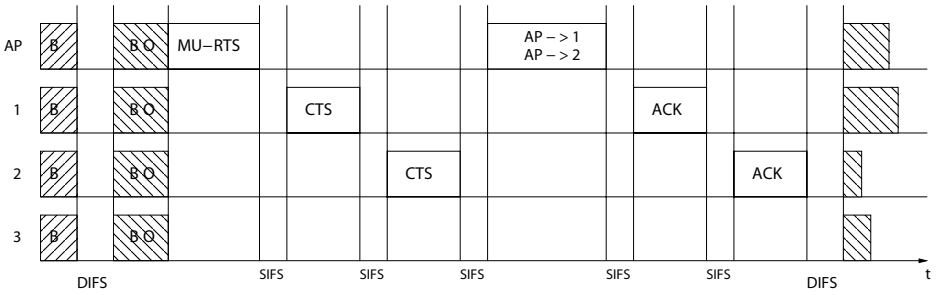

(b) Successful transmission of the AP

Figure 3.4: DCF/DSDMA Successful Transmissions

space (EIFS) time, as shown in Equation 3.2, and then start competing for the channel again.

$$CTS_{timer} = SIFS + CTS_{tx} \tag{3.1}$$

$$EIFS = SIFS + CTS_{tx} + DIFS \tag{3.2}$$

Accordingly, the CTS timer and EIFS have to set to the new values MU_CTS_{timer} and MU_EIFS (as shown in Equations 3.3 and 3.4). Both parameters have to consider the worst case to make sure that all STAs start competing for the channel at the same time.

It is important to note that in all situations these new values have to be considered for all STAs, even in the scenario when there are only collisions between STAs, as illustrated in Figure 3.5(b). This is because colliding STAs can not know if they are colliding with the AP or another STA. Obviously, these required changes introduce some overheads such as waiting a longer time when collisions occured among STAs or when the collisions are between the AP and STAs but the AP is sending a Space-batch with less than N frames.

$$MU\_CTS_{timer} = N \cdot (SIFS + CTS_{tx}) \tag{3.3}$$

$$MU\_EIFS = N \cdot (SIFS + CTS_{tx}) + DIFS \tag{3.4}$$

3.3.3 Other considerations

The AP will only send frames to those STAs whose channel conditions meet certain threshold. As illustrated in Figure 3.6, the channel between the AP and STA 1 does not meet the required quality, and therefore, the AP will send a frame to STA 2 only. Note that STA 2 has to wait for an extra $SIFS + ACK$ time before it can send its own ACK even if it is the only receiver. This is because the transmission duration and the sequence of sending CTS and ACK are decided in the MU-RTS and all STAs set their NAV timer based on that.

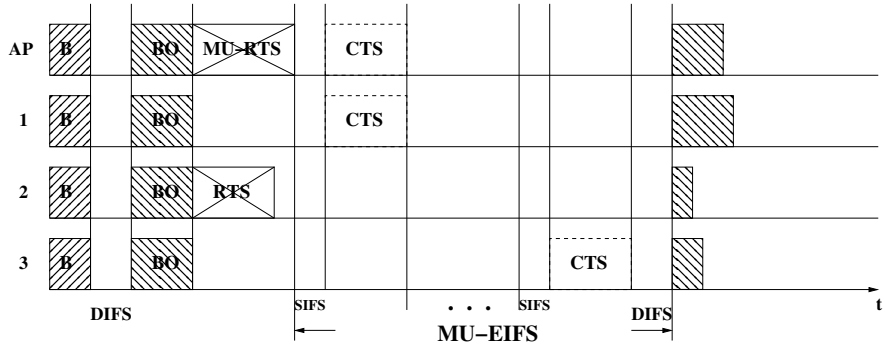

(a) Collision between the AP and a STA

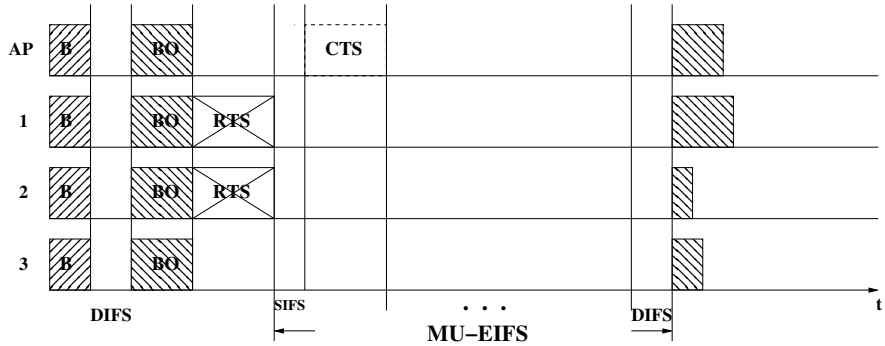

(b) Collision between two STAs

Figure 3.5: DCF/DSDMA: Recovering from collisions

3.4 Performance Evaluation

The parameters considered to evaluate the proposed DCF/DSDMA are listed in Table 3.1. The Component Oriented Simulation Toolkit (COST) [79] libraries have been used to implement and simulate the considered system.

The theoretical maximum throughput of the AP using N antennas is shown in Equation 3.5, where MU_RTS_{tx} denotes the transmission time of the MU_RTS frame with N receiving addresses. The subscript tx

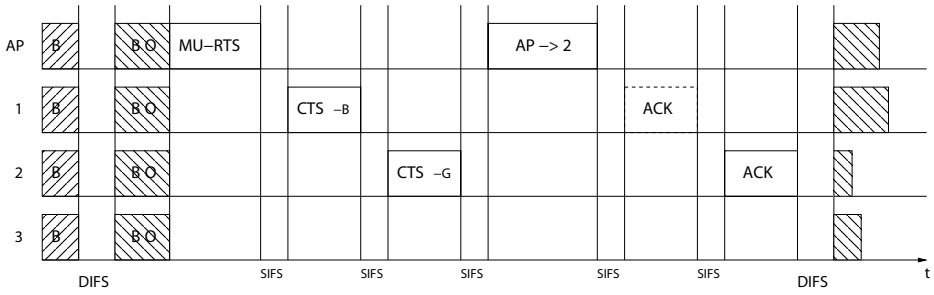

Figure 3.6: Unfeasible transmission due to the channel conditions between the AP and the 1-th STA. The (-G) in the CTS means 'good' and the (-B) means 'bad'.

$$S_{max}(N) = \frac{N \cdot L}{DIFS + \sigma CW_{min}/2 + MU\_RTS_{tx} + N(CTS_{tx} + ACK_{tx}) + FRAME_{tx} + (2N+1)SIFS} \quad (3.5)$$

means the transmission duration of the control or data frame. Note that the assumptions made for computing the theoretical maximum throughput are: 1) only the AP is transmitting and 2) the AP is saturated. For instance, considering a frame length L equal to 4000 bits, the maximum achievable throughput following the Equation 3.5 are $S_{max}(1) = 2.82$ Mbits/s, $S_{max}(2) = 4.24$ Mbits/s, and $S_{max}(4) = 5.66$ Mbits/s, for the AP with $N = 1$, $N = 2$ and $N = 4$ atennas respectively.

Figures 3.7(a) and 3.7(b) show the throughput of the AP and STAs. As we can see from Figure 3.7(a), the throughput of the AP with one antenna (AP-N=1) increases proportionally with the number of STAs until it saturates (around 2.54 Mbits/s). Given the considered downlink /uplink traffic distribution, the AP becomes saturated mainly due to its own traffic load, although collisions with STAs can not be neglected, which is why the throughput is decreasing as the number of STAs goes higher after the saturation.

In Figure 3.7(a), the considerable gain is observed in the AP throughput, from 2.54 Mbits/s with $N = 1$ antenna to 3.81 Mbits/s with 2 anten-

nas (AP-N=2) and 5.00 Mbits/s with 4 antennas (AP-N=4). A noticeable outcome is that the gain is not linear with the increase of the number of antennas, the reason of that is two-fold: 1) the higher service time for each frame due to the backoff interruptions and the higher collisions as the system gets more STAs and 2) the presence of a finite queue as shown in [80] can not take full benefits of employing more antennas at the AP. These reasons also justify the difference between the maximum throughput computed in Equation 3.5 increasing with N.

In Figure 3.7(b), significant gains are achieved if a longer frame length ($L = 8000$ bits) is used. For example, the maximum throughput of the AP with $N = 2$ antennas increases from 3.81 Mbits/s in Figure 3.7(a) to 6.39 Mbits/s in Figure 3.7(b) and the number of STAs that the wireless system can support goes from 20 to 32 STAs. The main reason is that each Space-batch now includes more bits as the frame length is longer, which makes the overhead of the control messages (i.e. $MU\_RTS_{tx}(N)$) less significant and the WLAN works more efficiently.

Note that in the considered scenario the STAs never become saturated as the aggregate throughput of STAs (Figures 3.7(a) and 3.7(b)) increases proportionally with the number of STAs regardless the number of the antennas at the AP.

In Figures 3.8(a) and 3.8(b) the delay of the AP is shown. Obviously the average delay decreases significantly by employing multiple antennas. A noticeable aspect here is that the average delay increases significantly at a certain region before the AP becomes saturated. It is called the turmoil region in this Chapter. For example, the turmoil region for the AP with one antenna in Figure 3.8(a) is from 10 to 15 STAs and for the AP with one antenna in Figure 3.8(b) is from 15 to 25 STAs, which could be useful for finding out what is the most suitable number that a wireless network can support.

Finally, it is interesting to observe the average Space-batch size in Figures 3.9(a) and 3.9(b) increases as the number of STAs increases. Note that it is load-aware as the size of the Space-batch increases with the number of STAs.

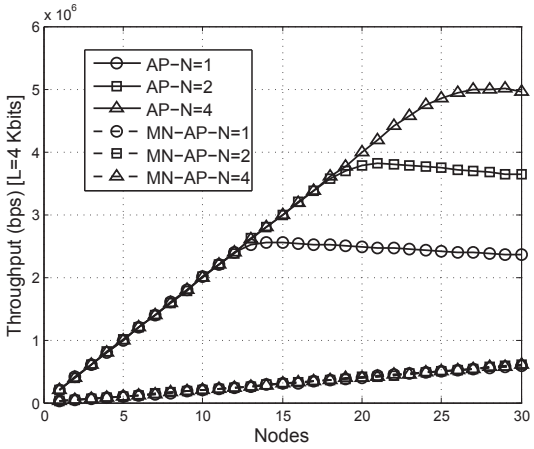

(a) Frame length=4000 bits

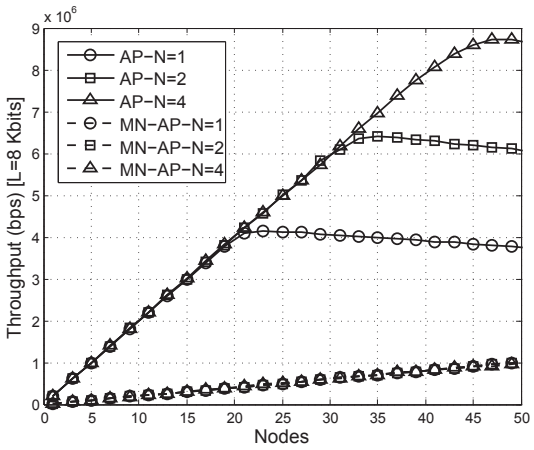

(b) Frame length=8000 bits

Figure 3.7: Throughput against the number of STAs with different antennas N

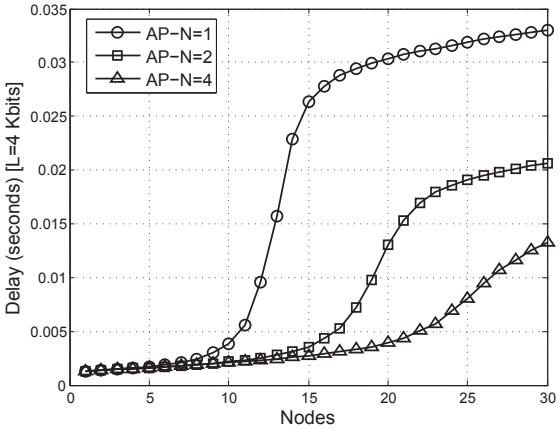

(a) Frame length=4000 bits

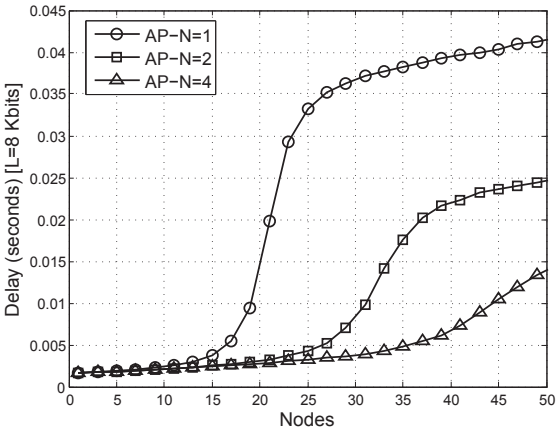

(b) Frame length=8000 bits

Figure 3.8: Average Delay against the number of STAs with different antennas N

3.5 Summary

In this Chapter, the DCF/DSDMA protocol has been presented. The results show that considerable performance gains, in terms of a higher

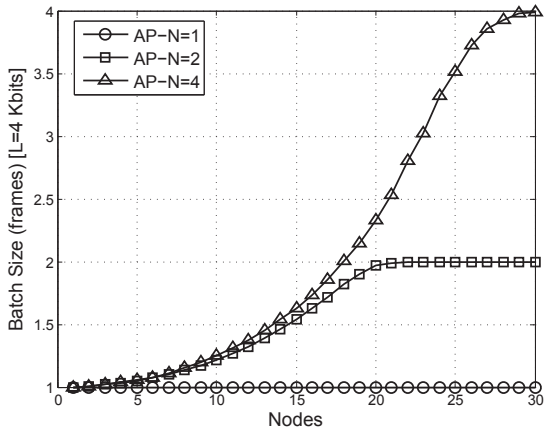

(a) Frame length=4000 bits

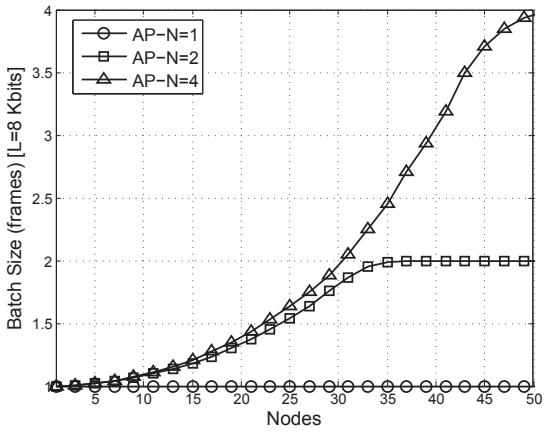

(b) Frame length=8000 bits

Figure 3.9: Average Space-batch against the number of STAs with different antennas N

throughput and lower delays, are achieved by employing multiple antennas at the AP. However, the results also show that the achieved gain is neither linear with the number of antennas nor the frame length due to the

extra overheads of the DCF/DSDMA, the own behavior of the DCF and the presence of a finite queue length.

Chapter 4

ENHANCED UPLINK TRANSMISSIONS IN WLANS

4.1 Introduction

The traditional IEEE 802.11 MAC schemes allow only one node to access the channel each time. In order to take the benefit of multiple simultaneous uplink transmissions when the AP is equipped with multiple antennas, a new MAC protocol called DCF/USDMA is presented. It extends the IEEE 802.11 DCF by introducing a second contention round, which is used to accommodate the multiple simultaneous transmissions from multiple stations.

A similar work has been presented in [60]. The authors devise a novel way to synchronize multiple uplink transmissions, which includes a random access part and a data transmission part. In the random access period, two new types of CTS frames are introduced: Pending CTS (PCTS) and Final CTS (FCTS). PCTS acts as an acknowledgment to the RTS, and FCTS is used to notify to the wireless nodes the start of the data transmission. Each pair of RTS/PCTS exchange is delimited by a combination of the DIFS plus a random back-off, which is intended to provide fairness among the multiple contenders. A special feature of this proposal is that it is able to dynamically adjust the contention period.

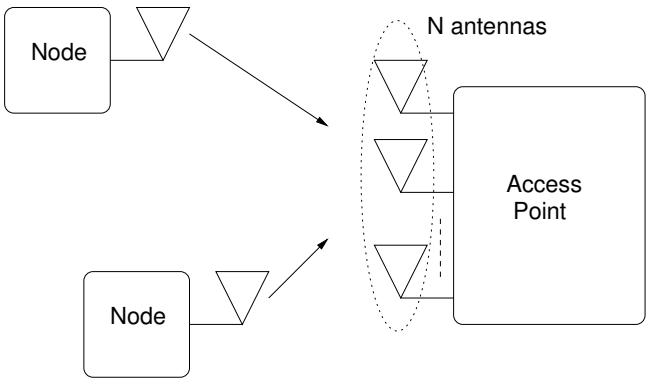

Figure 4.1: Multi-Packet Reception at the AP

In this Chapter, a more efficient communication procedure is proposed for multiple simultaneous uplink transmissions. In order to recruit more nodes for the uplink transmission, we extend the traditional one-round channel contention with an extra second round. However, compared to [60], our proposed 2-nd round stage is shorter as we send a single message to reply all successfully received 2-nd round RTSs. In addition, the 2-nd round stage finishes as soon as the available antennas counts to zero, without always waiting its maximum duration. We also introduce a new block ACK frame, the Group ACK (G-ACK), which significantly reduces the overheads caused by the transmission of multiple consecutive ACKs to each different destinations. Finally, we have extensively evaluated the performance of the DCF/USDMA protocol, specially focusing on tuning the parameters that control the 2-nd round contention stage.

4.2 DCF/USDMA: the MAC Design

4.2.1 Adapted Frame Format

The traditional IEEE 802.11 DCF MAC protocol relies on either the basic access scheme or the optional handshaking mechanism-RTS/CTS to share the wireless channel, both of which are based on CSMA/CA proto-

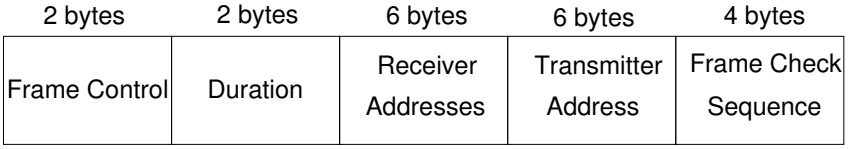

(a) Standard RTS Frame

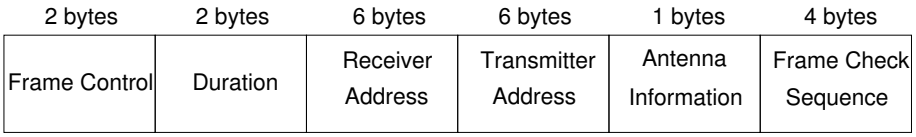

(b) MU-CTS Frame

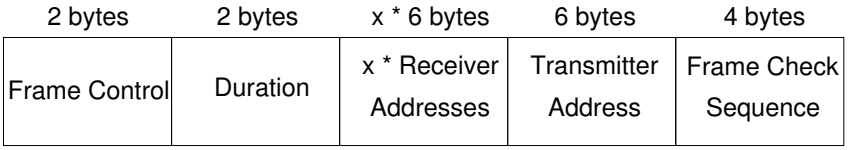

(c) G-CTS & G-ACK Frame

Figure 4.2: Adapted Frames

cols. The proposed DCF/USDMA MAC protocol extends the RTS/CTS handshaking mechanism to support simultaneous transmissions in the uplink.

The RTS/CTS mechanism is employed in the DCF/USDMA for the following reasons: Firstly, the RTS/CTS frames can be extended to include the antenna information. For example, the AP can embody the number of antennas it has so that the wireless nodes can behave accordingly. Moreover, by exchanging the control frames, the distributed wireless nodes are synchronized. Thirdly, the AP can receive or estimate the required CSI from the exchanged frames.

The adapted control frames for the DCF/USDMA are illustrated in Figure 4.2. The RTS frame keeps unchanged. The CTS is disabled and replaced by the Multi-User CTS (MU-CTS) and Group CTS (G-CTS) frames. MU-CTS is sent by the AP and acts as a response to a received

RTS, which includes the number of available spatial streams. The G-CTS and G-ACK have a common frame structure, where the receiver address field is of variable length, which depends on how many wireless nodes are involved in a simultaneous uplink transmission (x stands for the number of nodes). The G-CTS frame is utilized to inform the wireless nodes about the start of the data transmission phase while the G-ACK is used to notify the successful reception of data frames, both of which are sent by the AP.

A sounding sequence that includes some predefined Long Training Fields (LTF, known by both the transmitting and receiving sides) is added into the PHY Layer Convergence Procedure (PLCP) preamble, which is used by the AP to estimate the channel condition. Based on the estimated CSI, the AP can decode the simultaneously-transmitted uplink data frames. For example as illustrated in Figure 4.3, the AP can estimate the CSI based on the sounding sequence in the RTS sent from the 1-st node, 2-nd node and 3-rd node to decode next simultaneously-transmitted data frames.

The description of the DCF/USDMA uplink scheme is divided in two parts: successful transmission and frame collisions. Note that, the AP has N antennas and each wireless node is equipped with a single antenna. We assume that all nodes are in the transmitting range of each other. Initially the channel is assumed Busy (B) in all figures, the random back-off (BO) starts to count down after the channel is idle for a DIFS interval and is frozen as soon as the channel is detected busy.

4.2.2 Successful Transmissions

As illustrated in Figure 4.3, the 1-st node wins the channel access contention and sends a conventional RTS to the AP. Then, the AP broadcasts a MU-CTS to all wireless nodes instead of replying with a conventional CTS. Two important fields are included in the MU-CTS: 1) the address of the RTS sender, which is used to inform the 1-st node of the successful reception of its RTS, and 2) the number of available antennas, which is used to inform other nodes about how many available spatial streams are left.

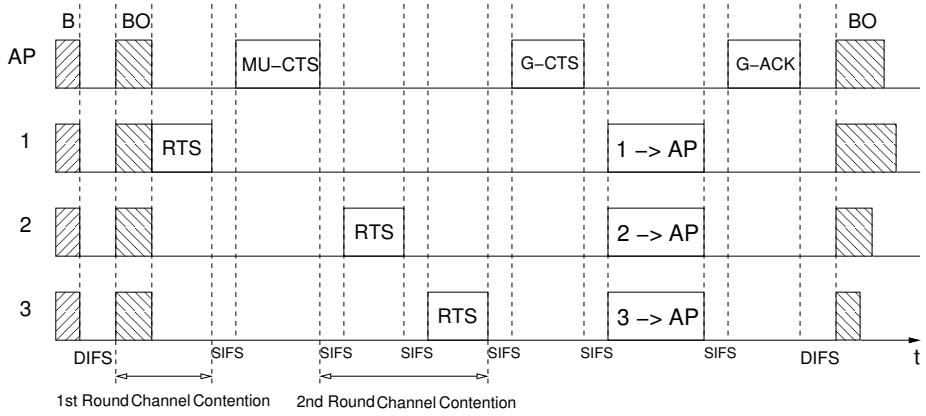

Figure 4.3: A successful transmission

The contention for the 2-nd round channel access starts immediately after the reception of the MU-CTS and is arbitrated by a new back-off instance with 2-nd round Contention Window (CW_{2nd}). For example, in a scenario where the AP has 3 antennas and CW_{2nd} equals to 2, as illustrated in Figure 4.3, 2-nd and 3-rd nodes choose a random back-off equal to 0 and 1 from CW_{2nd} respectively, which means that 2-nd and 3-rd nodes will send RTSs sequentially to bid for the available antennas in the 2-nd round channel access. After receiving the RTS from 2-nd and 3-rd nodes, the AP broadcasts the G-CTS frame to indicate the readiness for receiving multiple data frames in parallel. Note that the number of available spatial streams decreased by one each time the AP receives a RTS. The G-CTS includes the addresses of the wireless nodes who have successfully sent a RTS to the AP during the two contention rounds. Then the nodes which are listed in the G-CTS start sending data frames to the AP simultaneously. Finally the AP acknowledges the received data frames with a G-ACK frame.

It is important to point out that, in the 2-nd round channel access, the G-CTS will be sent out as soon as the number of available antennas counts to zero or the duration of 2-nd round contention elapses after waiting for CW_{2nd} slots, where CW_{2nd} is the maximum value of the 2-nd Contention

Window. The G-CTS timer is shown in Equation 4.1, which is set at the time that the MU-CTS is sent out.

$$GCTS_{timer} = CW_{2nd} \cdot (SIFS + RTS_{tx}) \tag{4.1}$$

4.2.3 Frame Collisions

Collisions occur if more than one node choose the same random back-off value (this is valid in both the 1-st and 2-nd rounds). If collisions occur in the 1-st round channel access, in order to be compatible with our previous MU-MIMO downlink implementation [13], the MU-CTS timer for receiving the expected MU-CTS is set to be Equation 4.2, where N is the number of antennas at the AP and the subscription tx represents the transmission duration of the frame. The Extended Inter Frame Space (EIFS) in DCF is modified to Equation 4.3 to obtain the same duration as the MU-CTS$_{timer}$ (Fig. 5.6, where the dashed MU-CTS means it would be there if there were no frame collisions). So after a collision, all nodes can recover and start to compete again for the channel at the same time.

$$MU\_CTS_{timer} = N \cdot (SIFS + MU\_CTS_{tx}) \tag{4.2}$$

$$MU\_EIFS = N \cdot (SIFS + MU\_CTS_{tx}) + DIFS \tag{4.3}$$

If collisions occurred in the 2-nd round channel access, those colliding nodes' addresses will not be added into the G-CTS, as illustrated in Figure 4.5.

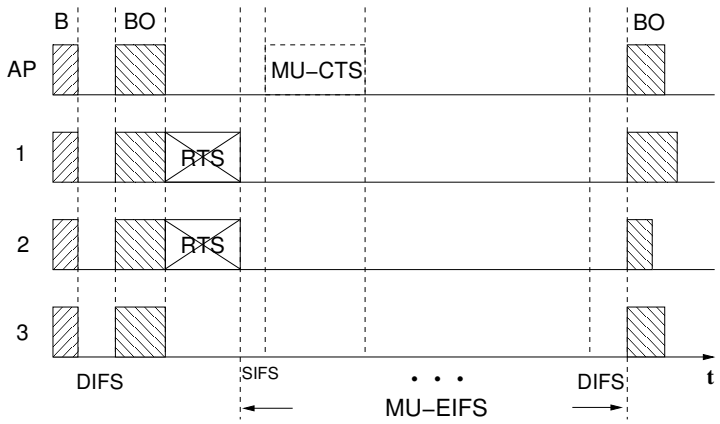

Figure 4.4: RTSs collision in the 1-st Contention Round

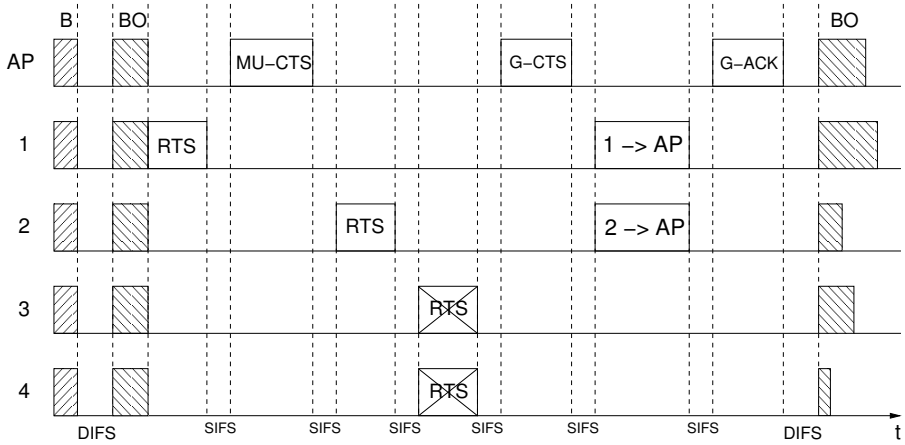

Figure 4.5: RTSs collision in the 2-nd Contention Round

4.2.4 Other Considerations

In order to avoid the collision, a random back-off value is chosen from the range $[0, CW - 1]$, where CW could be the Contention Window of the first or second round respectively. In the conventional IEEE 802.11 standard, a node will renew the random back-off value after transmitting

Table 4.1: System Parameters

Parameters	Values
Data & Basic Rate	54 & 6 Mbps
Queue Length	50 Frames
Frame Length (L)	8000 bits
PLCP Header & Preamble	40 & 96 bits
MAC Header & RTS	160 bits
MU-CTS	168 bits
G-CTS & G-ACK	$112 + 48 \cdot x$ bits
Slot Time (T_s)	9 μs
DIFS & SIFS	34 & 16 μs
CWmax & CWmin	1024 & 32
AP Antennas (N)	1, 2, or 4

to the channel. While for the other nodes that heard the transmission, the remaining back-off value will be frozen until they transmit. In this Chapter, the random back-off value for the 1-st contention round is only renewed after a collision in the 1-st round or if the node is the initiator of the two-round phase, where the node who successfully sends the first RTS is called the initiator of the two-round process. For example in Figure 4.5, although both 1-st node and 2-nd node transmit a packet, only the 1-st node is considered as the initiator. In other words, the 1-st node will pick a new random back-off value for the next 1-st round and the 2-nd node will use the remaining back-off from the previous attempt. With respect to the random back-off value for the 2-nd contention round, each node picks a new random value each time that the 2-nd round phase starts.

4.3 Performance Evaluation

The parameters considered to evaluate the proposed DCF/USDMA MAC protocol are listed in Table 4.1. The implementation and simulation are based on the COST libraries [79].

$$S_{max,N} = \frac{N \cdot L}{DIFS + 16T_s + MUCTS_{tx} + NRTS_{tx} + GCTS_{tx} + FRAME_{tx} + GACK_{tx} + (N+3)SIFS} \quad (4.4)$$

In this Chapter, the DCF/USDMA is evaluated in ideal conditions (i.e. an error-free channel and a MPT detector are assumed) to be able to focus on how it performs regardless other considerations which can distort the obtained results.

Equation 4.4 shows the maximum achievable throughput, which is used as a reference. For $N = 1$, $N = 2$ and $N = 4$ antennas, and $L = 8000$ bits, the maximum achievable throughput is $S_{max,1} = 14.61$ Mbits/s, $S_{max,2} = 22.99$ Mbits/s and $S_{max,4} = 37.28$ Mbits/s respectively. From these values, it is clear that the throughput does not grow linearly with the number of antennas, which is caused by the corresponding increase in protocol and frame overheads, although they show that notable gains on performance can be achieved by increasing the number of antennas at the AP.

4.3.1 System Performance with Saturated Traffic

Figures 4.6 and 4.7 show the system performance under saturated traffic conditions (i.e. all nodes always have a packet ready for transmissions). It is considered that the AP has $N = 4$ antennas and the traffic load of each node is 16 Mbps.

The system achieves its maximum performance when CW_{2nd} is slightly higher than the number of wireless nodes participating in the network. That is because the system obtains the best trade-off between the 2-nd round collision probability and service time (i.e., the higher CW_{2nd} means the smaller 2-nd round collision probability and the longer service time). Figure 4.6(a) shows that the throughput first increases with the CW_{2nd} until it reaches the its maximum value. After that, it starts to decrease as the larger 2-nd round duration does not compensate the lower collision probability.

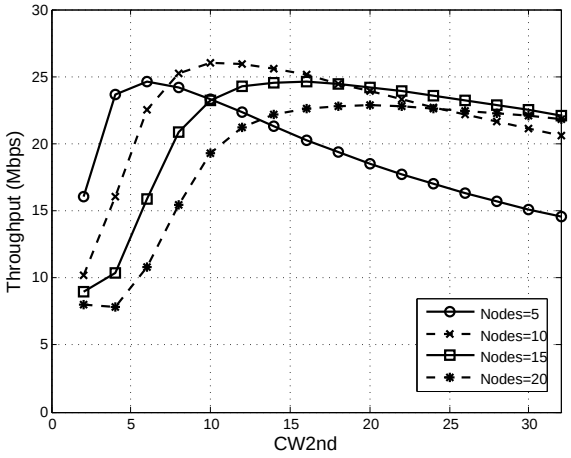

(a)

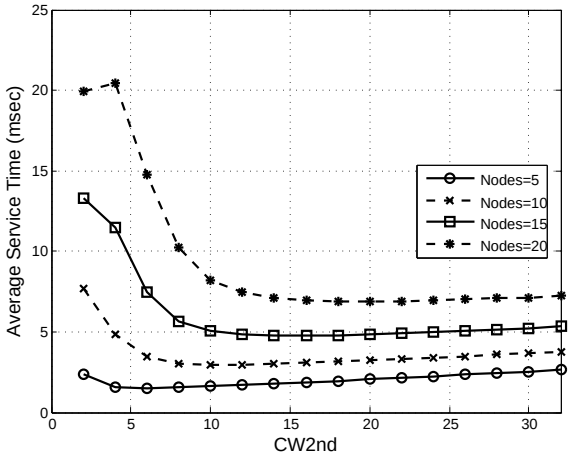

(b)

Figure 4.6: Throughput and delay with saturated wireless nodes

Another interesting point observed from Figure 4.6(a) is that the system throughput decreases when the number of wireless nodes is high,

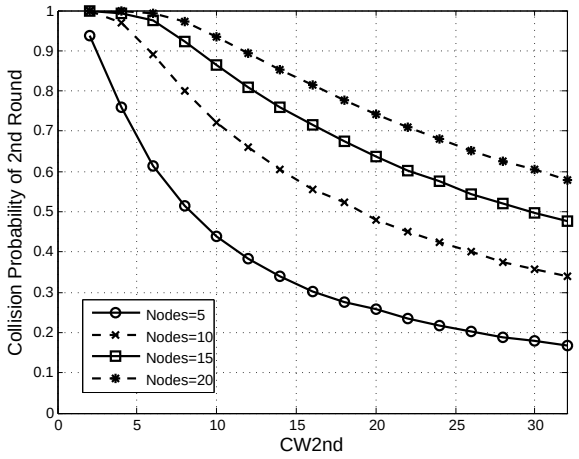

(a)

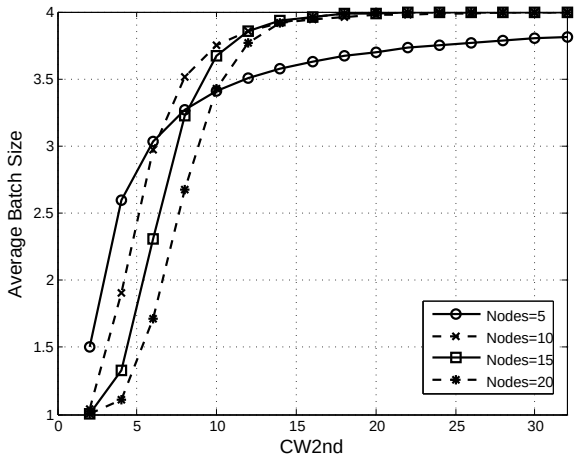

(b)

Figure 4.7: Collision probability and batch size with saturated wireless nodes

which is because the observed higher collision probability in both rounds.

Note that in saturated conditions all nodes always contend to access the channel in the first contention round, which means that the 1-st round collision probability will be constant and independent of the CW_{2nd}. In comparison, in the 2-nd round the collision probability decreases, as a larger CW_{2nd} leads to a lower 2-nd round collision probability (Figure 4.7(a)).

The average service time (Figure 4.6(b)) depends on both 1-st and 2-nd round collision probability, because collisions in the 1-st round will lead to retransmissions and collisions in the 2-nd round will result in a longer 2-nd round phase. As CW_{2nd} increases, the service time starts to decrease to a minimum value, and then slightly increases. This behavior is justified by the same reason that was given for the throughput: the continuous increase of CW_{2nd} breaks the best trade-off and the extra overheads does not compensate the reduction on the collision probability. The average batch size (the number of frames transmitted simultaneously) (Figure 4.7(b)) is straightforward. As CW_{2nd} increases, the average batch size keeps increasing until it approaches the number of antennas at the AP, which means that a higher CW_{2nd} value increases the probability to have more parallel transmissions.

4.3.2 System Performance with Different Traffic Conditions

Figures 4.8 and 4.9 show the system performance in non-saturated traffic conditions with a fixed number of nodes equal to 8, three different traffic load values for each node: 1, 2 and 3 Mbps, and two different number of antennas at the AP: 2 and 4.

Figure 4.8(a) shows the aggregate throughput for all different traffic loads and AP antennas. With a traffic load equal to 1 Mbps at each node, the network is always non-saturated, regardless the value of CW_{2nd}. For a traffic load equal to 2 Mbps, the system is only saturated when CW_{2nd} is 2 and then becomes non-saturated as CW_{2nd} increases, which is why there is no difference between using 2 and 4 antennas with both 1 and 2 Mbps traffic load. As the node's bandwidth increases to 3 Mbps, the

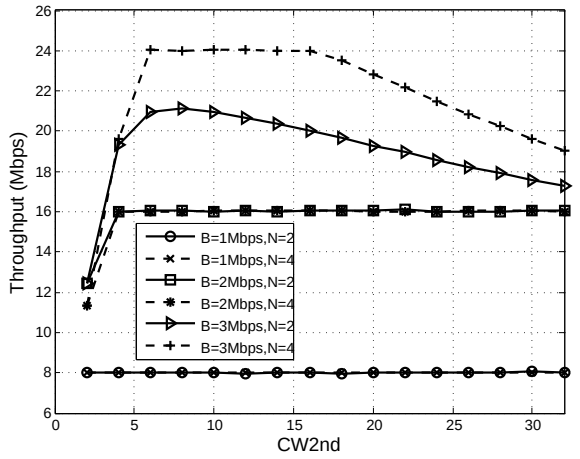

(a)

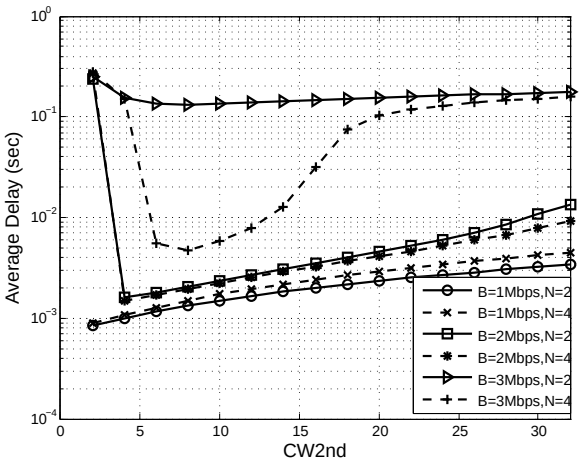

(b)

Figure 4.8: Throughput and delay with non-saturated wireless nodes

system becomes saturated except when the AP employs 4 antennas and CW_{2nd} falls on the region from 6 to 16. It is important to note that, in this

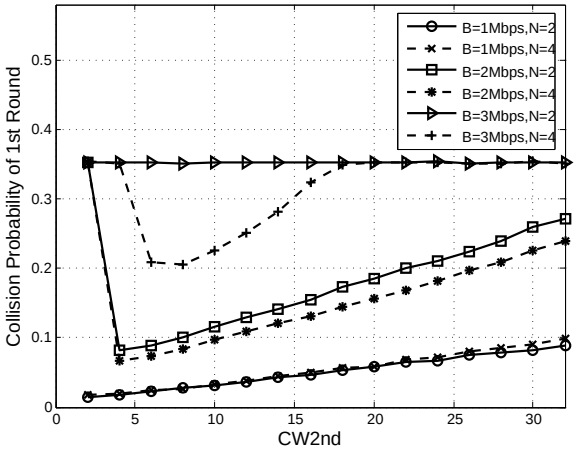

(a)

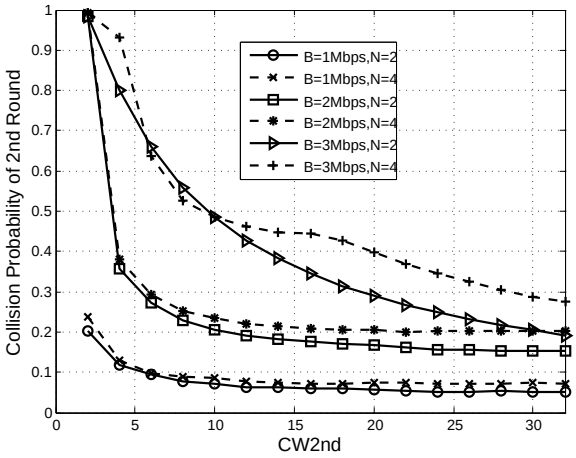

(b)

Figure 4.9: Collision probability with saturated wireless nodes

last case, the system evolves from saturation to non-saturation and again to saturation, which clearly shows the influence of the CW_{2nd} parameter

on the system performance and the importance of setting it properly.

The similar phenomenon is also observed in Figures 4.8(b), 4.9(a) and 4.9(b). In Figure 4.8(b), the average delay of node's load equal to 1 and 2 Mbps keeps increasing (except the saturated point) as CW_{2nd} increases, and shows light differences between using 2 and 4 antennas. The average delay with node's load equal to 3 Mbps keeps more or less constant when the system is saturated, while the average delay, for $N = 4$ antennas. shows a sharp drop in the region of non-saturation, which can be cross-verified in the Figures 4.9(a) and 4.9(b).

It is interesting to point out that, in contrast to what it could be expected, more antennas at the AP does not result in a lower collision probability. In Figure 4.9(a), with a load equal to 1 Mbps for $N = 2$ antennas, the 1-st round collision probability is lower than with $N = 4$ antennas. This is also observed in Figure 4.9(b) for all traffic loads, where the 2-nd round collision probability for $N = 2$ antennas is lower than for $N = 4$ antennas (except some saturated points). The reason is that, in case that more antennas are used at the AP, a longer duration of the 2-nd round increases the chances of more collisions in each transmission. For example, as illustrated in Figure 4.10, in case that the AP has 2 antennas, there are 7 nodes contending for the still-available spatial stream (one node has already obtained a spatial stream to transmit in the 1-st round channel access). Then, as soon as any one of the 7 nodes wins the 2-nd round channel contention, the 2-nd round channel access finishes and the system proceeds to the data transmission phrase. In the case that the AP has 4 antennas, the 2-nd round channel contention will continue until the available antennas count to 0 or all CW_{2nd} elapses.

4.4 Summary

It is well known that significant performance gains can be obtained by exploiting the spatial dimension using MIMO techniques. However, to effective use the spatial dimension a properly designed MAC protocol is required. In this Chapter, we have presented a novel MAC protocol,

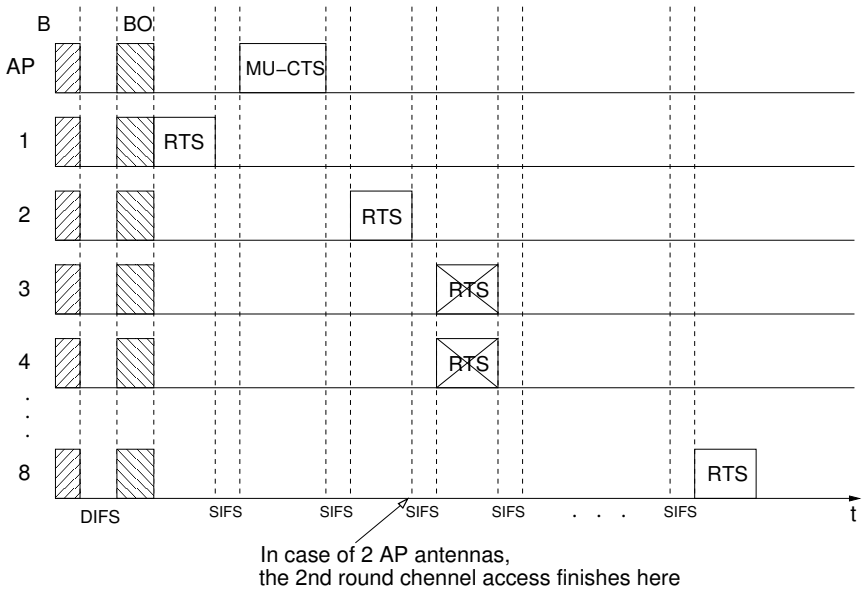

Figure 4.10: 2-nd Round Contention with 4 antennas

called DCF/USDMA, which supports simultaneous uplink transmissions in WLANs. Results show that DCF/USDMA is able to increase the performance of WLANs. In addition, the presented results provide some insights about how the different parameters that control the DCF/USDMA operation can be optimized.

Chapter 5

UNIFIED DOWN/UP-LINK MU-MIMO MAC

5.1 Introduction

The Internet traffic has shifted from web browsings and file transfers to a wide variety of applications, many of which integrate content-rich files provided by users [81, 82]. This shift, mainly driven by the bandwidth-hungry multimedia applications (e.g., the web HDTV, the video sharing and the wireless display), demands a capacity increase for both downlink and uplink in WLANs [83].

In response, we propose a unified downlink and uplink MU-MIMO MAC protocol called Uni-MUMAC to enhance the performance of IEEE 802.11ac WLANs by exploring the multi-user spatial multiplexing. Specifically, in the downlink, we implement an IEEE 802.11ac-compliant MU-MIMO transmission scheme to allow the AP to simultaneously send frames to a group of STAs [12]. In the uplink, we extend the traditional one round channel access contention to two rounds, which enable multiple STAs to transmit frames towards the AP in parallel. 2-nd round Contention Window (CW_{2nd}), a parameter that makes the length of the 2-nd contention round elastic according to the traffic condition, is introduced [13]. Uni-MUMAC is evaluated through simulations in saturated and non-saturated

conditions when both downlink and uplink traffic are present in the system. By properly setting CW_{2nd} and other parameters, a WLAN implementing Uni-MUMAC exhibits that the system not only performs well in the downlink traffic dominated scenario, but it is also able to balance both the downlink and uplink throughput in the emerging uplink bandwidth-hungry scenario.

5.2 Uni-MUMAC: the MAC Design

Uni-MUMAC is based on IEEE 802.11 Enhanced Distributed Channel Access (EDCA), which relies on the CSMA/CA mechanism to share the wireless channel. EDCA can operate in either the basic access mode or the optional RTS/CTS handshaking one. In this Chapter, Uni-MUMAC adopts and extends the RTS/CTS scheme for the following reasons: 1) The AP can notify the uplink contending STAs about the number of available antennas by using a modified control frame; 2) The AP can estimate the CSI from the RTS/CTS exchanging process; 3) The distributed STAs can be easily synchronized for simultaneous uplink transmissions from the RTS/CTS exchanging process.

5.2.1 Adapted Frame Format

The PHY frame structure of IEEE 802.11ac is shown in Figure 5.1, where VHT PLCP, PPDU and MPDU stand for Very High Throughput Physical Layer Convergence Protocol, PLCP Protocol Data Unit and MAC Protocol Data Unit respectively. As shown from the frame structure, PPDU consists of the PHY preamble and MPDUs. IEEE 802.11ac specifies that all MPDUs must be transmitted in the format of Aggregated-MPDU (A-MPDU), and aggregated MPDUs are separated by MPDU delimiters. Before being delivered to the PHY layer, a service field and a tail field are appended to the A-MPDU. The PHY preamble is formed by 3 legacy fields for the backward compatibility (i.e., L-STF, L-LTF and L-SIG) and some newly introduced VHT fields [2] [84].

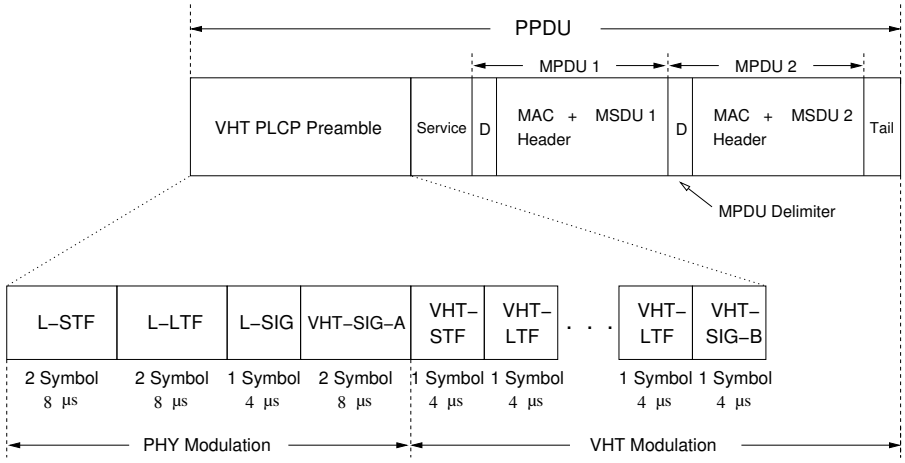

Figure 5.1: PHY frame format of IEEE 802.11ac

IEEE 802.11ac introduces these VHT fields to assist WLANs in obtaining the high performance. A Group Identifier (Group-ID) field is added in VHT Signal Field-A (VHT-SIG-A), which is used to inform the targeted STAs about the followed MU-MIMO transmission, the order and the position of each STA's corresponding stream [85]. VHT Long Training Field (VHT-LTF) can contain an orthogonal training sequence that is known by both the transmitter and the receiver to estimate the MIMO channel. The number of VHT-LTF fields should not be less than the number of transmitted spatial streams to precisely estimate the channel. The legacy and VHT-SIG-A fields adopt the low rate modulation scheme to make them understandable to all STAs, while the rest VHT fields and A-MPDU are transmitted using the VHT modulation scheme. In this Chapter, a single modulation and coding scheme (MCS), i.e., 16-QAM with $1/2$, is utilized for all frames to simplify the simulation, although the extension to various MCS for different frames and STAs is straightforward. Here, we only introduce the PHY features that are closely related to the proposed protocol. The readers please refer to [2] for details of other PHY features.

The control frames of Uni-MUMAC are shown in Figures 5.2 and

5.3. In the downlink, the control frames are MU-RTS, MU-CTS and MU-ACK. MU-RTS keeps the standard RTS frame structure, because the AP can utilize the Group-ID field of the PHY frame to notify multiple receivers. MU-CTS and MU-ACK add a transmitter address field to the original CTS and ACK frames in order to facilitate the AP to differentiate multiple responding STAs. Note that MU-CTS and MU-ACK coincidentally have the same frame structure as the standard RTS frame after adding a transmitter address field to the original CTS and ACK frames.

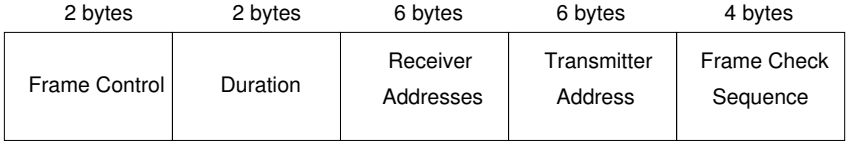

Figure 5.2: Frame structure of standard RTS

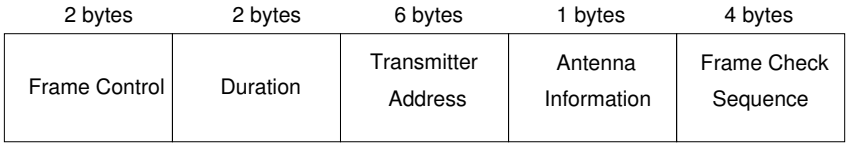

(a) Ant-CTS

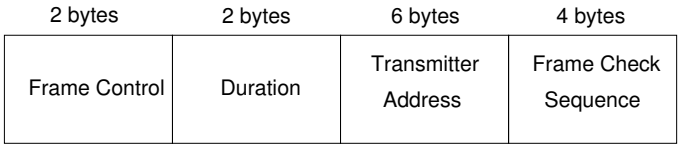

(b) G-CTS & G-ACK

Figure 5.3: Modified frames for uplink transmissions

In the uplink, all frame modifications are limited to the AP side to reduce STAs' computing consumption. These modified frames are Ant-CTS (CTS with the antenna information), G-CTS (Group CTS) and G-ACK (Group ACK), as shown in Figure 5.3. An Antenna Information

field is added to Ant-CTS, which is broadcast by the AP to announce the number of available antennas and the start of the 2-nd contention round. G-CTS and G-ACK have the identical frame structure, where the receiver address field is removed and replaced by the Group-ID field in the IEEE 802.11ac PHY frame, while a transmitter address field is added to indicate the AP address. The G-CTS frame is used to inform STAs the start of the data transmission, and G-ACK is used to indicate the successful reception of data frames.

5.2.2 Successful Downlink Transmissions

Figure 5.4 shows a successful Uni-MUMAC downlink transmission. Initially the channel is assumed busy (B). After the channel has been idle for an Arbitration Inter Frame Space (AIFS), a random back-off (BO) drawn from CW starts to count down and is frozen as soon as the channel is detected as busy.

Suppose the AP first wins the channel contention and sends a MU-RTS. Then, the STAs who are included in the Group-ID field reply with MU-CTSs sequentially as the indicated order. Those STAs who are not included in the MU-RTS will set the Network Allocation Vector (NAV) to defer their transmissions. After a MU-CTS is received, the AP will measure the channel through the training sequence included in the PHY preamble, and then uses the estimated CSI to precode the simultaneously-transmitted frames. As being precoded, the frames destined to different STAs will not interfere with each other. Finally, STAs send MU-ACKs at the same time to acknowledge the successful reception of data frames.

Note that, the uplink channel is assumed to be the same as the downlink one. In other words, the implicit CSI feedback, namely, the AP estimates the channel using the training sequence included in the MU-CTS, is adopted. The reason is that the explicit CSI feedback will need more computing capability at STAs and require an extra field with substantial volume in the MU-CTS to include the measured CSI, which may not be suitable for STAs in some capacity or power constraint scenarios.

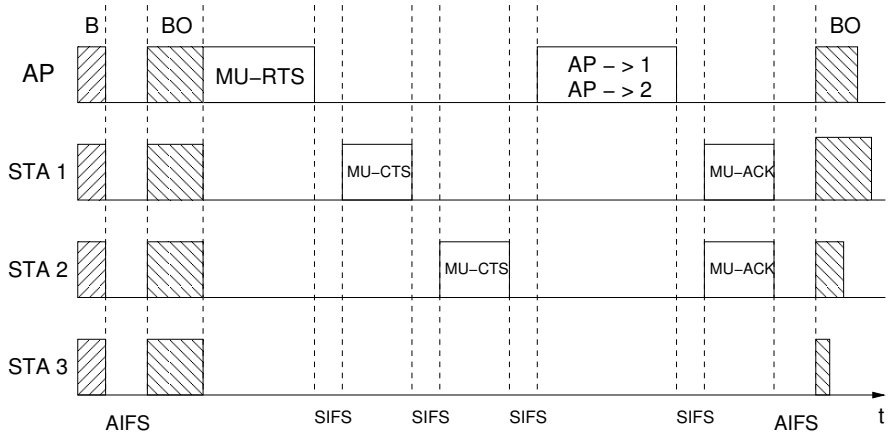

Figure 5.4: A successful Uni-MUMAC downlink transmission

5.2.3 Successful Uplink Transmissions

In the uplink, a standard RTS is sent to the AP by the STA that won the 1-st round channel contention. Instead of replying a CTS, an Ant-CTS is broadcast by the AP with two functions: 1) to notify the STA about the successful reception of the RTS, and 2) to inform other STAs that the number of available antennas and the start of the 2-nd contention round. The STAs who have frames to send will compete for the available spatial streams in the 2-nd contention round. A new random BO (BO_{2nd}) drawn from CW_{2nd} starts to count down, and a RTS will be sent if BO_{2nd} of a STA reaches 0. The number of available antennas of the AP decreases by one each time an uplink RTS is successfully received. The 2-nd contention round finishes as: 1) all available antennas of the AP are occupied or 2) a predefined duration of the 2-nd contention round elapses in case there are not enough contending STAs (the maximum duration of the 2-nd contention round is set to CW_{2nd} slots). As soon as the 2-nd contention round finishes, a G-CTS is sent by the AP to indicate the readiness for receiving multiple frames in parallel. The G-CTS frame includes the addresses of STAs who have successfully sent RTSs during both 1-st and 2-nd contention rounds. When the G-CTS is received by

the targeted STAs, they are synchronized to send data frames to the AP simultaneously. Finally, the AP acknowledges the received data frames with G-ACK.

An example of a successful uplink transmission is shown in Figure 5.5, where the AP has 3 antennas, STA 2 picks $BO_{\text{2nd}} = 0$ and STA 3 picks $BO_{\text{2nd}} = 1$ from $[0, CW_{\text{2nd}} - 1]$ respectively.

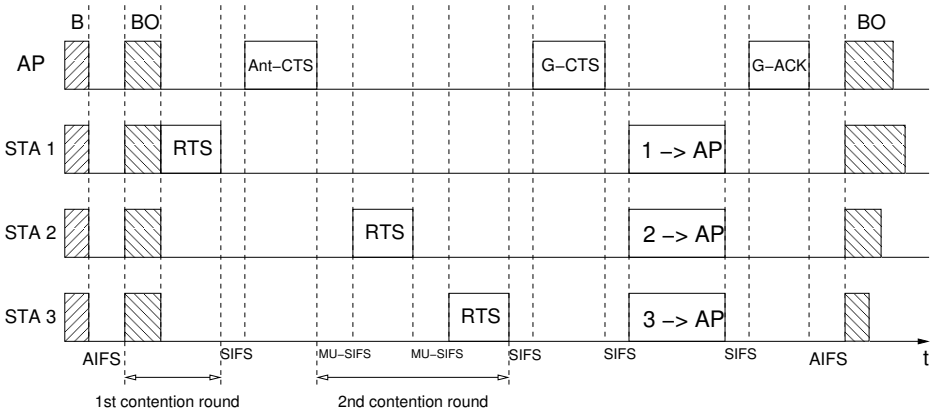

Figure 5.5: A successful Uni-MUMAC uplink transmission

It is important to point out that the RTSs sent by STAs in the 2-nd contention round could collide with G-CTS sent by the AP. For example, the RTS sent by a STA who claims the AP's last available antenna is not heard by some STAs (hidden terminals), which therefore believe that the AP still has available antennas. Then, after a SIFS interval, the G-CTS sent by the AP and RTSs sent by the hidden STAs would collide. To avoid this unexpected scenario, STAs are forced to wait for a Multi-User SIFS interval (MU-SIFS, an interval that is longer than SIFS but shorter than AIFS) in the 2-nd contention round, which gives the AP a priority to send the G-CTS.

5.2.4 Frame Collisions

Collisions will occur in both 1-st and 2-nd contention rounds if more than one STA choose the same random back-off value. On sending a RTS, EDCA specifies that the STA has to set a timer according to Equation (5.1) to receive the expected CTS, where T_{CTS} represents the transmission duration of a CTS frame. If CTS is not received before the timer expires, the STAs who previously sent RTSs assume that collisions occurred. These RTS-sending STAs will compete for the channel access after the expiration of the timer. For the RTS-receiving STAs, none of RTSs can be decoded correctly. Therefore, after the collision time, the receiving STAs will wait for an Extended Inter Frame Space (EIFS, as shown in Equation (5.2)) interval to compete for the channel access together with those RTS-sending STAs.

As shown in Figure 5.6 (Ant-CTS and MU-CTSs with dotted lines mean these frames would be transmitted if there were no collisions), collisions in the 1-st contention round include two cases: 1) collisions among STAs; 2) collisions between STAs and the AP. Since STAs can not differentiate these two cases, the collision time has to be set according to the duration of the longer frame, which is $T_{\text{MU-RTS}}$. In addition, the $\text{CTS}_{\text{timer}}$ and the EIFS interval also have to be extended according to $\text{MU-CTS}_{\text{timer}}$ (as shown in Equation (5.3), where N is the number of AP's antennas) and Multi-User EIFS (MU-EIFS, as shown in Equation (5.4)), to take the scenario that the AP is involved in collisions into account.

$$\text{CTS}_{\text{timer}} = \text{SIFS} + T_{\text{CTS}} \tag{5.1}$$

$$\text{EIFS} = \text{SIFS} + T_{\text{CTS}} + \text{AIFS} \tag{5.2}$$

$$\text{MU-CTS}_{\text{timer}} = N \cdot (\text{SIFS} + T_{\text{MU-CTS}}) \tag{5.3}$$

$$\text{MU-EIFS} = N \cdot (\text{SIFS} + T_{\text{MU-CTS}}) + \text{AIFS} \tag{5.4}$$

If collisions occur in the 2-nd contention round, the colliding STAs will not be indicated as the receivers in the Group-ID field of G-CTS. Therefore, only the STAs that have successfully sent RTSs in both contention rounds are allowed to transmit frames to the AP at the same time, as illustrated in Figure 5.7.

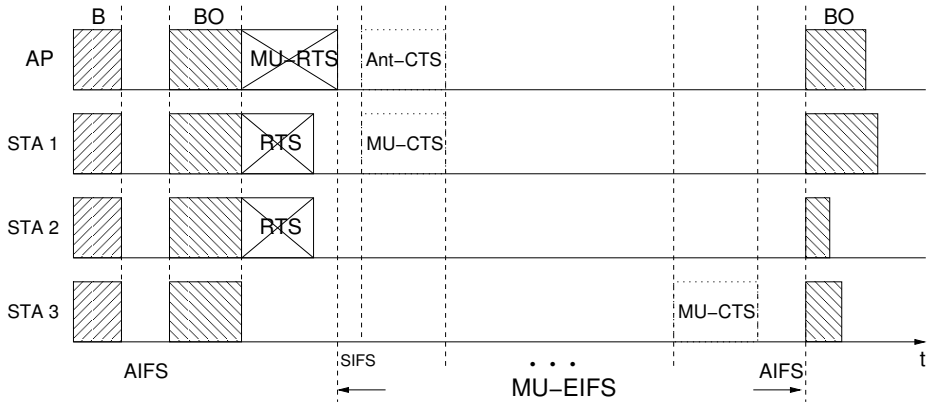

Figure 5.6: Collisions in the 1-st contention round

5.2.5 Other Considerations

In IEEE 802.11 EDCA, a STA renews its BO if the channel contention was successful. For the STAs who did not win the contention, the frozen BO is used for the next channel contention. In this Chapter, BO of the 1-st contention round is renewed after collisions in the 1-st round or if the STA is the initiator of the two-round process. Although both STA 1 and STA 2 participate in the transmission as shown in Figure 5.7, STA 1 is considered to be the initiator. In other words, STA 1 will have a new random BO in the followed 1-st contention round, while STA 2 will use the frozen BO.

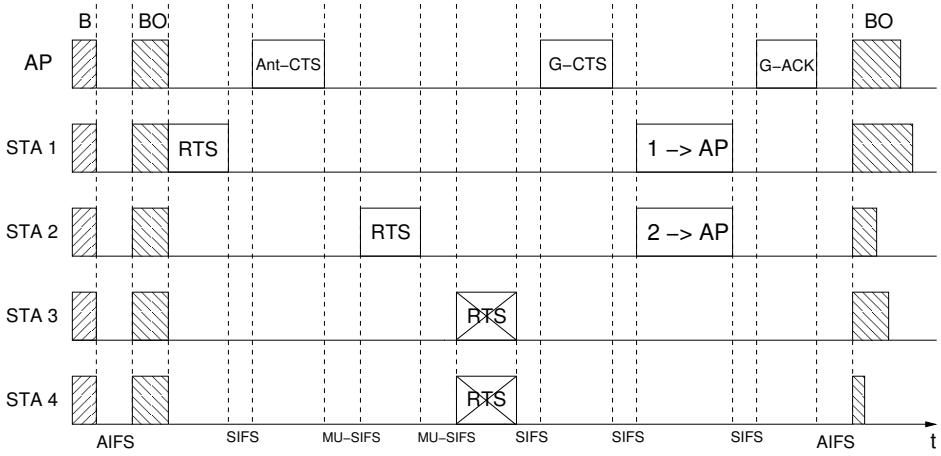

Figure 5.7: RTS collisions in the 2-nd contention round

It is more straightforward regarding BO_{2nd}. Each STA draws a fresh BO_{2nd} from CW_{2nd} as soon as a new 2-nd contention round starts.

G-CTS will be sent out by the AP depending on whether the number of available antennas reaches zero or the duration of the 2-nd contention round drains. As soon as the Ant-CTS is sent, the AP sets the G-CTS timer according to Equation (5.5).

$$\text{G-CTS}_{\text{timer}} = CW_{\text{2nd}} \cdot (\text{MU-SIFS} + T_{\text{RTS}}) \tag{5.5}$$

5.3 Performance Evaluation

Uni-MUMAC is implemented in C++ using the COST library [79] and evaluated in the SENSE simulator [86].

5.3.1 Considered Scenarios and Maximum Throughput

A single-hop WLAN implementing Uni-MUMAC is considered, as shown in Figure 5.8. It consists of one AP and M STAs with an error-

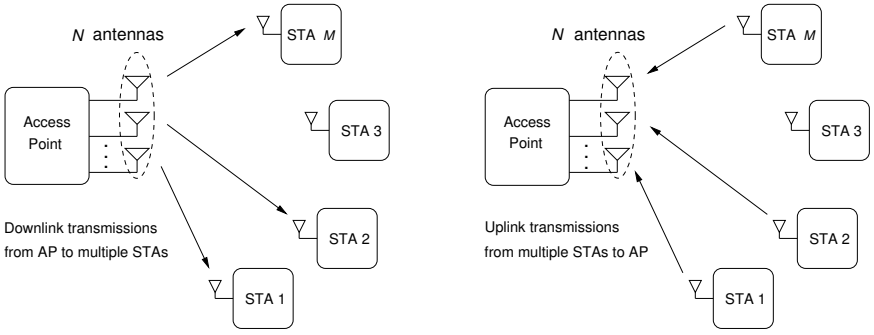

Figure 5.8: Down/Up-link Uni-MUMAC transmissions

Table 5.1: System parameters

Parameters	Values
Channel Bandwidth	40 MHz
Modulation & Coding Scheme	16-QAM with $1/2$
Guard Interval	0.8 μs
Queue Length of STA & AP	$Q_{\text{sta}} = 50$, $Q_{\text{ap}} = M^2$
Frame Length (L)	8000 bits
MAC Header (L_{MAC})	272 bits
MPDU Delimiter ($L_{\text{delimiter}}$)	32 bits
Service Bits (L_{service})	16 bits
Tail Bits (L_{tail})	6 bits
RTS/MU-RTS/MU-CTS/MU-ACK	160 bits
Ant-CTS	120 bits
G-CTS/G-ACK	112 bits
Slot Time (T_{s})	9 μs
SIFS and AIFS	16 and 34 μs
MU-SIFS	20 μs
CW	32
AP Antennas (N)	1, 2, 4

free channel. The AP employs an array of N antennas, while each STA

has only one antenna. The data frame has a fixed length of L bits. The parameters used to evaluate Uni-MUMAC are listed in Table 5.1. An example to calculate the duration of a MU-RTS frame and a data frame using these parameters is given in Equation (5.6). $T_{\text{PHY}}(N) = 36 + N \cdot 4$ μs are the duration of PHY header (the number of the VHT-LTF fields is proportional to the number of AP antennas N); L_{service}, L_{tail} and $L_{\text{delimiter}}$ are the length of the service field, the tail field and the MPDU delimiter; L_{DBPS} and T_{symbol} are the number of data bits in a symbol and the symbol duration; N_{f} is the number of aggregated frames in an A-MPDU; $L_{\text{MU-RTS}}$ and L_{MAC} are the length of MU-RTS and the MAC header respectively. More detailed calculation of the frame duration can be found in [87].

$$\begin{cases} T_{\text{MU-RTS}} = T_{\text{PHY}}(N) + \left\lceil \frac{L_{\text{service}} + L_{\text{MU-RTS}} + L_{\text{tail}}}{L_{\text{DBPS}}} \right\rceil T_{\text{symbol}} \\ T_{\text{A-MPDU}} = T_{\text{PHY}}(N) + \left\lceil \frac{L_{\text{service}} + N_{\text{f}} \cdot (L_{\text{MAC}} + L + L_{\text{delimiter}}) + L_{\text{tail}}}{L_{\text{DBPS}}} \right\rceil T_{\text{symbol}} \end{cases} \tag{5.6}$$

The theoretical maximum saturation throughput of the downlink and the uplink of Uni-MUMAC are given in Equations (5.7) and (5.8) to compare with what can be obtained from simulations. The maximum throughput is calculated by assuming: 1) no collisions in both contention rounds; 2) only one-way traffic is present; 3) the number of STAs M is always higher than the number of antennas at the AP, which enables all AP's antennas to be fully utilized. In the case of $N = 4$ and $N_{\text{f}} = 1$, the maximum downlink throughput and the uplink throughput from Equations (5.7) and (5.8) are $S_{\text{down}} = 39.6085$ Mbps and $S_{\text{up}} = 36.0053$ Mbps respectively.

$$S_{\text{down}} = \frac{N \cdot N_{\text{f}} \cdot L}{\text{AIFS} + (T_{\text{s}} \cdot CW/2) + T_{\text{MU-RTS}} + N \cdot (T_{\text{MU-CTS}} + \text{SIFS}) + T_{\text{A-MPDU}} + T_{\text{MU-ACK}} + 2 \cdot \text{SIFS}} \tag{5.7}$$

$$S_{\text{up}} = \frac{N \cdot N_{\text{f}} \cdot L}{\text{AIFS} + (T_{\text{s}} \cdot CW/2) + T_{\text{RTS}} + T_{\text{Ant-CTS}} + (N-1) \cdot (T_{\text{RTS}} + \text{MU-SIFS}) + T_{\text{G-CTS}} + T_{\text{A-MPDU}} + T_{\text{G-ACK}} + 4 \cdot \text{SIFS}} \tag{5.8}$$

5.3.2 System Performance against CW_{2nd}

In this sub-section, the performance of Uni-MUMAC is evaluated by increasing CW_{2nd}, with the goal to find a suitable CW_{2nd} that maximizes the system performance. Two traffic conditions are considered: 1) the saturated one, as shown in Figure 5.9, and 2) the non-saturated one, as shown in Figure 5.10. Note that the saturated condition refers to that both the AP and STAs always have frames to transmit. Obviously, there is no 2-nd round channel access when the AP has 1 antenna, which is why the results keep constant as $N = 1$.

When the WLAN is in the saturated condition (i.e., both downlink and uplink are saturated), the impact of increasing CW_{2nd} on the downlink throughput (AP's throughput) is very small. However, for the uplink, a clear advantage of using the higher number of antennas and the importance of choosing an appropriate CW_{2nd} are observed. For example, the uplink throughput (STAs' throughput) approaches its maximum when $CW_{\text{2nd}} \in [8, 12]$ as $M = 8$ (Figure 5.9(a)) and when $CW_{\text{2nd}} \in [12, 16]$ as $M = 15$ (Figure 5.9(b)).

In the non-saturated condition, we set the traffic load for each STA and the AP to 1.4 Mbps and 11.2 Mbps, respectively. In Figure 5.10(a), the downlink throughput when the AP has 2 and 4 antennas obtains the highest value when $CW_{\text{2nd}} \in [4, 8]$ and then decreases as CW_{2nd} keeps increasing. The reason for that is the continuous increase of CW_{2nd} leads to longer uplink transmissions that harm the downlink. Figure 5.10(b) shows that the average delay increases as CW_{2nd} increases. Note that, the average delay remains at a relatively low level when the system is in the non-saturated condition, for example, the average delay of STAs when $CW_{\text{2nd}} \in [4, 34]$ and the average delay of the AP when $N = 4$ and $CW_{\text{2nd}} \in [4, 8]$. However, the average delay of the AP (for $N = 4$) increases sharply as the downlink traffic approaches saturation.

It is also observed that the downlink throughput, as the network becomes saturated, is much lower than both the uplink one and the theoretical one. The reasons are as follows. First, the AP bottle-neck effect. It is caused because the AP manages all traffic to and from STAs in a WLAN,

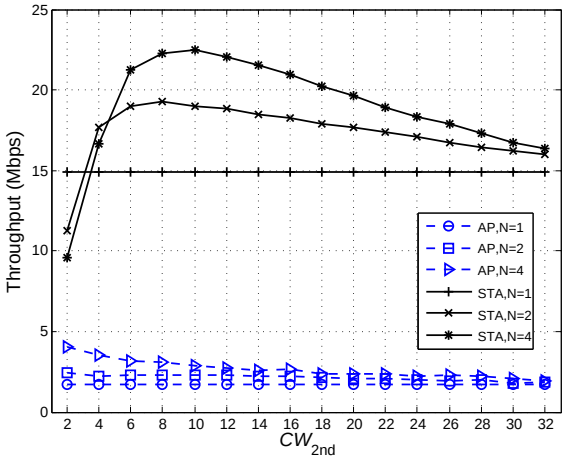

(a) $M = 8$

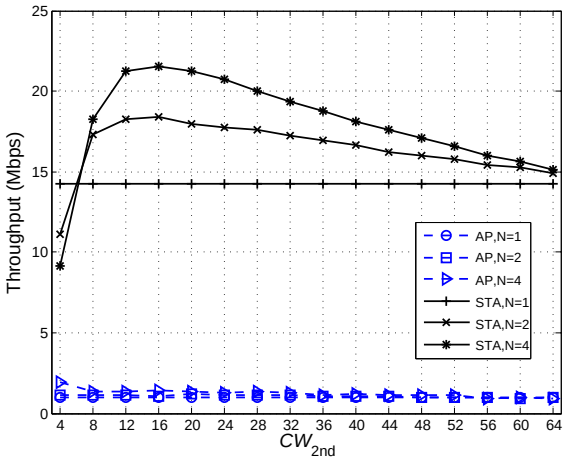

(b) $M = 15$

Figure 5.9: Saturated throughput against $CW_{2\text{nd}}$

while it has the same probability to access the channel as the STAs due to the random back-off mechanism of CSMA/CA. In addition, the inher-

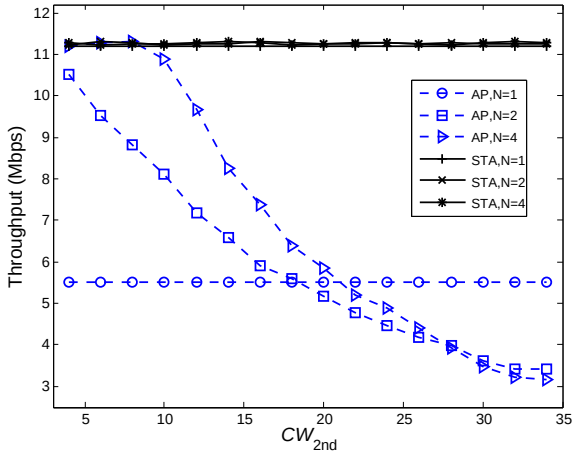

(a) $M = 8$, STA 1.4 Mbps, AP 11.2 Mbps

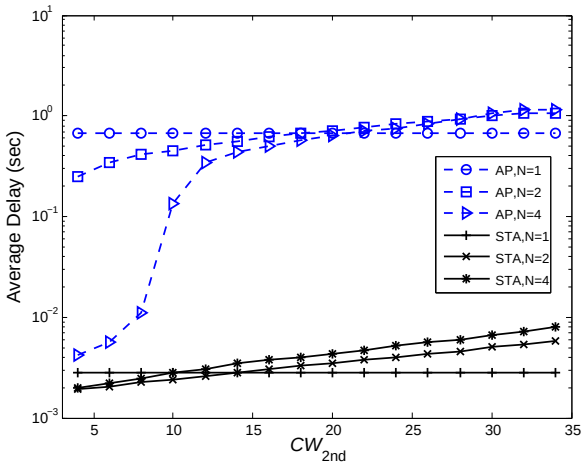

(b) $M = 8$, STA 1.4 Mbps, AP 11.2 Mbps

Figure 5.10: Non-saturated throughput & Average delay

ently high traffic load at the AP results in that the downlink is saturated most of the time. Thirdly, a favorable value of CW_{2nd} for the uplink does

not mean the same benefit to the downlink. For example, as shown in the Figure 5.9, the uplink obtains the highest throughput when CW_{2nd} is closer to the number of STAs, while the downlink transmission prefers a value of CW_{2nd} as small as possible.

In order to mitigate the AP bottle-neck effect and compensate the downlink disadvantage when STAs choose a big CW_{2nd}, we set the maximum number of frames the AP can aggregate to be the number of STAs ($N_{\text{f}} \leq M$), while keeping the number of frames aggregated by each STA to 1 in the following simulations. Also, the queue length of the AP is set to quadratically increase with the number of STAs ($Q_{\text{ap}} = M^2$) to statistically guarantee that there are enough frames destined to different STAs [87].

In Figures 5.11 and 5.12, the performance of Uni-MUMAC is evaluated in the same condition as done in Figures 5.9 and 5.10 except that the AP applies the new frame aggregation scheme (AP's $N_{\text{f}} \leq M$, STA's $N_{\text{f}} = 1$) and the new queue length ($Q_{\text{ap}} = M^2$, $Q_{\text{sta}} = 50$). The results show that Uni-MUMAC manages to avoid the extreme-low downlink throughput when the system is saturated (Figure 5.11) and keeps the downlink transmission always in the non-saturation area (Figure 5.12(a), which is not achieved in Figure 5.10(a)). The average delay of the AP (Figure 5.12(b)) is much lower compared to that of the AP in 5.10(b), which is because the system remains in the non-saturated condition by employing the frame aggregation scheme. The results from Figure 5.11 also show that the system can roughly obtain the maximum performance when $CW_{\text{2nd}} \in [M-4, M+4]$. For example, in the case that the AP has 4 antennas, the system throughput (AP+STA) reaches its maximum when $CW_{\text{2nd}} \in [6, 8]$ as $M = 8$ and $CW_{\text{2nd}} \in [12, 16]$ as $M = 15$ respectively. Therefore, the optimum value of CW_{2nd} is fixed to M in the following simulations.

5.3.3 System Performance against M

In this sub-section, the performance of Uni-MUMAC is evaluated against the number of STAs in the downlink-dominant and the down/up-

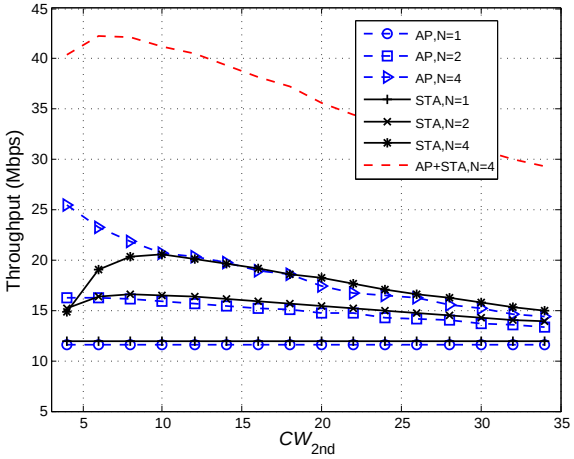

(a) $M = 8$

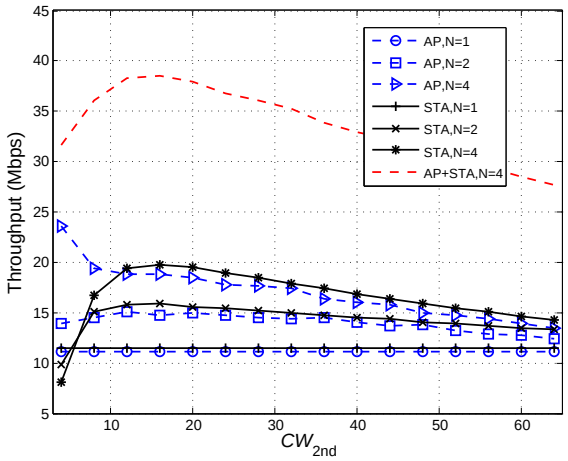

(b) $M = 15$

Figure 5.11: Saturated throughput when AP aggregates frames

link balanced traffic scenarios, where M is increased from 1 to 35, the maximum number of frames aggregated at the AP is set to M and the

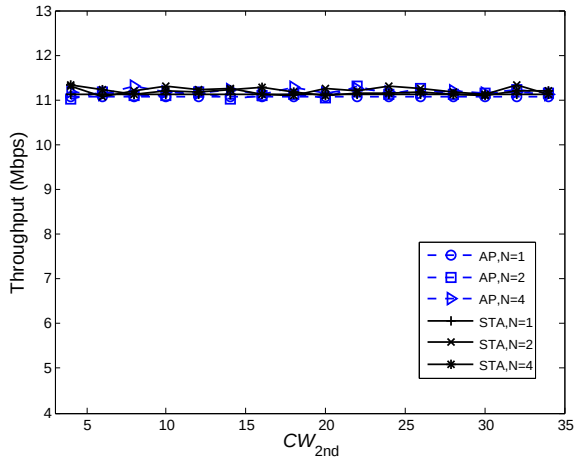

(a) $M = 8$, STA 1.4 Mbps, AP 11.2 Mbps

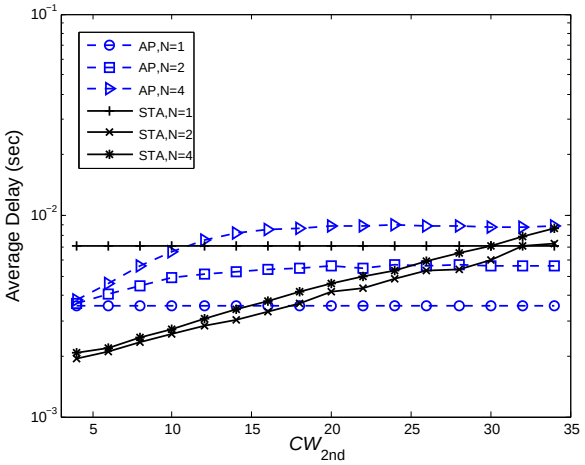

(b) $M = 8$, STA 1.4 Mbps, AP 11.2 Mbps

Figure 5.12: Non-saturated throughput & Average delay when AP aggregates frames

2-nd round Contention Window is also set to M.

1. **Downlink-dominant**: This is the traditional WLAN traffic scenario, where the AP manages a much heavier traffic load compared to that of STAs. Therefore, the traffic load of the AP is set to be 4 times higher than that of each STA. For example, in case the traffic load of a STA is 0.8 Mbps and there are 5 STAs, the traffic load of the AP will be $4 \cdot 0.8 \cdot 5 = 16$ Mbps.

2. **Down/up-link balanced**: This is one of the WLAN traffic types that not only includes P2P applications, which have already been around for some years, but also includes those emerging content-rich file sharing and video calling applications, where the traffic of downlink and uplink is balanced. Therefore, the traffic load of the AP is set to be the same as that of each STA. In this case, if there are 5 STAs, and each STA has 0.8 Mbps traffic load, the traffic load of the AP will be $0.8 \cdot 5 = 4$ Mbps.

Figure 5.13(a) shows the throughput by increasing the number of STAs M in the downlink-dominant traffic scenario. The advantage of employing a higher number of antennas at the AP is obvious. The downlink throughput is much higher than the uplink one before the system gets saturated. The reasons for that are twofold: 1) the AP traffic load is inherently higher than that of STAs, and 2) the AP adopts the frame aggregation scheme. As the system becomes saturated, the AP and all STAs always have frames ready for transmissions, therefore, the throughput of both downlink and uplink decreases as M increases.

Figure 5.13(b) shows the throughput against M in the down/up-link balanced traffic scenario. As expected, Uni-MUMAC achieves the balanced downlink and uplink throughput. This is because the AP and STAs are set to have the same traffic load, and more importantly, the frame aggregation scheme (AP's $N_{\mathrm{f}} \leq M$, STA's $N_{\mathrm{f}} = 1$) counteracts the STAs' collective advantage on the channel access.

Figure 5.14 shows the average delay against M. Both downlink and uplink delays increase with M, and grow significantly as the downlink or

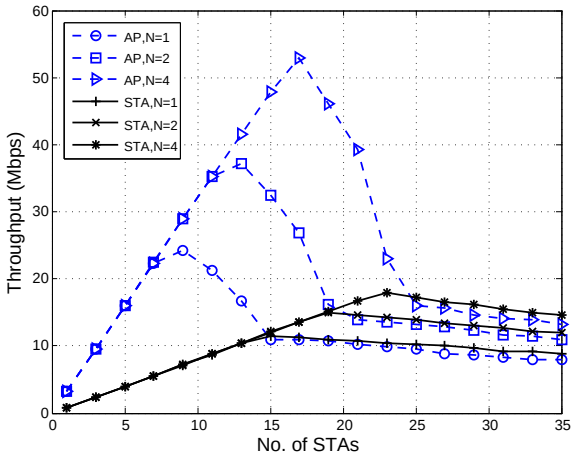

(a) Downlink-dominant: STA 0.8 Mbps, AP 3.2 Mbps

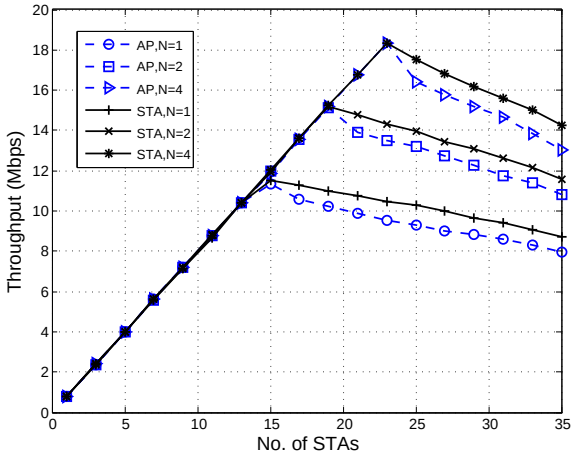

(b) P2P Scenario: STA 0.8 Mbps, AP 0.8 Mbps

Figure 5.13: Throughput against M

the uplink traffic approaches the saturation. After the system gets saturated, the average delay becomes steady. It is worth pointing out that the

average delay of STAs is higher than that of the AP when M becomes bigger. The reason for that is that the transmission duration of the AP gets longer as M increases (due to the frame aggregation scheme), which makes STAs waiting longer to access the channel.

Figure 5.15 shows that the 1-st round collision probability of the AP and STAs increases with M and converges when the system becomes saturated, which confirms the down/up-link saturation trend as discussed in Figures 5.13 and 5.14. It is interesting to note that the collision probability of STAs is higher than that of the AP when the system is non-saturated. The reason for that is a STA transmits less frequently than the AP in the non-saturated condition, which results in a lower conditional collision probability for the AP. It can be clearly explained by Equation 5.9, where p_{ap} and τ_{ap} (p_{sta} and τ_{sta}) are the 1-st round collision probability and the transmission probability of the AP (or a STA).

$$\begin{cases} p_{\text{ap}} = 1 - (1 - \tau_{\text{sta}})^{M} \\ p_{\text{sta}} = 1 - (1 - \tau_{\text{sta}})^{M-1} \cdot (1 - \tau_{\text{ap}}) \end{cases} \tag{5.9}$$

Figure 5.16 shows the 2-nd round collision probability against M. It is clear that the 2-nd round collision probability is higher when the system traffic load is higher. In the low number of STAs area, the 2-nd round collision probability when the AP has 2 antennas is sometimes lower than that when the AP has 4 antennas. The reason is that, a higher number of antennas at the AP usually means a longer duration of the 2-nd contention round, which increases the chances of collisions in the 2-nd round. For example, in a case that the AP employs 2 antennas, the 2-nd contention round finishes as soon as a STA successfully wins the still-available antenna of the AP; while in a case that the AP employs more than 2 antennas, the 2-nd contention round continues, therefore increasing the 2-nd round collision probability.

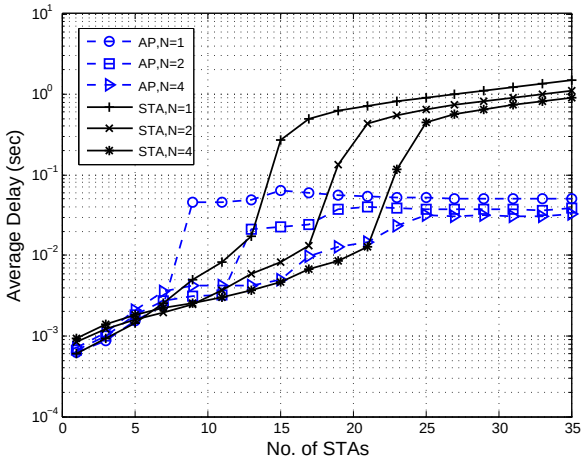

(a) Downlink-dominant: STA 0.8 Mbps, AP 3.2 Mbps

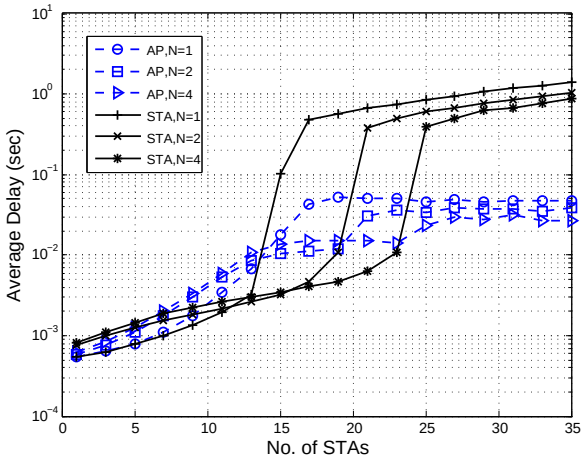

(b) P2P Scenario: STA 0.8 Mbps, AP 0.8 Mbps

Figure 5.14: Average delay against M

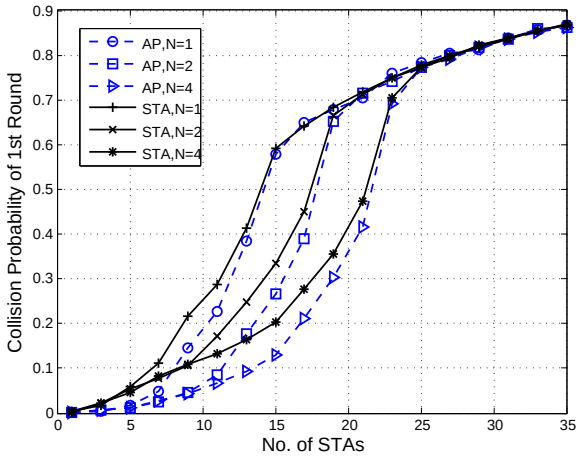

(a) Downlink-dominant: STA 0.8 Mbps, AP 3.2 Mbps

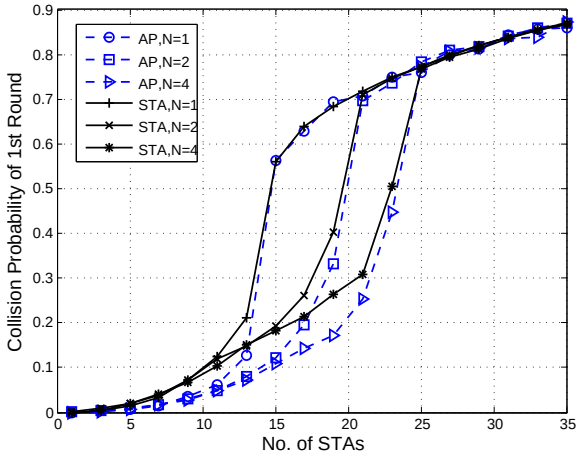

(b) P2P Scenario: STA 0.8 Mbps, AP 0.8 Mbps

Figure 5.15: 1-st round collision probability against M

5.4 Summary

In this Chapter, we propose and evaluate a unified MU-MIMO MAC

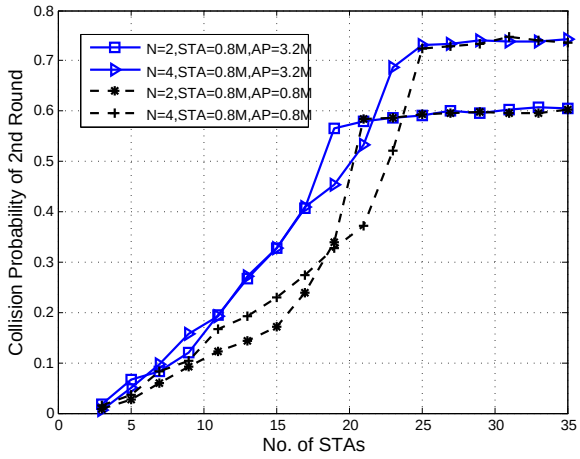

Figure 5.16: 2-nd round collision probability against M

protocol, which supports simultaneous downlink and uplink transmissions for IEEE 802.11ac WLANs. By analyzing the simulation results, we observe that the 2-nd round Contention Window CW_{2nd}, which is tuned to optimize the uplink transmission, is however not bringing the same benefit to the downlink one. An adaptive frame aggregation scheme and queue scheme are applied at the AP to offset this disadvantage. By properly setting all the parameters, the results show that a WLAN implementing Uni-MUMAC is able to avoid the AP bottle-neck problem and performs very well in both the traditional downlink-dominant and emerging down/up-link balanced traffic scenarios. The results also show that a higher system capacity can be achieved by employing more antennas at the AP.

Uni-MUMAC gives us insight about the interaction of down/up-link transmissions and how different parameters that control the system can be tuned to achieve the maximum performance. Based on the study of this Chapter, we considered the following aspects as the next steps for Uni-MUMAC.

1. **Adaptive Scheduling Scheme**: As discussed in the paper, a param-

eter that optimizes the uplink could be unfavorable to the downlink. Therefore, an adaptive scheduling algorithm that takes several key parameters into account and compensates those STAs whose interests are harmed would play a significant role on obtaining the maximum performance while maintaining the fairness. As implied from the results, these parameters include: the size of A-MPDU, the queue length, the spatial-stream/frame allocation, the number of nodes/antennas, and other key parameters that control down/uplink transmissions.

2. **Traffic Differentiation**: Another future research challenge is to provide new traffic differentiation capability in the uplink in addition to the one defined in IEEE 802.11e amendment [26]. The traffic differentiation can be used to limit the number of STAs that can participate in the 2-nd contention round to reduce 2-nd round collisions. A solution could be to create a table at the AP with information about the the priority of each traffic flow and the queue length of each STA, and then to utilize this table to control the 2-nd contention round.

3. **Multi-hop Mesh Networks**: There are more challenges that need to be considered to design MAC for operating in multi-hop wireless networks. First, the hidden-node problem. To find mechanisms that efficiently solve the collisions caused by hidden nodes is still an open challenge. A collision-free scheme [88] could be a good option in wireless mesh networks. Secondly, due to the heterogeneity of mesh nodes (e.g., different number of antennas at nodes), MAC protocols for wireless mesh networks need to be able to flexibly switch among MU-MIMO, SU-MIMO, multi-packet and single-packet transmission schemes. Thirdly, MAC and routing protocols need to be jointly designed. There could be multiple destinations involved in a MU-MIMO transmission and some destinations could be out of the one-hop transmitting range, in which case, routing strategies should be able to forward multiple packets to different nodes in parallel.

Chapter 6

EVALUATING STANDARD AND ENHANCED IEEE 802.11AC MAC IN WIRELESS MESH NETWORKS

6.1 Introduction

According to the latest IEEE 802.11ac amendment, the wireless network is about to embrace the gigabit-per-second raw data rate. Compared with previous IEEE standards, this significant performance improvement can be attributed to the novel PHY and MAC features, such as MU-MIMO transmissions, the frame aggregation and the channel bonding. In this chapter, we first briefly survey the main features of IEEE 802.11ac; and then, we evaluate these new features in a fully-connected wireless mesh network using an analytic model and simulations. More specifically, the performance of the MAC scheme defined by the IEEE 802.11ac, which employs the Explicit Compressed Feedback (ECFB) mechanism for the channel sounding, is evaluated. In addition, we propose an extended RTS/CTS scheme that integrates the ECFB operation to compare with the IEEE 802.11ac defined one in saturated conditions. The comparison

of the two MAC schemes is conducted through three spatial-stream allocation algorithms. A simple but accurate analytical model is derived for the two MAC schemes, the results of which are validated with simulations. The observations of the results not only reveal the importance of the spatial-stream allocations but also provide insight into how the newly introduced features could affect the performance of IEEE 802.11ac-based wireless mesh networks.

IEEE 802.11 [18] is the de-facto standard of the widely-deployed WLANs. Since its debut in 1997, it comes a way from megabits per second to the upcoming gigabits per second [89], which was achieved by the cable technology not long ago. The IEEE 802.11ac amendment [2] aims to provide an aggregated multi-station throughput of at least 1 gigabit per second on the 5 GHz band. This performance improvement, compared to IEEE 802.11n [19], is obtained by introducing novel PHY and MAC features, including: 1) wider channel bandwidths, 2) a higher modulation scheme, 3) downlink MU-MIMO transmissions, and 4) a compulsory frame aggregation mechanism. IEEE 802.11ac also introduces other novel features, e.g., the TXOP Sharing, while we only focus on those tightly related to this Chapter.

Some previous work has investigated the performance of IEEE 802.11ac focusing on one of the features. In [90], Redieteab et al. utilize a PHY and MAC cross-layer simulation platform to explore the impact of the training interval on the system performance. The results show that a frequent training process helps to increase the throughput in spite of the associated overhead. In [71], Cha et al. compare the performance of a downlink MU-MIMO scheme with a Space Time Block Coding (STBC) based frame aggregation scheme. The authors claim that the MU-MIMO scheme produces a higher throughput than the frame aggregation one if transmitted frames are of similar length. In [84], Ong et al. compare the MAC throughput of IEEE 802.11ac with that of IEEE 802.11n over different frame aggregation schemes. The results suggest that a hybrid scheme of Aggregated MAC Protocol Data Unit (A-MPDU) and Aggregated MAC Service Data Unit (A-MSDU) yields the best performance. In [87], Bellalta et al. present a frame aggregation scheme for

IEEE 802.11ac WLANs and evaluate its performance in non-saturated conditions. The results show that both the number of active nodes and the queueing length have significant impacts on the system performance. In [91], Nojima et al. measure the performance of an MU-MIMO WLAN system in a realistic channel, where two linear precoding schemes-Channel Inversion (CI) and Block Diagonalization (BD) are applied and compared. From the results, the authors conclude that the BD precoding scheme is more effective than the CI one.

Bianchi in [49] considers a legacy IEEE 802.11 network using DCF and derives the prominent saturation throughput analytical model for both basic access and RTS/CT) schemes. This saturation throughput analytic model is extended to support the MU-MIMO transmission and conform to the parameter configuration of IEEE 802.11ac in this Chapter. Regarding MU-MIMO transmissions in WLANs, Li et al. propose an integrated MU-MAC protocol that includes both Multi-Packet Transmission (MPT) and Multi-Packet Reception (MPR) in [64], where the perfect CSI is assumed to be obtained by the RTS/CTS training. The authors claim that the integration of MPT and MPR can obtain a significant performance improvement in terms of the number of supported nodes. Some related performance evaluation on MPT, MPR or a combination of MPT and MPR schemes for wireless networks can be found in [92] [39] [93].

In this Chapter, we capture the most important features of 802.11ac (e.g., MU-MIMO, the channel sounding interval, the number of antennas, the size of aggregated frames and the channel bandwidth) to get insight into how these parameters can affect the system performance. The considered scenario is a fully-connected wireless mesh network (fully-connected means that all nodes are directly connected), which is targeted by the IEEE 802.11ac usage models [94]. As it can be seen in Figure 6.1, mesh nodes are equipped with two interfaces: an IEEE 802.11ac one, which is used to communicate with mesh nodes, and an IEEE 802.11n one, which is used to communicate with the associated stations of each WLAN. In this Chapter, we focus on the performance analysis of the wireless mesh backhaul network, assuming that all the mesh nodes have the same number of antennas, which enables the transmission of multiple

frames to the same or different destinations.

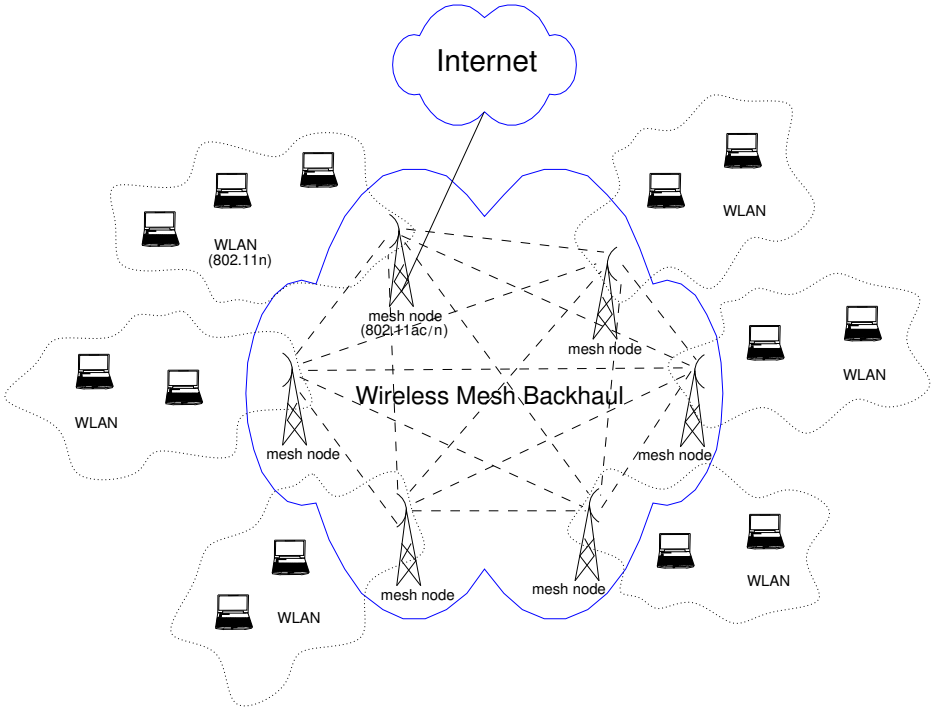

Figure 6.1: A wireless mesh backhaul network and associated WLANs

In what follows, the basic access scheme defined by IEEE 802.11ac and the extended RTS/CTS scheme proposed by us are named as MU-Basic and MU-RTS/CTS respectively.

6.2 IEEE 802.11ac

This section briefly surveys the latest amendment-IEEE 802.11ac, including the PHY layer and the MAC layer enhancements. This review does not go through every aspect of IEEE 802.11ac, but focusing on those techniques and parameters which are needed to understand how the IEEE

802.11ac based protocols work and how they could affect the system performance. A summary of IEEE 802.11ac main characteristics is shown in Table 6.1.

Table 6.1: IEEE 802.11ac Parameters

Parameters	Values
Spectrum	5 GHz
Max no. of Receiving Nodes	4
Max no. of Streams to a Node	4
Max no. of Streams to all Nodes	8
Aggregation Scheme	A-MPDU, A-MPDU of A-MSDU
Maximum A-MPDU Size	1048575 Bytes
CSI Feedback	ECFB Training Protocol (optional)
Modulation Schemes	BPSK, QPSK, 16-QAM, 64-QAM, 256-QAM (optional)
Channel Bandwidth	20, 40 and 80 MHz, 160 and 80+80 MHz (optional)
Guard Interval	0.8 μs, 0.4 μs (optional)
Forward Error Correction	Binary Convolutional Coding, Low Density Parity Check (optional)
Bandwidth Indication	CTS, RTS (optional)

6.2.1 Main Features

Wider Channel Bandwidth

Compared to the legacy standard, IEEE 802.11ac operates exclusively on the 5 GHz band, which avoids interferences from many legacy devices as well as household appliances that operate at 2.4 GHz. In addition, there are more non-overlapping channels at 5 GHz, which can be bonded together to obtain wider channels. IEEE 802.11ac adds 80 MHz and 160 MHz (optional) channels into its specification, where the 80 MHz channel

is formed by combining 2 adjacent 40 MHz channels, and the 160 MHz one is built up by combining 2 adjacent or non-adjacent 80 MHz channels [95].

Higher Modulation and Coding Scheme

64-QAM with $5/6$ coding rate is the highest Modulation and Coding Scheme (MCS) employed in IEEE 802.11n, which is extended to 256-QAM in IEEE 802.11ac. With 256-QAM, each symbol can carry 8 information bits, increasing the number of transmitted bits per hertz. However, 256-QAM requires a higher SNR at the receiving end in order to keep a low bit-error probability compared with other modulation schemes included in IEEE 802.11ac [96].

CSI Feedback for Multi-user Beamforming

IEEE 802.11ac utilizes a channel sounding protocol called Explicit Compressed Feedback (ECFB, as shown in Figure 6.2) to obtain the required CSI for Multi-user Beamforming [95] [97]. The ECFB protocol works as follows. The beamformer first sends a Null Data Packet Announcement (NDPA) to initiate the training process, which includes the addresses of the targeted nodes. After a SIFS interval, the beamformer will send a Null Data Packet (NDP), where a set of training sequences that are known by both the beamformer and the beamformees will be included into the Very High Throughput Long Training Field (VHT-LTF). The node that is identified as the first responder in the NDPA utilizes the training sequence in the NDP to estimate the channel, and compresses the measured channel information, which is then fed back in a VHT compressed beamforming frame. The volume of the CSI feedback depends on the number of antennas and sub-carriers. Other nodes who are addressed in the NDPA will respond if they are explicitly polled. With these replied VHT compressed beamforming frames, the beamformer can calculate the weight and precisely steer each beam to the targeted receiver. For the detailed structure of NDPA, NDP, VHT compressed beamforming frame and Poll, readers can refer to [2] [19].

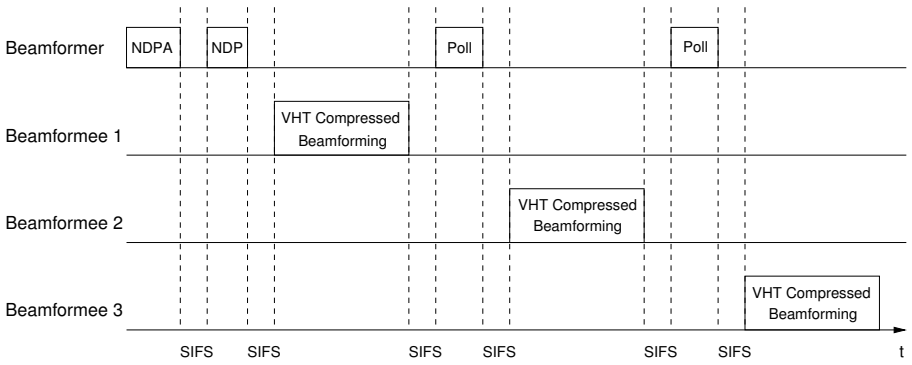

Figure 6.2: An example of ECFB of 3 Beamformees

Spatial Multiplexing

A maximum number of 4 spatial streams is defined in IEEE 802.11n for the point-to-point communication mode (Single-user MIMO). IEEE 802.11ac extends this maximum number from 4 to 8. In order to restrict the MU-MIMO transmission to a manageable scale, IEEE 802.11ac specifies the following two rules to the 8 spatial streams: 1) The maximum number of simultaneous beams directed to different nodes is 4, which means that the maximum number of simultaneous receivers of an MU-MIMO transmission is 4; 2) The maximum number of simultaneous spatial streams inside a beam towards a node is 4, which means that the maximum number of spatial streams that each receiver can have is also 4 [95] [96].

6.2.2 PHY Frame Format

Figure 6.3 shows the structure of the IEEE 802.11ac PHY frame, where PLCP and PPDU stand for Physical Layer Convergence Protocol and PLCP Protocol Data Unit respectively. A service field and a tail field are appended to the A-MPDU before being processed by the PHY layer. The PHY header starts with a preamble that includes 3 legacy fields [2]: the Legacy Short Training Field (L-STF), the Legacy Long Training Field

(L-LTF) and the Legacy Signal Field (L-SIG). L-STF and L-LTF have functions such as detecting the signal, synchronization and frequency offset estimation. L-SIG contains information about the data rate and the length of the transmitted frame. These legacy fields are kept for the backward compatibility.

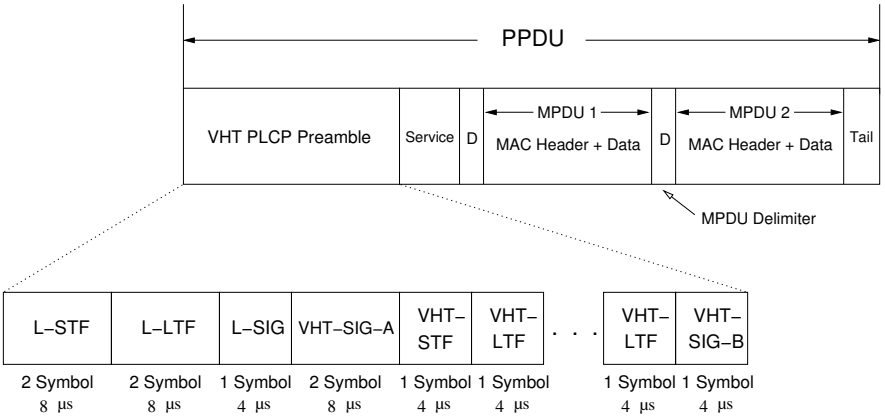

Figure 6.3: PHY Frame Format of IEEE 802.11ac

The following Very High Throughput (VHT) fields are introduced by IEEE 802.11ac to assist the novel PHY and MAC features in obtaining the required information [2] [84]. VHT-SIG-A consists of two Orthogonal Frequency Division Multiplexing (OFDM) symbols: VHT-SIG-A1 and VHT-SIG-A2, each containing 24 bits. Note that there is a Group Identifier (Group-ID) field in VHT-SIG-A1, which is utilized to notify those nodes about the following MU-MIMO transmission. VHT-STF is a short training field that is used to compute the transmission power assigned to that transmission. VHT-LTF allows a receiver to estimate the MIMO channel by containing a training sequence that is known by both the transmitting and the receiving nodes. IEEE 802.11ac supports up to 8 VHT-LTF fields, each of which contains an orthogonal training sequence. In order to precisely estimate the MIMO channel, the number of VHT-LTF fields should be equal to or higher than the number of transmitted spatial streams. The VHT-SIG-B field contains the length of data and the

MCS used for each beam.

6.2.3 MAC Enhancements

A-MPDU

IEEE 802.11n introduces the A-MSDU and the A-MPDU frame aggregation schemes to improve the MAC efficiency. MSDUs who share a common MAC header are aggregated into an A-MSDU, which is then encapsulated into an MPDU. Multiple MPDUs with different MAC headers are aggregated into an A-MPDU. In IEEE 802.11ac, the maximum size of A-MSDU and A-MPDU has been increased to 11406 and 1048575 bytes respectively, and all frames are required to be transmitted as the format of A-MPDU even if there is only one MPDU [2] [95].

Group-ID

Group-ID is a field defined in VHT-SIG-A1 to signal a group of selected receivers. More specifically, the Group-ID field is utilized by a receiving node to decide if it is targeted in the followed MU-MIMO transmission. Depending on whether a node is targeted, it will either check the User Position field (a field defined in VHT-SIG-A1) to identify the spatial streams that correspond to itself, or will not process the rest of the PPDU [2]. Although Group-ID is specified in the frame of PHY layer, it actually benefits the MAC layer. Because the control frame (e.g., RTS) or the MAC header of data frames does not need to be extended to accommodate multiple receivers' addresses.

6.2.4 Data Rate

In IEEE 802.11ac, the data rate is $R_{\text{data}} = \frac{N_{\text{DBPS}}}{T_{\text{symbol}}}$, where N_{DBPS} is the number of data bits per OFDM symbol and T_{symbol} is the symbol duration. N_{DBPS} is determined by the number of data sub-carriers (N_{dsc}) and MCS, while T_{symbol} is determined by the employed bandwidth and the Guard Interval (GI).

An example to calculate the maximum data rate of a single spatial stream is shown as follows. In a scenario where the channel bandwidth is 160 MHz and GI is 0.4 μs, there will be 468 data sub-carriers out of 512 OFDM sub-carriers; each OFDM symbol of a sub-carrier can carry up to $8 \cdot 5/6$ information bits if 256-QAM with $5/6$ coding rate is employed. The total number of data bits in a symbol, N_{DBPS}, equals $468 \cdot 8 \cdot 5/6 = 3120$ bits/symbol; the symbol duration, T_{symbol}, is equal to $512/160$ μs $+$ 0.4 μs $= 3.6$ μs; then the maximum single-stream data rate is obtained: $\frac{N_{\text{DBPS}}}{T_{\text{symbol}}} \approx 866.7$ Mbps.

6.3 Standard & Enhanced MAC Protocols for IEEE 802.11ac

In this Section, the IEEE 802.11ac defined basic access scheme (MU-Basic) and the proposed one (MU-RTS/CTS) are introduced, both of which are based on the Enhanced Distributed Channel Access (EDCA).

6.3.1 Standard MAC Scheme: MU-Basic

A node running in the MU-Basic scheme switches between two modes: the ECFB training (CSI mode) and the multi-user data transmission (data mode). The ECFB training is periodically ($T_{\text{2-CSI-Req}}$) performed by each node to obtain the required CSI from its neighbours. $T_{\text{2-CSI-Req}}$ is the interval between two CSI requests of a node. The operations of ECFB have been described in Section 6.2.1. This section focuses on the multi-user data transmission.

The MU-Basic scheme is based on EDCA, with the difference that a node who wins the channel is able to send frames to multiple receivers. After the channel has been idle for an Arbitration Inter Frame Space (AIFS), a back-off (BO) starts to count down. As soon as a node's BO first reaches zero, it simultaneously transmits multiple A-MPDUs. If all frames are successfully received, the receiving nodes will send Block ACKs (B-ACKs) sequentially. Note that a node has a unique BO no mat-

ter whether it is in the CSI mode or in the data mode, which is to say, if the node switches to the CSI mode in the middle of the data mode's BO count-down process, it will utilize the ongoing BO for the ECFB frames.

In this Chapter, the bitmap field of B-ACK is set to be a variable to account for the number of aggregated MPDUs (N_{f}) in each A-MPDU. The frame structure of B-ACK is shown in Figure 6.4.

2 bytes	2 bytes	6 bytes	6 bytes	2 bytes	2 bytes	$\lceil N_{\mathrm{f}}/8 \rceil$ bytes	4 bytes
Frame Control	Duration	Receiver Addresses	Transmitter Address	B–ACK Control	Starting Sequence Control	B–ACK Bitmap	Frame Check Sequence

Figure 6.4: Frame Structure of B-ACK

An example of a successful MU-Basic transmission is illustrated in Figure 6.5. Initially the channel is assumed Busy (B) in Figures 6.5, 6.6 and 6.8. Suppose Node 1 wins the channel contention and simultaneously transmits two A-MPDUs, one is directed to Node 2 and the other is directed to node 4. After the successful reception of the A-MPDUs, Node 2 and 4 send the B-ACK sequentially.

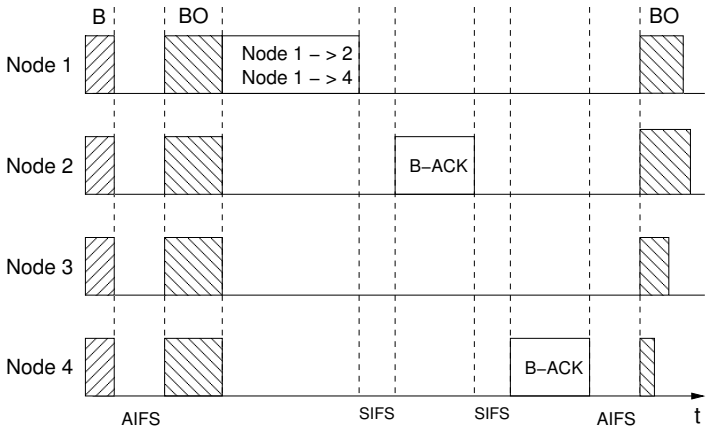

Figure 6.5: A Successful Transmission of the MU-Basic Scheme

If collisions occur, as illustrated in Figure 6.6, no frames can be re-

ceived successfully, where the dashed frames mean that these frames would be there if the transmission was successful (no collisions). ECFB-EIFS and MUBasic-EIFS represent the Extended Inter Frame Space for each case, examples of the calculation of which can be found in [12] [13].

6.3.2 Enhanced MAC Scheme: MU-RTS/CTS

The MU-RTS/CTS scheme is proposed as an alternative to the MU-Basic one, where the ECFB training protocol is integrated into the RTS and MU-CTS handshaking process. More specifically, the training sequence is included into the VHT-LTF field of the RTS control frame. The nodes who are targeted in the Group-ID field will estimate the channel and feed back the measured CSI through MU-CTSs to the RTS sender. The frame structure of MU-CTS is shown in Figure 6.7. The channel information field contains the measured CSI, which has the same size as that of the VHT compressed beamforming frame, and is equal to $M \cdot N_{\text{dsc}} \cdot 8$ bits, where M is the number of antennas of each node, N_{dsc} is the number of data sub-carriers and 8 is the number of bits required to estimate the channel gain of each data sub-carrier.

The benefits of employing the MU-RTS/CTS scheme are as follows: 1) It eliminates the need to periodically execute the ECFB protocol; 2) It reduces the collision time, because the length of RTS is much shorter than that of A-MPDU; 3) The data-sender can also obtain CSI by estimating the training sequence included in MU-CTSs, which enables it to receive B-ACKs in parallel, therefore further reducing temporal overheads.

The MU-RTS/CTS scheme works as illustrated in Figure 6.8(a). Suppose that Node 1 initiates the transmission by sending an RTS, in which the targeted nodes are mapped in the Group-ID field, and the training sequence is added in the VHT-LTF field of the PHY preamble. The targeted nodes will estimate the channel, include the measured CSI into the channel information field of MU-CTS and send it back in the same order as indicated in the Group-ID field. With these MU-CTSs that include the required CSI, Node 1 is able to create multiple beams towards the selected destinations. In order to take benefits of receiving multiple B-ACKs in

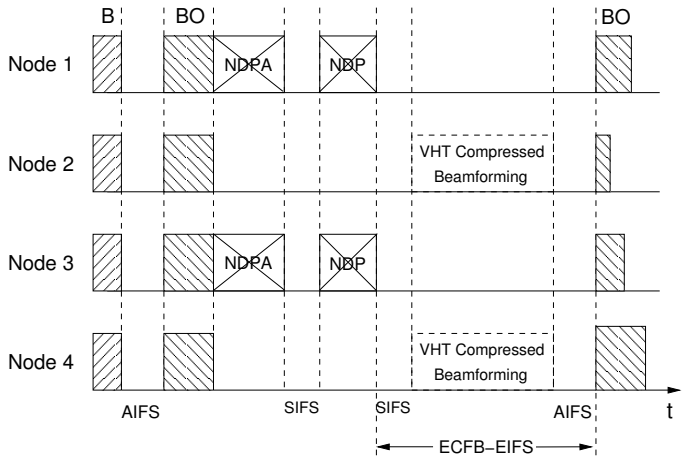

(a) Collisions between Multiple NDPAs

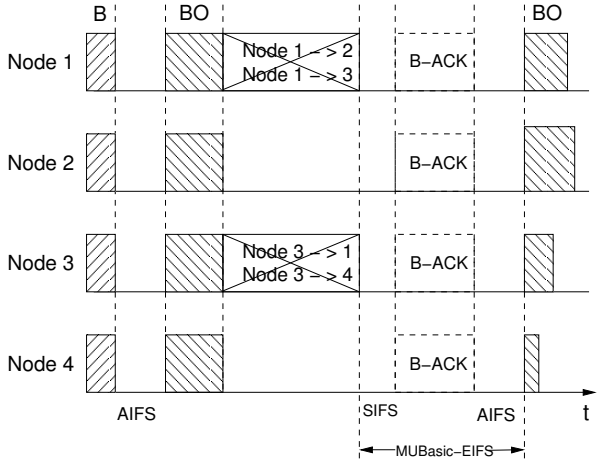

(b) Collisions between Multiple Data Frames

Figure 6.6: Collisions in the MU-Basic Scheme

parallel, Node 1 will also measure the channel from the training sequence of MU-CTS's VHT-LTF field.

If collisions happen, as shown in Figure 6.8(b), MURTS/CTS-EIFS,

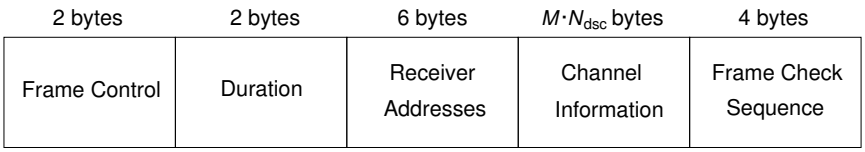

Figure 6.7: Frame Structure of MU-CTS

which is set according to the MU-CTS timer, will make all nodes recover from collisions at the same time [12] [13].

6.4 Analysitic and Simulation Results

The considered wireless mesh backhaul network is shown in Figure 6.9. There are n identical mesh nodes, each of which is equipped with M antennas. All these nodes are within the transmitting range of each other, hence forming a fully-connected mesh network. A single transmission rate is used for both control frames and the data frames. An error-free channel is considered.

All nodes are saturated and transmit fixed length frames of L bits. Frames destined to the same node are assembled into an A-MPDU, which will be assigned to a beam. Each beam contains one or more spatial streams. The A-MPDU payload is served by the spatial streams of a beam, therefore, the transmission duration of a beam with more spatial streams is shorter than that of a beam with fewer spatial streams. In order to make all beams of a transmission have the same duration, we assume that a node assigns the same number of spatial streams to different beams in each transmission.

6.4.1 Spatial-stream Allocation Algorithms

Three spatial-stream allocation schemes are designed to investigate whether it is better to employ more beams or more spatial streams in MU-MIMO transmissions. The algorithms seek the maximum product of

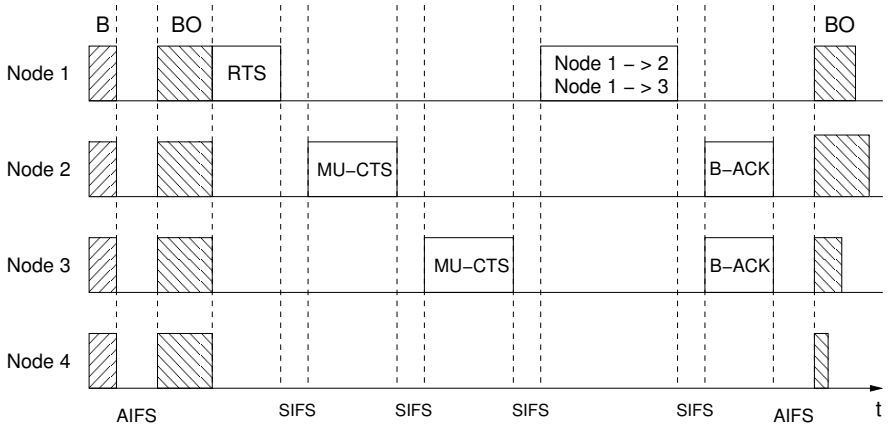

(a) A Successful Transmission of the MU-RTS/CTS Scheme

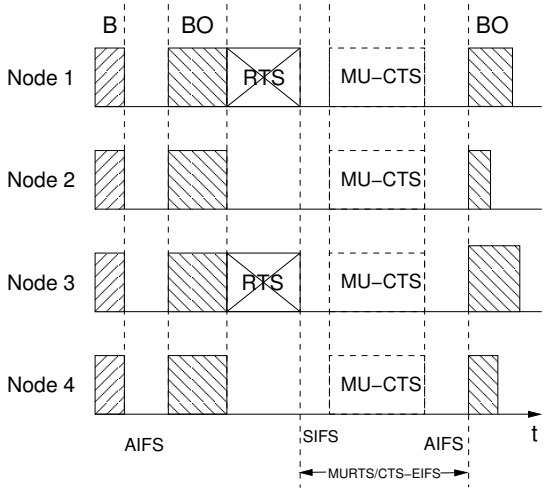

(b) Collisions between RTSs

Figure 6.8: MU-RTS/CTS Scheme

the number of beams (N_{b}) and the number of spatial streams (N_{s}), which can be formulated as Equation (6.1). $N_{\mathrm{s},i} = N_{\mathrm{s},j}$ is the constraint that all beams have to contain the same number of spatial streams, where i and j

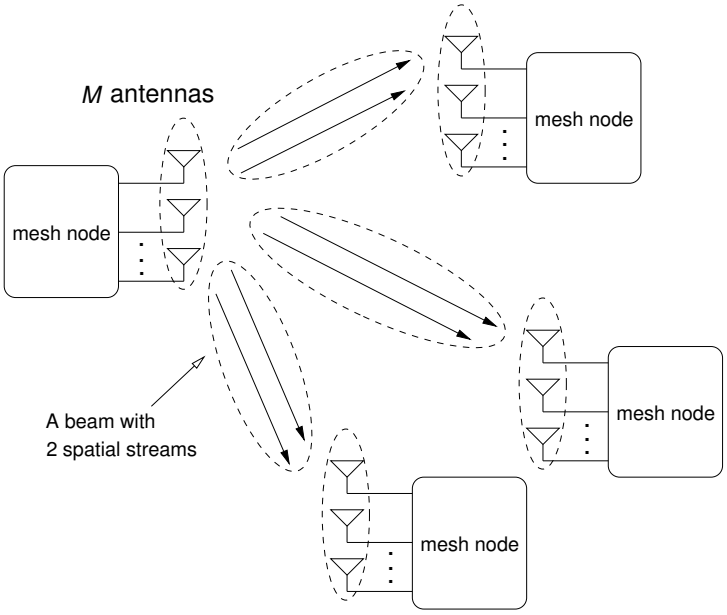

Figure 6.9: A Wireless Mesh Backhaul Network

refer to any pair of beams.

$$\begin{aligned} \text{maximize} \quad & N_{\text{b}} \cdot N_{\text{s}} \\ \text{subject to} \quad & N_{\text{b}} \leq \min(M, \min(n-1, 4)) \\ & N_{\text{s}} \leq \min(M, 4) \\ & N_{\text{b}} \cdot N_{\text{s}} \leq \min(M, 8) \\ & N_{\text{s},i} = N_{\text{s},j} \end{aligned} \tag{6.1}$$

1. **Stream-greedy algorithm**: It tries to maximize the number of spatial streams assigned to a beam, taking into account that the maximum number is 4. The duration of a transmission is reduced if more spatial streams are assigned to a beam. Therefore, nodes will be able to transmit more frequently, which is expected to improve the network performance. Note that this scheme only parallelizes

the payload of A-MPDU over the spatial streams, but not the protocol overheads, such as control frames (e.g., RTS and B-ACK) and the PHY header.

2. **Beam-greedy algorithm**: It tries to maximize the number of parallel beams, taking into account that the maximum number is 4. This scheme tries to increase the number of nodes that can simultaneously receive A-MPDUs, which makes the transmission more efficient as the PHY header is also transmitted in parallel. However, the channel will remain busy for a longer period, because the duration of each transmission is longer, thus reducing the frequency that nodes can transmit new frames.

3. **Stream-independent algorithm**: It considers each spatial stream is independent and responsible for transmitting an A-MPDU, regardless of that if A-MPDUs are destined to different nodes or to the same node. Therefore, $N_{\text{b}} \leq \min(M, \min(n-1, 4))$ reduces to $N_{\text{b}} \leq \min(M, n-1)$. This ideal scheduler aims to further extend the advantages of the *Beam-greedy* algorithm by removing the limitation on the number of beams that can be simultaneously transmitted.

An example to obtain the solution for each algorithm is as follows. In a scenario where $M = 6$ and $n = 8$, the maximum value of $N_{\text{b}} \cdot N_{\text{s}}$ is 6 according to Equation (6.1). Three solutions are therefore obtained: **Solution** 1: $N_{\text{b}} = 2$, $N_{\text{s}} = 3$; **Solution** 2: $N_{\text{b}} = 3$, $N_{\text{s}} = 2$; and **Solution** 3: $N_{\text{b}} = 6$, $N_{\text{s}} = 1$. Based on the characteristics of the scheduling algorithms, each one chooses a solution. In other words, the *Stream-greedy* one chooses **Solution** 1, the *Beam-greedy* one takes **Solution** 2, while the *Stream-independent* one goes for **Solution** 3.

6.4.2 Saturation Throughput Analysis

In order to simplify the analysis for the MU-Basic scheme, we assume that a slot is previously assigned to either the ECFB training part or the

data transmission one. Therefore, only collisions among data transmissions or collisions among NDPA frames are counted. γ is used to refer to the probability that one slot is allocated for ECFB and $1-\gamma$ to refer to the probability that one slot is allocated for data transmissions.

Regardless if the MU-Basic scheme or the MU-RTS/CTS scheme is used, nodes will start a random back-off counter to compete for the channel access if the channel has been idle for AIFS. Then, each node decreases its random back-off counter by one if the channel is detected as free; otherwise, it freezes the counter. In the latter case, the frozen counter will be reused in the next channel access contention. That is to say, in between each decrement of the back-off counter, a node could observe the channel in either an empty state (no transmission activities) or a busy state (a successful transmission or collisions). Therefore, a slot time could be a constant value σ if the channel is empty, T_{s} if there is a successful transmission or T_{c} if there are collisions.

Let the transmission probability of each node in a randomly chosen slot be τ. Then, the probability that the channel is empty, p_{e}, is given in Equation (6.2), which is the probability that no node transmits in that slot.

$$p_{\mathrm{e}} = (1-\tau)^n \tag{6.2}$$

The probability that a slot contains a successful transmission, p_{s}, is based on the fact that there are n nodes and only one single node transmits.

$$p_{\mathrm{s}} = \binom{n}{1}\tau(1-\tau)^{n-1} = n\tau(1-\tau)^{n-1} \tag{6.3}$$

Thus, the collision probability in a slot, p_{c}, is obtained as follows.

$$p_{\mathrm{c}} = 1 - p_{\mathrm{e}} - p_{\mathrm{s}} \tag{6.4}$$

The saturation throughput S, as shown in Equation (6.5), is expressed as the ratio of the frame payload successfully transmitted in a slot and the average duration of a slot, where γ is the probability that a slot is labeled as ECFB, N_{f} is the number of frames in each A-MPDU and N_{b} is the number of parallel beams towards multiple nodes. L is the length of a data frame. $T_{\text{data,s}}$ and $T_{\text{data,c}}$ represent the duration of a successful data transmission and the duration of collisions between data transmissions ($T_{\text{csi,s}}$ and $T_{\text{csi,c}}$ have the similar definition for ECFB frames). Note that Equation (6.5) can be transformed to the Bianchi's model if γ equals zero, which means the ECFB protocol is disabled or the MU-RTS/CTS scheme is in operations.

$$S = \frac{(1-\gamma)\cdot p_{\mathrm{s}}\cdot N_{\mathrm{f}}\cdot N_{\mathrm{b}}\cdot L}{\gamma\cdot(p_{\mathrm{s}}T_{\text{csi,s}}+p_{\mathrm{c}}T_{\text{csi,c}})+(1-\gamma)\cdot(p_{\mathrm{s}}T_{\text{data,s}}+p_{\mathrm{c}}T_{\text{data,c}})+p_{\mathrm{e}}\sigma} \tag{6.5}$$

τ, as given in Equation (6.6), is the sum of the probability that the back-off counter reaches zero, no matter which stage the back-off is in, where m is the maximum back-off stage.

$$\tau = \frac{2(1-2p)}{(1-2p)(CW_{\text{min}}+1)+pCW_{\text{min}}(1-(2p)^m)} \tag{6.6}$$

p is the conditional collision probability for a node that transmits a frame, and in that slot, at least one of the $n-1$ nodes is also transmitting.

$$p = 1-(1-\tau)^{n-1} \tag{6.7}$$

γ can be derived through a given $T_{\text{2-CSI-Req}}$ value as follows.

1. The total number of slots in $T_{\text{2-CSI-Req}}$ is $N_{\text{slots}} = \frac{T_{\text{2-CSI-Req}}}{E[T_{\text{slot}}]}$, where $E[T_{\text{slot}}]$ is the average slot duration (the denominator of Equation (6.5)).

2. The average number of slots in the CSI mode during $T_{\text{2-CSI-Req}}$ is $\gamma \cdot N_{\text{slots}} \cdot (p_{\text{e}} + p_{\text{c}}) + n$, where n represents the number of successful ECFB transmissions, one for each node, observed in every $T_{\text{2-CSI-Req}}$ interval.

3. Lastly, the probability of ECFB, i.e., the probability that the channel is in the CSI mode is $\gamma = \frac{\gamma \cdot N_{\text{slots}} \cdot (p_{\text{e}} + p_{\text{c}}) + n}{N_{\text{slots}}}$, which can be simplified to Equation (6.8). It shows that the probability of being in the CSI mode can be represented as the number of successful slots in the CSI mode divided by the total number of successful slots in $T_{\text{2-CSI-Req}}$.

$$\gamma = \frac{n}{p_{\text{s}} \cdot N_{\text{slots}}} \tag{6.8}$$

Equations (6.5), (6.6), (6.7) and (6.8) present a non-linear system, which can be resolved using the iterative numerical technique as used in [49] [98].

If we replace a slot duration of Equation (6.5) with corresponding item as shown in Equations (6.9) and (6.10), the saturation throughput S is valid for either the MU-Basic scheme or the MU-RTS/CTS scheme.

$$\begin{cases} T_{\text{data,c}}^{\text{MU-Basic}} = T_{\text{A-MPDU}} + \text{SIFS} + T_{\text{B-ACK}} + \text{AIFS} + \sigma \\ T_{\text{csi,c}}^{\text{MU-Basic}} = T_{\text{NDPA}} + \text{SIFS} + T_{\text{NDP}} + \text{SIFS} + T_{\text{BF-Feedback}} + \text{AIFS} + \sigma \\ T_{\text{data,c}}^{\text{MU-RTS/CTS}} = T_{\text{RTS}} + \text{SIFS} + T_{\text{MU-CTS}} + \text{AIFS} + \sigma \end{cases} \tag{6.9}$$

$$\begin{cases} T_{\text{data,s}}^{\text{MU-Basic}} = T_{\text{A-MPDU}} + N_{\text{b}} \cdot (\text{SIFS} + T_{\text{B-ACK}}) + \text{AIFS} + \sigma \\ T_{\text{csi,s}}^{\text{MU-Basic}} = T_{\text{NDPA}} + T_{\text{NDP}} + (n-1) \cdot T_{\text{BF-Feedback}} + (n-2) \cdot T_{\text{Poll}} \\ \qquad\qquad + (2n-2) \cdot \text{SIFS} + \text{AIFS} + \sigma \\ T_{\text{data,s}}^{\text{MU-RTS/CTS}} = T_{\text{RTS}} + \text{SIFS} + N_{\text{b}} \cdot (T_{\text{MU-CTS}} + \text{SIFS}) + T_{\text{A-MPDU}} \\ \qquad\qquad + \text{SIFS} + T_{\text{B-ACK}} + \text{AIFS} + \sigma \end{cases} \tag{6.10}$$

The duration of each frame transmission can be calculated as shown in Equation (6.11), where $T_{\text{VHT}}(M) = (36 + M \cdot 4)\ \mu$s are the duration of the IEEE 802.11ac PHY preamble (the number of VHT-LTF is proportional to the number of antenna M). N_{s} is the number of spatial streams in each beam; L_{service}, L_{tail} and $L_{\text{delimiter}}$ are the length of the service field, the tail field and the MPDU delimiter; L_{MAC} is a MAC header that will be added to the calculation if it is a data frame; N_{DBPS} and T_{symbol} are the number of data bits in a symbol and the symbol duration; L_{RTS}, $L_{\text{MU-CTS}}$ and $L_{\text{B-ACK}}$ are the length of RTS, MU-CTS and B-ACK respectively. The detailed calculation of the frame duration can be found in [87].

$$\begin{cases} T_{\text{A-MPDU}} = T_{\text{VHT}}(M) + \left\lceil \frac{L_{\text{service}} + N_{\text{f}} \cdot (L_{\text{MAC}} + L + L_{\text{delimiter}}) + L_{\text{tail}}}{N_{\text{s}} \cdot N_{\text{DBPS}}} \right\rceil T_{\text{symbol}} \\ T_{\text{RTS}} = T_{\text{VHT}}(M) + \left\lceil \frac{L_{\text{service}} + L_{\text{RTS}} + L_{\text{tail}}}{N_{\text{DBPS}}} \right\rceil T_{\text{symbol}} \\ T_{\text{MU-CTS}} = T_{\text{VHT}}(M) + \left\lceil \frac{L_{\text{service}} + L_{\text{MU-CTS}} + L_{\text{tail}}}{N_{\text{DBPS}}} \right\rceil T_{\text{symbol}} \\ T_{\text{B-ACK}} = T_{\text{VHT}}(M) + \left\lceil \frac{L_{\text{service}} + L_{\text{B-ACK}} + L_{\text{tail}}}{N_{\text{DBPS}}} \right\rceil T_{\text{symbol}} \end{cases} \tag{6.11}$$

6.4.3 Results

The parameters considered for the performance evaluation of MU-Basic and MU-RTS/CTS are shown in Table 6.2. A simulator has been developed in C++ using the COST library [79]. Results obtained by simulations are compared with those of the analytical model.

Figures 6.10(a) and 6.10(b) show the system throughput against the interval between 2 CSI Requests ($T_{\text{2-CSI-Req}}$). The results clearly show that the system (MU-Basic) obtains a higher throughput if CSI is less frequently updated. The throughput of the MU-RTS/CTS scheme is not affected by increasing $T_{\text{2-CSI-Req}}$, because the channel sounding process is integrated into the RTS and MU-CTS exchanges.

Note that the results of analytical model and simulations for the MU-RTS/CTS scheme match very well, while there are some gaps for the MU-Basic scheme. It is because, in the MU-Basic scheme, we leave collisions

Table 6.2: System Parameters

Parameters	Values
Channel Bandwidth	160 MHz
Modulation & Coding Scheme	256-QAM with $5/6$
Guard Interval	0.8 μs
Frame Length (L)	20000 bits
MAC Header (L_{MAC})	272 bits
MPDU Delimiter ($L_{\text{delimiter}}$)	32 bits
Service Bits (L_{service})	16 bits
Tail Bits (L_{tail})	6 bits
RTS	160 bits
MU-CTS	$112 + (M \cdot N_{\text{dsc}} \cdot 8)$ bits
B-ACK	$192 + \lceil N_{\text{f}}/8 \rceil \cdot 8$ bits
NDPA	$152 + n \cdot 16$ bits
NDP	$36 + M \cdot 4$ μs
VHT Compressed Beamforming Frame	$40 + (M \cdot N_{\text{dsc}} \cdot 8)$ bits
Poll	168 bits
Slot Time (σ)	9 μs
SIFS and AIFS	16 and 34 μs
CW_{min} and CW_{max}	16 and 1024
Maximum Back-off Stage (m)	6

between ECFB frames and data frames out of the analytical model to simplify the calculation, however, these collisions are counted in the simulation to resemble the real scenario. Therefore, the analytical results of MU-Basic are slightly more optimistic than those of simulations. It is also observed that the results (the analytical and simulations) of the Stream-greedy algorithm match better than the other two algorithms, which is because the channel sees a lower percentage of γ if the Stream-greedy algorithm is running (the more streams the shorter data transmission duration, and the more data slots in $T_{\text{2-CSI-Req}}$), therefore reducing the impact of the assumption of the analytical model compared to the other two algorithms.

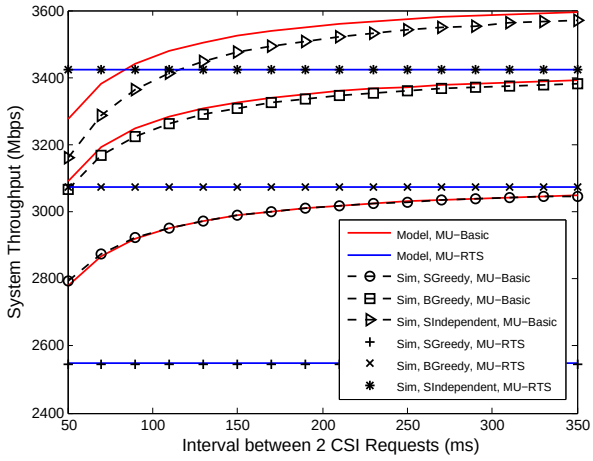

(a) $n = 5$

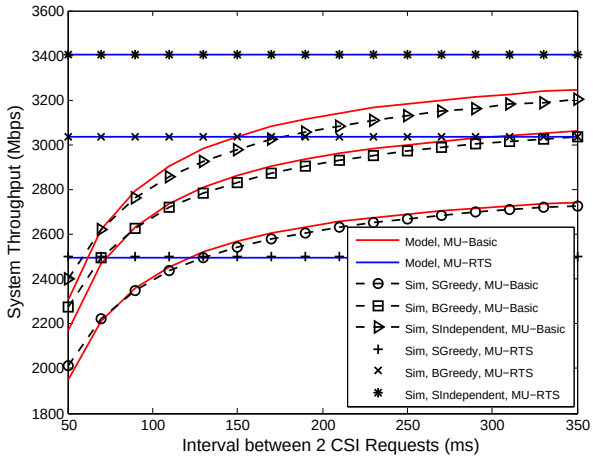

(b) $n = 10$

Figure 6.10: Throughput against $T_{\text{2-CSI-Req}}$

As shown in Figure 6.10, the system throughput of MU-Basic increases as the CSI updates less frequently (lower γ). In a slow mobility

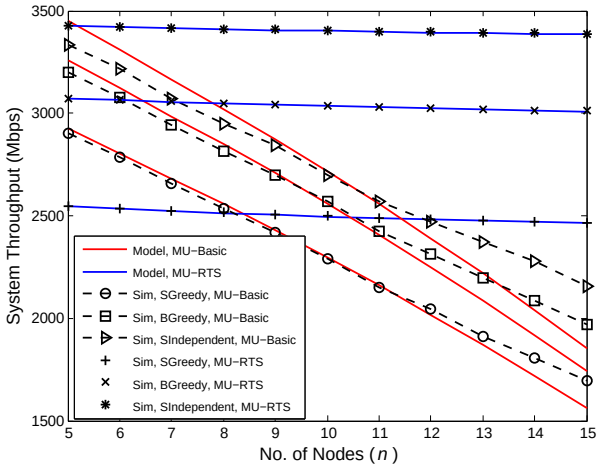

Figure 6.11: Throughput against n

scenario (the maximum Doppler shift is 12 Hz), the coherence time of a 5 GHz channel is in the range of 50 ms to 80 ms [99] [100]. Therefore, we set $T_{\text{2-CSI-Req}}$ to 80 ms in the following simulations.

Figure 6.11 shows the throughput against the number of nodes, where $N_{\text{f}} = 64$, $M = 8$ and $T_{\text{2-CSI-Req}} = 80$ ms. The results show that the Beam-greedy scheme outperforms the Stream-greedy one, although the ideal Stream-independent scheme performs the best. The throughput of all schemes decreases as the number of nodes increases. However, the decreasing rate of the MU-Basic scheme is higher than that of the MU-RTS/CTS one. The reason is that, collisions occur more frequently as the number of nodes increases, however, the collision time of the MU-RTS/CTS scheme is less than that of the MU-Basic scheme, as RTS is much shorter than the data frame in length.

The other hint from Figure 6.11 is that the size of the IEEE 802.11ac wireless mesh network could be heavily limited if the MU-Basic scheme is adopted due to the CSI overhead.

Figure 6.12 shows the throughput against M, where $N_{\text{f}} = 64$, $T_{\text{2-CSI-Req}}$

$= 80$ ms and $n = 5$ and 10. The throughput of the Stream-independent scheme always increases with M and outperforms the other schemes. It is because the Stream-independent scheme not only transmits data in parallel, but also transmits overheads concurrently. The system throughput of Stream-greedy and Beam-greedy increases in the following ranges: $M = 2$ to $M = 4$, $M = 5$ to $M = 6$, and $M = 7$ to $M = 8$. This is due to the increase of N_{s} and N_{b}, which either decreases the transmission duration or increases the number of simultaneously transmitted A-MPDUs. The system throughput of Stream-greedy and Beam-greedy slightly decreases in the ranges of $M = 4$ to $M = 5$ and $M = 6$ to $M = 7$, which is because N_{s} and N_{b} do not increase there, while the CSI overhead increases proportionally to M.

Figure 6.13 shows the throughput against N_{f}, where $M = 8$, $T_{\text{2-CSI-Req}}$ $= 80$ ms and $n = 5$ and 10. It clearly shows that the system throughput increases as N_{f} becomes larger. At the points where N_{f} is large, the performance of the MU-RTS/CTS scheme exceeds that of the MU-Basic one, which is because the RTS and MU-CTS exchanging process is more effective in case of collisions, given that the extra overheads of MU-RTS/CTS are compensated by the shorter collision duration.

Figure 6.14 shows the throughput against the channel bandwidth, where $M = 8$, $T_{\text{2-CSI-Req}} = 80$ ms, $N_{\mathrm{f}} = 64$, $n = 5$ and 10. It shows that the system throughput increases if a wider channel bandwidth is used, however, the increase is not linear with the channel bandwidth. It is due to the increase of CSI overheads (i.e., the size of the CSI feedback increases with the channel bandwidth), as well as the constant PHY header duration (as described in Section 6.2.2). An effective way to compensate the growth of overheads is to increase N_{f} together with the bandwidth, which reveals that the system parameters have to be jointly considered to maximize the system performance.

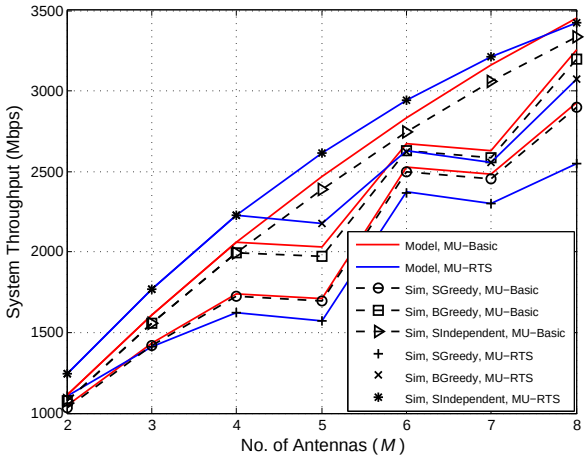

(a) $n = 5$

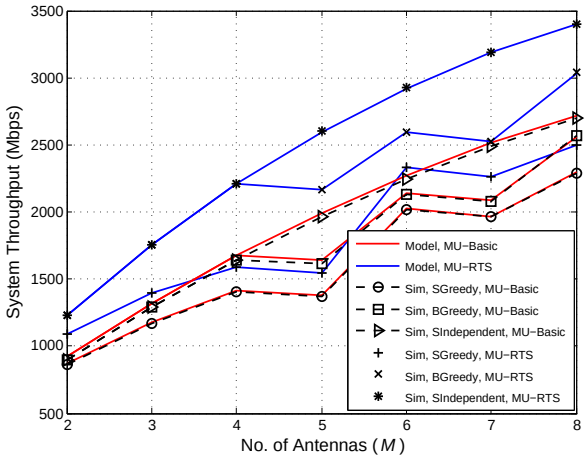

(b) $n = 10$

Figure 6.12: Throughput against M

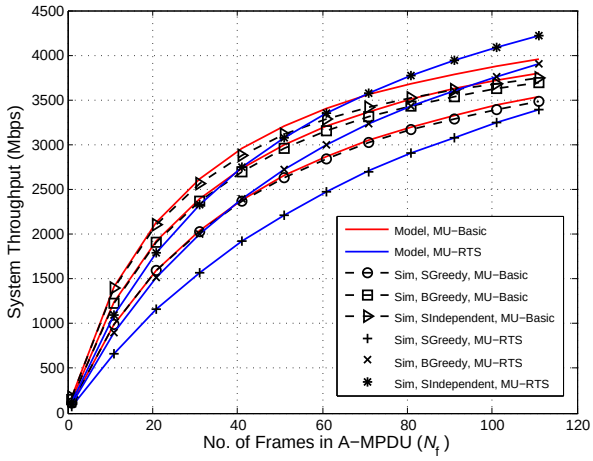

(a) $n = 5$

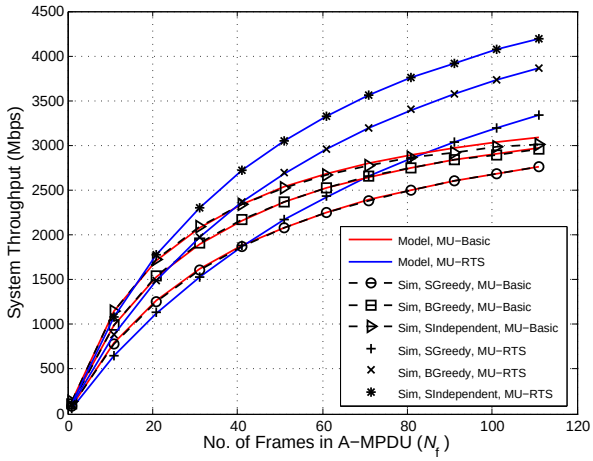

(b) $n = 10$

Figure 6.13: Throughput against N_{f}

6.5 Summary

In this Chapter, a simple but accurate analytical model is presented for IEEE 802.11ac wireless mesh backhaul networks in saturated conditions.

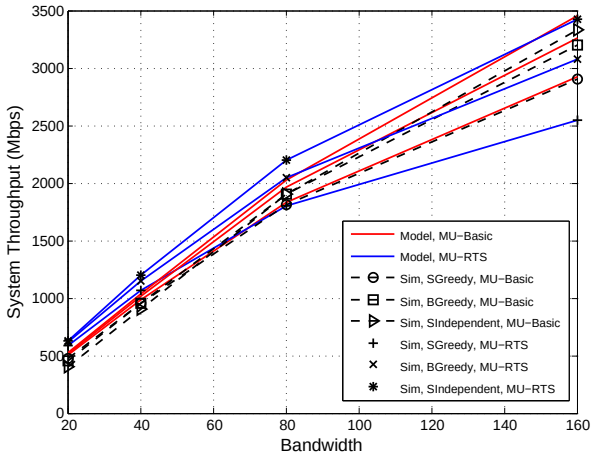

(a) $n = 5$

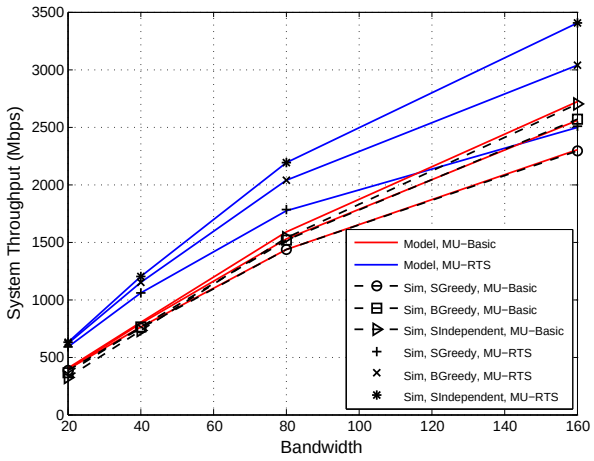

(b) $n = 10$

Figure 6.14: Throughput against Bandwidth

The IEEE 802.11ac defined basic access scheme (MU-Basic) and proposed MU-RTS/CTS scheme are evaluated and compared through three

spatial-stream allocation algorithms by the analytical model and simulations. The results show that MU-RTS/CTS is more efficient than MU-Basic as the number of nodes and the size of A-MPDU increase. Regarding the spatial-stream allocation algorithms, the Beam-greedy algorithm outperforms the Stream-greedy one, but the ideal Stream-independent algorithm is the one that provides the best performance.

From the presented results, it is clear that the novel PHY and MAC features introduced by IEEE 802.11ac, such as the downlink MU-MIMO, the frame aggregation and the channel bonding, are able to provide significant performance gains. However, the results also point out the importance of the spatial-stream allocation algorithm and the high overheads introduced by the CSI acquisition procedure. The wireless mesh network may not work well in some scenarios where the number of nodes is high and CSI is updated frequently if MU-MIMO transmissions are considered.

Based on the work of this Chapter, the following two points that can be considered in the future work:

1. **Multi Packet Reception (MPR)**: In this Chapter, we proposed an MU-RTS/CTS scheme that allows a node to simultaneously transmit frames to multiple nodes. However, MPR (i.e., simultaneous transmissions from multiple nodes to one node), which is able to reduce the collision probability and therefore improve the system performance, has not been considered. Normally, MPR requires the synchronization among distributed nodes, which makes the MU-RTS/CTS handshaking process a better candidate than the MU-Basic one to be extended to support MPR.

2. **Non-saturated Conditions**: In non-saturated conditions, the ECFB channel sounding policy should be redesigned to reduce overheads. An easiest option is to make the on-demand CSI request to some specified nodes only when the transmitter has frames directed to them; while a more complex option can be that a node caches the obtained CSI for a predefined time, and only requests the CSI updates if it has frames to send and the cached CSI is outdated.

Chapter 7

MODELLING AND ENHANCING FULL-DUPLEX MAC

7.1 Introduction

Traditional wireless systems are not able to transmit and receive frames using the same frequency simultaneously. The reason of that is the strong signal presented at the receiving antenna from the same node's transmitting end, i.e., the self interference. Recent advances in the antenna design and the analog/digital interference cancellation [6–9] have lifted this limitation, and pave the way for full-duplex (FD) transmissions in wireless networks.

The adoption of FD transmissions will positively impact the IEEE 802.11 standard on improving its current performance. However, it is inevitable to introduce modifications to DCF based MAC protocols to take full benefits of FD transmissions. In order to avoid collisions, the authors in [101] restrict only the receiver of a successful transmission to activate the FD mode. A history based list of interfering nodes is also proposed by the authors to select less-interfered nodes. In order to be compatible with legacy nodes, [102] specifies that only symmetric FD transmissions are

allowed, and all nodes will wait for EIFS instead of DIFS after a successful FD transmission. [103] recommends the use of a new FD header with a shared random field among pairs of FD nodes to reduce collisions. [104] introduces a new two-bit notification field to indicate the node's willingness for FD transmissions, and [105] proposes pseudo-random noise sequences to enable multi-mode operations, e.g., symmetric, asymmetric and uni-directional FD transmissions. The above-mentioned works have evaluated their proposals in testbeds or/and simulations, but no analytic model for FD transmissions has been presented. This Chapter analytically investigates FD transmissions by taking MAC operations and overheads into account. An enhanced FD MAC (FD+) that can convert the under-utilized FD transmission scenarios to the preferred symmetric one is proposed to further improve the transmission efficiency. Using IEEE 802.11 DCF as a reference, analytic and simulation results of FD and FD+ are compared and discussed.

7.2 Full-duplex Transmission Scenarios and MAC Schemes

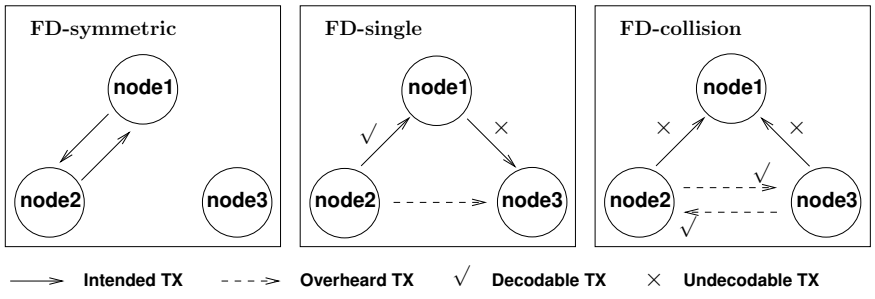

Figure 7.1: Scenarios of FD two-node transmissions

7.2.1 Considered FD & FD+ MAC Scenarios

The considered wireless network consists of n nodes, each of which is equipped with one single antenna.

IEEE 802.11 DCF deals with a single-node transmission as a successful attempt, and more-than-one-node transmissions as collisions, respectively. Thanks to the FD capability, two-node simultaneous transmissions that are traditionally considered as collisions now become feasible. Therefore, we expand nodes' transmission to three scenarios, namely, single-node, two-node and more-than-two-node. This section only focuses on two-node simultaneous transmissions, as the single-node or more-than-two-node transmissions are dealt with the same mechanism as done in the baseline DCF, and readers' familiarity with DCF is assumed.

Depending on nodes' targeting addresses, two-node simultaneous transmissions have three sub-scenarios: FD-symmetric, FD-single and FD-collision (Figure 7.1). Among them, FD-symmetric is the most desired one due to its high spectrum efficiency. However, it only occurs when two nodes start to transmit at the same time, and they are targeting at each other.

FD-single occurs when one node targets a second node, and this "second node" targets one of the rest nodes in the network. The difference between the single-node and the FD-single transmissions is that FD-single is a sub-scenario of two-node simultaneous transmissions, where only one node's transmission succeeded. For example, node2 transmits to node1, and node1 transmits to node3, in which case, the transmission from node2 to node1 is successful, while the transmission from node1 to node3 is undecodable due to node2's interference. The MAC operation of FD-single is shown at the fore part of Figure 7.2(a).

FD-collision occurs when two nodes transmit at the same time, while neither of them targets the other node. Although the frames are bound for some other nodes in the network, the two transmitting nodes can decode the frames from overheard transmissions. The MAC operation of FD-collision is shown at the rear part of Figure 7.2(a).

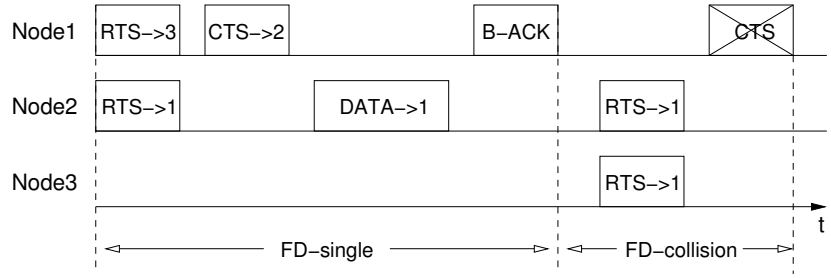

(a) FD MAC

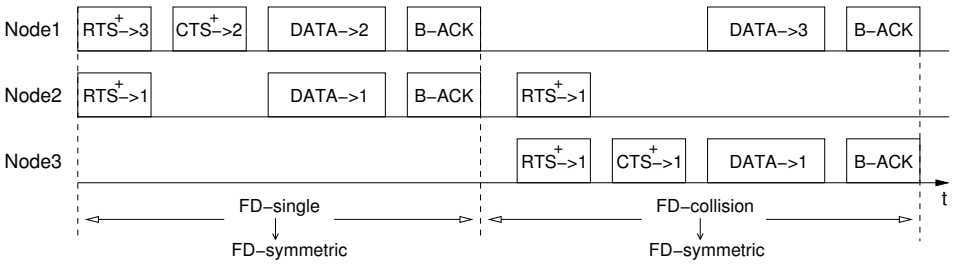

(b) FD+ MAC

Figure 7.2: FD & FD+ MAC Operations

7.2.2 Enhanced FD MAC Operations

As discussed in the above section, FD-symmetric, FD-single and FD-collision achieve paired, partial and zero data receptions, respectively. Unfortunately, the probability of FD-symmetric is fairly low in comparison to other scenarios, which makes the FD capability significantly underutilized (the compound probability of FD-symmetric, FD-single and FD-collision is $1 : 2(n-2) : (n-2)^2$, as shown in Figure 7.3).

FD+ is proposed to convert the single-node, FD-single and FD-collision transmitting scenarios to the preferred FD-symmetric one to increase the transmission efficiency. The RTS/CTS exchanging process is employed in FD+ to facilitate the conversion. RTS+, an extended version of RTS, introduces an octal field that generates a random number when RTS+ is sent. This random number is used together with the node's MAC address

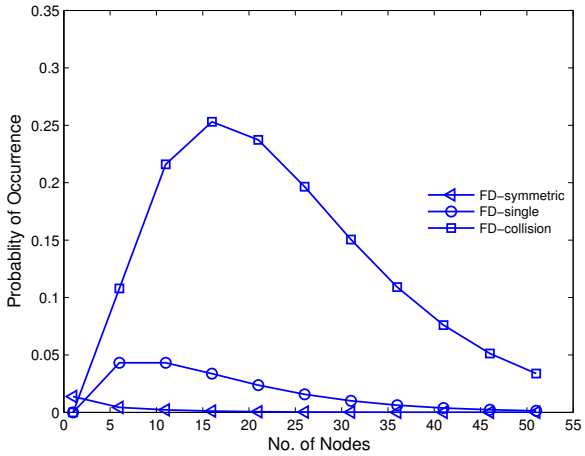

Figure 7.3: Compound probability of occurrence

to produce a priority value, which grants the priority-arbitration wining node to proceed and lead a node to form FD-symmetric transmissions by sending out a CTS+. The destination address of CTS+ is decided based on the following two rules: 1) if the winning node is targeted by its counterpart in RTS+, CTS+ will be addressed to this ”counterpart”; 2) if the winning node is not targeted by its counterpart in RTS+, CTS+ will be addressed to the winning-node’s original destination. Note that CTS+ not only informs the receiving node to send frames, but also hints the receiving node to receive frames. The two CTS+ addressing rules can secure at least one successful transmission in the non-saturated condition, and FD-symmetric transmissions in the saturated condition.

The fore part of Figure 7.2(b) depicts that FD+ converts an FD-single transmission to the FD-symmetric one. In this example, node1 wins the priority arbitration, sends a CTS+, and will transmit data along with node2. The rear part of Figure 7.2(b) shows that FD+ converts an FD-collision transmission to the FD-symmetric one, where node3 wins the priority arbitration. Both parts are illustrated in the saturated condition.

In the single-node transmitting case, by receiving RTS+, the receiver

will follow the initiator's transmission to form an FD-symmetric transmission, if the receiver has frames for the initiator.

7.3 Full-duplex MAC Analytic Models

Bianchi in [49] presented a saturation throughput model for DCF based WLANs. This DCF throughput model is utilized as a benchmark, and also extended to account for FD and FD+ transmissions in the Chapter.

7.3.1 FD Saturation Throughput Analysis

In order to facilitate the analysis, we divide the channel utilization time by slots. Three different types of slots are identified depending on the channel status: 1) an idle slot, where the channel sees no transmission activities, 2) a successful slot, where the channel observes successful transmissions, and 3) a collision slot, where the channel experiences collisions.

Let $\tau = 2/(CW + 1)$ be the transmission probability of a node in a random slot, which is computed as the probability that the backoff counter reaches zero at that slot, where CW is the size of the contention window.

Then, the probability that the channel sees an idle slot is obtained as follows:

$$p_{\text{i}} = (1 - \tau)^n. \tag{7.1}$$

A successful slot includes three cases: 1) the single-node transmission, 2) the FD-symmetric transmission and 3) the FD-single transmission. The probability of the first case, $p_{\text{s,single}}$, is given by:

$$p_{\text{s,single}} = \binom{n}{1} \tau(1 - \tau)^{n-1} = n\tau(1 - \tau)^{n-1}, \tag{7.2}$$

which accounts for that a single node successfully wins the channel contention.

$p_{\text{s,fd-symm}}$ and $p_{\text{s,fd-single}}$ are the probabilities of FD-symmetric and FD-single transmissions, respectively:

$$\begin{aligned} p_{\text{s,fd-symm}} &= \binom{n}{2}\tau\frac{1}{n-1}\tau\frac{1}{n-1}(1-\tau)^{n-2} \\ &= \frac{n}{2(n-1)}\tau^2(1-\tau)^{n-2} \end{aligned} \tag{7.3}$$

and

$$\begin{aligned} p_{\text{s,fd-single}} &= 2\cdot\binom{n}{2}\tau\frac{1}{n-1}\tau\frac{n-2}{n-1}(1-\tau)^{n-2} \\ &= \frac{n(n-2)}{(n-1)}\tau^2(1-\tau)^{n-2}. \end{aligned} \tag{7.4}$$

Note that $\frac{1}{n-1}\cdot\frac{1}{n-1}$ in (7.3) is the probability that both nodes are targeting each other, while $2\cdot\frac{1}{n-1}\cdot\frac{n-2}{n-1}$ in (7.4) is the probability that one node targets a second node and this "second node" targets one of the rest nodes in the network (multiplied by 2 explains the other way around).

Hence, the probability that the channel observes a successful slot has three components, $p_{\text{s,fd}} = p_{\text{s,single}} + p_{\text{s,fd-symm}} + p_{\text{s,fd-single}}$. By deducting p_{i} and $p_{\text{s,fd}}$, the collision probability of a slot, $p_{\text{c,fd}}$, is obtained:

$$p_{\text{c,fd}} = 1 - p_{\text{i}} - p_{\text{s,fd}}. \tag{7.5}$$

The frame error probability (p_{fer}) of each link is related to the signal-to-noise ratio (SNR) value of the receiver. Each individual link of an FD transmission will experience an independent frame error probability, and frames are assumed to be corrupted if the instantaneous SNR of a link is below a threshold [106]. Thus, the successfully received number of bits ($N_{\text{b,fd}}$) of an FD transmission is expressed as:

$$\begin{aligned} N_{\text{b,fd}} =& N_{\text{f}}\cdot L\cdot\Bigg((1-p_{\text{fer}})(p_{\text{s,single}} + p_{\text{s,fd-single}}(1-\alpha))\cdot 1 \\ &+\sum_{k=1}^{2}\binom{2}{k}(1-p_{\text{fer}})^k p_{\text{fer}}^{2-k} p_{\text{s,fd-symm}}(1-\alpha)\cdot k\Bigg), \end{aligned} \tag{7.6}$$

where N_{f} is the number of assembled frames in an aggregated MAC protocol data unit (A-MPDU), L is the length in bits of each data frame, and α is the FD Error Ratio that captures the case that an FD transmission fails due to the node is not able to successfully remove the self-interference.

The saturation throughput S_{fd} is expressed as the ratio of the successfully transmitted payload in bits of a slot and the average duration of a slot:

$$S_{\mathrm{fd}} = \frac{N_{\mathrm{b,fd}}}{p_{\mathrm{i}}\sigma + p_{\mathrm{s,fd}}T_{\mathrm{s}} + p_{\mathrm{c,fd}}T_{\mathrm{c}}}, \tag{7.7}$$

where σ is a constant value when the channel is idle; T_{s} and T_{c} represent the average duration of a successful and a collision slot, respectively:

$$\begin{cases} T_{\mathrm{s}} = T_{\mathrm{RTS}} + T_{\mathrm{CTS}} + T_{\text{A-MPDU}} + T_{\text{B-ACK}} + 3 \cdot \mathrm{SIFS} + \mathrm{DIFS} + \sigma \\ T_{\mathrm{c}} = T_{\mathrm{RTS}} + T_{\mathrm{CTS}} + \mathrm{SIFS} + \mathrm{DIFS} + \sigma. \end{cases} \tag{7.8}$$

p_{fd}, is the conditional collision probability of a node:

$$\begin{aligned} p_{\mathrm{fd}} =& 1 - \sum_{k=0}^{1} \binom{n-1}{k} \tau^k (1-\tau)^{n-1-k} \\ &+ \binom{n-2}{1} \tau (1-\tau)^{n-2} \\ =& 1 - (1-\tau)^{n-2}. \end{aligned} \tag{7.9}$$

The first two terms, $1 - \sum_{k=0}^{1} \binom{n-1}{k} \tau^k (1-\tau)^{n-1-k}$, represent the conditional collision probability when there are more than two nodes simultaneously transmitting. The third one, $\binom{n-2}{1} \tau (1-\tau)^{n-2}$, represents the conditional collision probability of a node when another node other than the node's target transmits. For example, as shown in Figure 7.1, it is a collision for node1 if it transmits to node3, while node3 is not transmitting (the FD-single scenario); or it is a collision for node2 if it transmits to node1, while node1 is silent (the FD-collision scenario).

7.3.2 FD+ Saturation Throughput Analysis

The analysis process of FD+ is similar to the FD scheme, so only the different probabilities and equations are given.

The probability that a slot contains successful transmissions in FD+, $p_{\text{s,fd+}}$, is when there are only one or two nodes simultaneously transmitting:

$$p_{\text{s,fd+}} = \sum_{k=1}^{2} \binom{n}{k} \tau^k (1-\tau)^{n-k}. \tag{7.10}$$

Then, the probability that a slot sees collisions in FD+ is derived as: $p_{\text{c,fd+}} = 1 - p_{\text{i}} - p_{\text{s,fd+}}$.

In FD+, the successfully received number of bits ($N_{\text{b,fd+}}$) is always contributed from both directions of paired nodes:

$$N_{\text{b,fd+}} = N_{\text{f}} \cdot L \cdot \sum_{k=1}^{2} \binom{2}{k} (1-p_{\text{fer}})^k p_{\text{fer}}^{2-k} p_{\text{s,fd+}} (1-\alpha) \cdot k. \tag{7.11}$$

Thus, by updating items in (7.7), the saturation throughput of FD+ is derived:

$$S_{\text{fd+}} = \frac{N_{\text{b,fd+}}}{p_{\text{i}}\sigma + p_{\text{s,fd+}} T_{\text{s+}} + p_{\text{c,fd+}} T_{\text{c+}}}. \tag{7.12}$$

Finally, the conditional collision probability of a node is when there are more than two nodes simultaneously transmitting:

$$p_{\text{fd+}} = 1 - \sum_{k=0}^{1} \binom{n-1}{k} \tau^k (1-\tau)^{n-1-k}. \tag{7.13}$$

7.4 Performance Evaluation

IEEE 802.11ac [2] parameters, as given in Table 7.1, are utilized for evaluating DCF, FD and FD+ transmissions. An event-driven simulator has been developed in C++ to compare with results obtained from the analytic models.

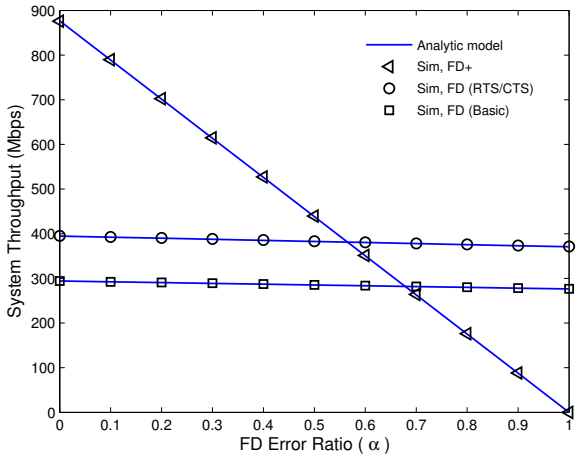

Figure 7.4: Throughput versus α

Table 7.1: **System parameters**

Parameters	**Values**
Channel bandwidth	160 MHz
Modulation and coding	256-QAM with 5/6
Guard interval	0.8 μs
Preamble	40 μs
Frame length (L)	12,000 bits
A-MPDU size (N_{f})	32
MAC header	272 bits
MPDU delimiter	32 bits
Service & Tail	16 and 6 bits
RTS & RTS+	160 and 168 bits
CTS/CTS+ & B-ACK	112 and 256 bits
SIFS and DIFS	16 and 34 μs
Idle slot time (σ)	9 μs

Figure 7.4 shows the system throughput of FD and FD+ when α increases from 0 to 1, where 0 means the perfect self-interference cancel-

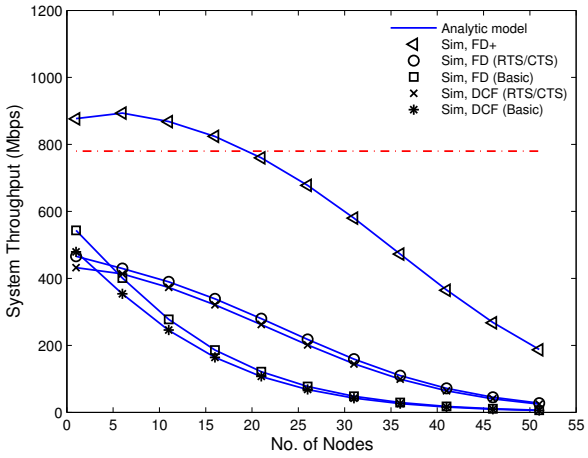

(a) Throughput versus nodes, $CW = 16$

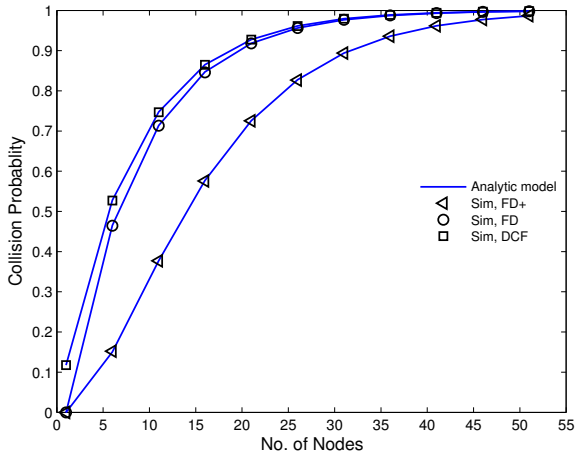

(b) Collision probability versus nodes, $CW = 16$

Figure 7.5: System performance versus number of nodes, $p_{\text{fer}} = 0.1$

lation, while 1 implies all full-duplex transmissions are corrupted. As we can see from the figure, FD+ is more vulnerable to the increase of

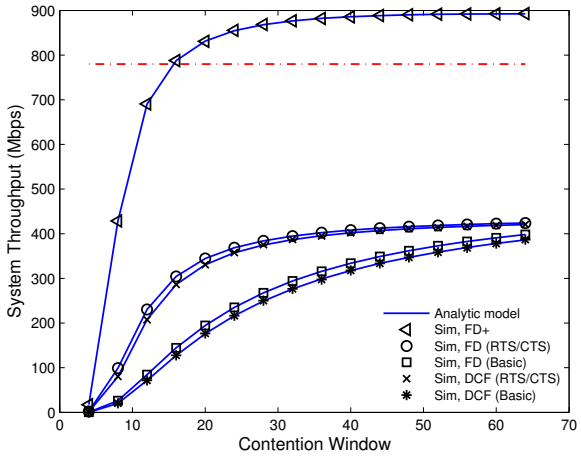

(a) Throughput versus contention window, Nodes=20

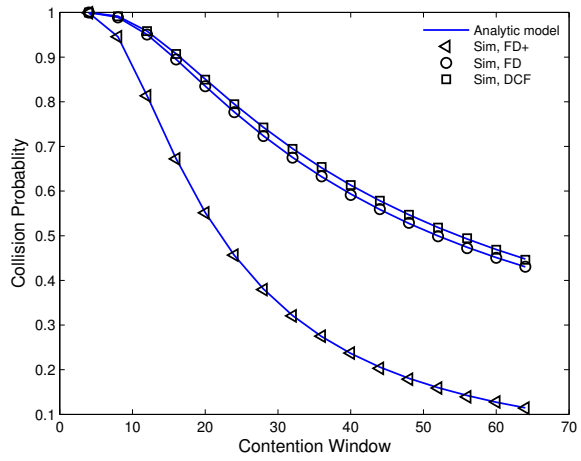

(b) Collision probability versus contention window, Nodes=20

Figure 7.6: System performance versus contention window, $p_{\text{fer}} = 0.1$

α, which is because FD+ will always operate in the FD-symmetric mode,

while FD has only small portion of operations in the FD-symmetric mode. In the randomly distributed nodes' topology, we fix $\alpha = 0.1$ in the following simulations. However, it is straightforward to adapt α to any value based on practical experimental or prototype tests.

Figures 7.5 and 7.6 show the system throughput and collision probability versus the number of nodes and contention window. The 802.11ac theoretic physical rate (780 Mbps), obtained using the parameters in Table 7.1, is also plotted as a reference (the red dotted lines). As we can see from the figures, the FD schemes only perform slightly better than the DCF ones, while the proposed FD+ scheme achieves significant throughput gains compared to FD and DCF (with an average factor of 2.3 increase). The reason is that FD can only exploit full-duplex capability in the FD-symmetric scenario, while FD+ is able to take full potentials of full-duplex transmissions by converting single-node, FD-single and FD-collision scenarios to the desired FD-symmetric one.

Figure 7.5(a) shows that the throughput decreases when the number of nodes increases, which is because the collision probability (Figure 7.5(b)) increases significantly as more nodes join. On the other hand, Figure 7.6(a) shows that the throughput increases as the size of contention window becomes larger. It is because the collision probability (Figure 7.6(b)) decreases when nodes have a bigger pool of backoff values, which enables FD+ transmissions to take more advantages.

Figures 7.5(a) and 7.6(a) also show that, in most cases, the DCF and FD throughput are less than half of what the physical rate offers, except when the number of nodes is very low or the size of contention window is large. This is caused by the so called overheads, which mainly include four aspects: the physical preambles, the compulsory idle time (e.g., DIFS and random back-off), the control frames (e.g., RTS/CTS) and the collisions. In the current communication structure of IEEE 802.11, these four aspects are either pre-determined or difficult to be eliminated. However, as we can see from the results, by properly designing the MAC scheme, the full-duplex transmissions are able to increase the system performance significantly.

7.5 Summary

This Chapter models the full-duplex transmission by considering the MAC operations and overheads. An enhanced FD MAC scheme is proposed to exploit full potentials of simultaneous transmissions with the same frequency. The analytic and simulation results show that the performance gains of FD+ are significant (an average factor of 2.3) against that of the IEEE 802.11 DCF and the under-utilized FD schemes. This promising improvement enables the full-duplex transmission to become a key technique candidate for next-generation wireless standards beyond IEEE 802.11ac.

Chapter 8

CONCLUSIONS

8.1 Concluding Remarks

In this thesis, we focused on studying and proposing enhanced MAC schemes to utilize the MU-MIMO and FD techniques to improve the performance of IEEE 802.11 networks.

In Chapter 2, we have surveyed and categorized prominent MAC proposals in the liturature. Some typical MUD and MUIC techniques for de/pre-coding are sampled, and the key requirements of designing efficient MAC protocols for next generation wireless networks are identified.

In Chapter 3, we have proposed a DCF/DSDMA protocol, which supports the AP to simultaneously send frames to multiple STAs. The results show that considerable performance gains, in terms of a higher throughput and lower delays, are achieved by exploring multiple antennas employed at the AP.

In Chapter 4, we have presented a novel two-round MAC protocol, called DCF/USDMA, which supports multi-STA simultaneous uplink transmissions in WLANs. The results show that DCF/USDMA is able to boost the performance of WLANs by synchronizing STAs' uplink access. In addition, the presented results provide some insights about how the different parameters that control the DCF/USDMA operation can be optimized.

In Chapter 5, we proposed a unified MU-MIMO MAC protocol called

Uni-MUMAC, which supports simultaneous downlink and uplink transmissions for IEEE 802.11ac WLANs. By analyzing the simulation results, we observe that the 2-nd round Contention Window CW2nd, which is tuned to optimize the uplink transmission, is however not bringing the same benefit to the downlink one. An adaptive frame aggregation scheme and queue scheme are applied at the AP to offset this disadvantage. By properly setting all the parameters, the results show that a WLAN implementing Uni-MUMAC is able to avoid the AP bottle-neck problem and performs very well in both the traditional downlink-dominant and emerging down/up-link balanced traffic scenarios.

In Chapter 6, the IEEE 802.11ac defined basic access scheme (MU-Basic) and proposed MU-RTS/CTS scheme are evaluated and compared through three spatial-stream allocation algorithms by the analytical model and simulations. The results show that MU-RTS/CTS is more efficient than MU-Basic as the number of nodes and the size of A-MPDU increase. Regarding the spatial-stream allocation algorithms, the Beam-greedy algorithm outperforms the Stream-greedy one, while the ideal one Stream-independent is the one that provides the best performance.

From the presented results, it is clear that the novel PHY and MAC features introduced by IEEE 802.11ac, such as the downlink MU-MIMO, the frame aggregation and the channel bonding, are able to provide significant performance gains. However, the results also point out the importance of the spatial-stream allocation algorithm and the high overheads introduced by the CSI acquisition procedure. The wireless mesh network may not work well in some scenarios where the number of nodes is high and CSI is updated frequently if MU-MIMO transmissions are considered.

In Chapter 7, we modelled full-duplex transmissions by considering MAC operations and overheads. We have proposed an enhanced FD MAC scheme to exploit full potentials of simultaneous transmissions in the same frequency. The analytic and simulation results show that the performance gains of FD+ are significant against that of the IEEE 802.11 DCF and the under-utilized FD schemes. This exciting improvement enables the full-duplex transmission to become a key technique candidate

for next-generation wireless standards beyond IEEE 802.11ac.

Despite considerable research has been conducted, there still exists under-explored areas toward simple, but highly efficient MAC protocols for MU-MIMO based WLANs, especially in the context of the rapid growth of wireless devices. Therefore, we have given some of our thoughts in that regard in the Section-Future Directions 8.2.

8.2 Future Directions

Based on the work of the thesis, we discuss possible future research directions for MU-MIMO MAC protocols through a micro perspective (i.e., the further research efforts needed for MU-MIMO transmissions in WLANs) and a macro perspective (i.e., the potential research aspects rising from possible cooperation or integration between MU-MIMO based WLANs and other networks).

8.2.1 Micro Perspective: Within WLANs

What Does 802.11ac Not Specify?

The downlink MU-MIMO transmission is one of the most significant features introduced by IEEE 802.11ac. In order to perform multi-user transmissions, the amendment proposes the ECFB scheme to feedback the AP with the required CSI, and devises a group identifier (Group-ID) field in the PHY preamble to facilitate grouping STAs. However, the following two related factors are not specified in the amendment.

- **Scope and frequency of CSI feedback**: [90] and [15] have shown the significant impact of the CSI feedback on the system performance. A clear dilemma regarding the scope and the frequency of the CSI feedback is that a large scale (e.g., all STAs in the network) and frequent CSI requests will introduce huge overheads, while the opposite way leads to that the rendered channel information might be outdated. Therefore, adaptive algorithms are needed to dynamically adjust the scope and the frequency of CSI feedback.

- **Conditions to group/re-group STAs**: Although it can be argued that the way of grouping STAs depends on the specific application, a smart grouping algorithm has to be designed to identify STAs that can be co-scheduled as well as conditions that would trigger STAs' re-grouping.

How to Improve MAC Efficiency?

As shown in the thesis, significant research efforts have been made to adapt the IEEE 802.11 MAC to advances such as the multi-antenna technique. However, the MAC throughput is still much lower than the PHY raw rate (lower than 70% in most cases [95]). The throughput loss mainly comes from the so-called overheads, which include the management frames (e.g., association requests/responses), control frames (e.g., RTS/CTS/ACK), frame headers (e.g., PHY preambles, PHY/MAC headers) and the compulsory idle duration (e.g., the random BO, DIFS/SIFS). Other non-overhead factors contributing to the throughput loss include frame collisions and the airtime unfairness caused by low rate STAs that monopolize the channel. These fundamental IEEE 802.11 mechanisms and features limit the MAC efficiency. In a packet capture test conducted in a dense area of Tokyo [107], the results show that data frames only account for 23% of all types of frames (46% management frames, 30% control frames, 1% others), and moreover, most of management frames are in the 802.11b format and transmitted at 1 Mbps to ensure the interoperability.

IEEE has recently approved a new task group-802.11ax [20]. It aims to improve the efficiency of WLANs by not only increasing the peak data rate, but also trying to focus on the throughput improvement of each STA in both indoor and outdoor heavily-loaded environments. Here, we give our thoughts on possible solutions to improve the MAC efficiency.

- **Cooperation among multiple bands**: Management frames, control frames and frames headers are necessary to facilitate correct receptions of data. They can not be eliminated in the current 802.11 communication architecture. At least from the legacy IEEE 802.11-

1997 to 802.11ac, what we have seen is an ever-increasing length of PHY preamble. Cooperation among multiple bands could be an effective way to control overheads. More specifically, a future smart device is likely to be equipped with multiple interfaces operating in multiple bands [108]. Thus, 802.11ac at 5 GHz, could be a candidate for the carrier sense and data transmissions across rooms; 802.11ah below 1 GHz, could be utilized to transmit management and control frames; while 802.11ad at 60 GHz, could be used for very high speed data transmissions in the line of sight. [109] has already suggested a possible usage model that using 802.11ah for signalling among APs while 802.11ac for data frames.

- **Revise the backoff scheme**: The random BO scheme is a key function employed by IEEE 802.11 to avoid collisions. Unfortunately, collisions can not be eliminated and remain as one of the most degrading factors to the system performance. [110] proposes a collision-free solution, where STAs adopt a deterministic BO instead of a random one after successful transmissions for single-antenna based WLANs. This innovative idea can be considered to extend to multi-antenna based WLANs in both downlink and uplink.

- **Uplink MU-MIMO transmissions**: The Internet traffic has evolved from mainly web browsing and file transfers to a wide variety of applications, which include considerable amount of content-rich files generated by users, such as the video conferencing, social networks and cloud uploading services. Although the enhancement for uplink transmissions has recently gained attention, there is still much space for improvements since IEEE 802.11ac will not support uplink MU-MIMO transmissions. In addition, there are a few works that focus on unifying MU-MIMO downlink and uplink in a single communication system.

- **Full-duplex transmissions**: The current form of communications in WLANs is half-duplex, namely, transmissions and receptions are

allocated to different time slots or frequency bands. The full-duplex transmission has the potential to double the channel capacity by allowing simultaneous transmissions and receptions with the same frequency [111] [112]. On the other hand, the coming of full-duplex transmissions hints us to rethink the IEEE 802.11 fundamental MAC mechanism-CSMA/CA, which is employed based on the long-held assumption that radios can not transmit and receive at the same time [113]. The research on full-duplex transmissions has just started in recent years. Although the challenging part is to cancel self-interference at the full-duplex transceiver, the MAC scheme needs to be revised as well [114] [115].

8.2.2 Macro Perspective: Heterogeneous Networks

It seems to be a trend that in the future there will be a huge and smart network that integrates heterogeneous networks (e.g., WLANs, broadband mobile networks and sensor networks), which means individual network will have to collaborate with others to provide services, rather than just coexist. Obviously, the integration and the inclusion of WLANs require some unique changes at the MAC layer.

How, who and when to collaborate?

With the PHY layer's focus on the air interface and the network layer's focus on the routing, the MAC layer plays a role in deciding how to collaborate, who to collaborate and when to collaborate [116] [117]. For example, imagining a scenario that a sink of a smart metering sensor network requests an AP to forward the collected data to a user's mobile phone, the AP first checks whether the mobile phone is in its vicinity to decide whether to forward the data by itself or to relay the data to other APs. And then, the AP checks the channel condition and the queueing status to decide who and when to transmit the data. Regardless the scale and the type of collaborations, management frames and control frames exchanges to build connections with other entities are needed. Note that

today's device-to-device communications already account for a significant part of total wireless traffic, and they are regarded as one of the most important challenges for 5G networks [118] [119]. Therefore, the MAC scheme for the integrated network has to take how, who and when to collaborate into account.

Multi-hop links

In addition to the above consideration, it is inevitable for MAC protocols of integrated networks to support multi-hop indirected links, where the hidden-node problem, cooperative diversity, MPT/MPR functionalities and the joint MAC-routing design need to be addressed [120].

Outdoor and mobile WLANs

The inclusion of WLANs to outdoors presents some significant challenges to the traditional MAC, as which is designed to support limited mobility. First, due to the user movement and the large scale fading, the outdoor channel is varying faster than that of indoors, even with the same moving speed [121]. For that reason, the CSI feedback scheme needs to be reconsidered to report the channel state timely, while maintaining low channel estimation overheads. Secondly, the cellular operators may offload traffic to public or proprietary WLANs (e.g., the carrier class Wi-Fi [122]) in a dense public stadium, in which case, the seamless transfer and the QoS promised by the cellular network need to be assured at the MAC layer.

Bibliography

[1] Cisco, "The Zettabyte Era-Trends and Analysis," in *Cisco White Paper*, pp. 1–19, 2013.

[2] "IEEE Standard for Information technology-Telecommunications and Information Exchange Between Systems-Part 11-Amendment 4: Enhancements for Very High Throughput for Operation in Bands below 6 GHz," *IEEE 802.11ac*, pp. 1–425, 2013.

[3] A. Goldsmith, S. A. Jafar, N. Jindal, and S. Vishwanath, "Capacity limits of MIMO channels," *IEEE Journal on Selected Areas in Communications*, vol. 21, no. 5, pp. 684–702, 2003.

[4] G. Caire and S. Shamai, "On the achievable throughput of a multiantenna Gaussian broadcast channel," *IEEE Transactions on Information Theory*, vol. 49, no. 7, pp. 1691–1706, 2003.

[5] D. Gesbert, M. Kountouris, R. W. Heath, C.-B. Chae, and T. Salzer, "Shifting the MIMO paradigm: From Single User to Multiuser Communications," *IEEE Signal Processing Magazine*, vol. 24, no. 5, pp. 36–46, 2007.

[6] J. I. Choi, M. Jain, K. Srinivasan, P. Levis, and S. Katti, "Achieving single channel, full duplex wireless communication," in *Proceedings of the sixteenth annual international conference on Mobile computing and networking*, pp. 1–12, ACM, 2010.

[7] M. Duarte and A. Sabharwal, "Full-duplex wireless communications using off-the-shelf radios: Feasibility and first results," in *Forty Fourth Asilomar Conference on Signals, Systems and Computers (ASILOMAR)*, pp. 1558–1562, IEEE, 2010.

[8] E. Aryafar, M. A. Khojastepour, K. Sundaresan, S. Rangarajan, and M. Chiang, "Midu: enabling mimo full duplex," in *Proceedings of the 18th annual international conference on Mobile computing and networking*, pp. 257–268, ACM, 2012.

[9] D. Bharadia, E. McMilin, and S. Katti, "Full duplex radios," in *Proceedings of the ACM SIGCOMM*, pp. 375–386, ACM, 2013.

[10] L. Cariou, "Usage models for IEEE 802.11 High Efficiency WLAN study group (HEW SG)." https://mentor.ieee.org/802.11/dcn/13/11-13-0657-06-0hew-hew-sg-usage-models-and-requirements-liaison-with-wfa.ppt. [Accessed 02 June 2014].

[11] R. Liao, B. Bellalta, M. Oliver, and Z. Niu, "Mu-mimo mac protocols for wireless local area networks: A survey," *arXiv preprint arXiv:1404.1622*, 2014.

[12] R. Liao, B. Bellalta, C. Cano, and M. Oliver, "DCF/DSDMA: Enhanced DCF with SDMA Downlink Transmissions for WLANs," in *BCFIC*, pp. 96–102, 2011.

[13] R. Liao, B. Bellalta, and M. Oliver, "DCF/USDMA: Enhanced DCF for Uplink SDMA Transmissions in WLANs," in *IWCMC*, pp. 263–268, 2012.

[14] R. Liao, B. Bellalta, T. C. Minh, J. Barcelo, and M. Oliver, "Uni-MUMAC: A Unified Down/Up-link MU-MIMO MAC Protocol for IEEE 802.11 ac WLANs," *arXiv preprint arXiv:1309.5049*, 2013.

[15] R. Liao, B. Bellalta, J. Barcelo, V. Valls, and M. Oliver, "Performance analysis of IEEE 802.11 ac wireless backhaul networks in saturated conditions," *EURASIP Journal on Wireless Communications and Networking*, vol. 2013, no. 1, pp. 1–14, 2013.

[16] R. Liao, B. Bellalta and M. Oliver, "Modelling full-duplex mac for wireless networks," in *Submitted for publication*.

[17] IEEE, "IEEE STANDARDS BOARD OPERATIONS MANUAL." http://standards.ieee.org/develop/policies/opman/sect1.html. [Accessed 02 June 2014].

[18] "IEEE Standard for Information technology–Telecommunications and information exchange between systems Local and metropolitan area networks–Specific requirements Part 11: Wireless LAN Medium Access Control (MAC) and Physical Layer (PHY) Specifications," *IEEE Std 802.11-2012*, pp. 1–2793, 2012.

[19] "IEEE Standard for Information technology–LAN/MAN– Specific requirements– Part 11: Wireless LAN Medium Access Control and Physical Layer Specifications Amendment 5: Enhancements for Higher Throughput," *IEEE 802.11n*, pp. 1–565, 2009.

[20] I. 802.11ax, "Project IEEE 802.11ax High Efficiency WLAN (HEW)." http://grouper.ieee.org/groups/802/11/Reports/tgax_update.htm. [Accessed 02 June 2014].

[21] H. Z. Y. S. L. C. Z. L. J. Z. H. K. S. C. Lei Wang, Hui-Ling Lou and R. Taori, "Proposed 802.11ax Functional Requirements." https://mentor.ieee.org/802.11/dcn/14/11-14-0567-03-00ax-proposed-tgax-functional-requirements.doc. [Accessed 02 June 2014].

[22] IEEE 802.11ad, "Very High Throughput in 60 GHz." http://www.ieee802.org/11/Reports/tgad_update.htm. [Accessed 02 June 2014].

[23] IEEE 802.11af, "Wireless LAN in the TV White Space." http://grouper.ieee.org/groups/802/11/Reports/tgaf_update.htm. [Accessed 02 June 2014].

[24] IEEE 802.11 11ah, "Proposed TGah Draft Amendment." http://www.ieee802.org/11/Reports/tgah_update.htm. [Accessed 02 June 2014].

[25] T. Adame, A. Bel, B. Bellalta, J. Barcelo, J. Gonzalez, and M. Oliver, "Capacity Analysis of IEEE 802.11 ah WLANs for M2M Communications," in *Multiple Access Communcations*, pp. 139–155, Springer, 2013.

[26] "IEEE Standard for Information Technology–LAN/MAN–Part 11: Wireless LAN Medium Access Control and Physical Layer Specifications–Amendment: Medium access control (MAC) Enhancements for Quality of Service," *IEEE 802.11e*, pp. 1–211, 2005.

[27] G. Bianchi, I. Tinnirello, and L. Scalia, "Understanding 802.11 e contention-based prioritization mechanisms and their coexistence with legacy 802.11 stations," *Network, IEEE*, vol. 19, no. 4, pp. 28–34, 2005.

[28] E. Charfi, L. Chaari, and L. Kamoun, "PHY/MAC enhancements and QoS mechanisms for very high throughput WLANs: a survey," *IEEE Communications Surveys & Tutorials*, 2013.

[29] M. Jiang and L. Hanzo, "Multiuser MIMO-OFDM for next-generation wireless systems," *Proceedings of the IEEE*, vol. 95, no. 7, pp. 1430–1469, 2007.

[30] F. Khalid and J. Speidel, "Advances in MIMO Techniques for Mobile Communications-A Survey," *Int'l J. of Communications, Network and System Sciences*, vol. 3, no. 3, pp. 213–252, 2010.

[31] A. Paulraj, R. Nabar, and D. Gore, *Introduction to space time wireless communications*. Cambridge university press, 2003.

[32] M. Costa, "Writing on dirty paper (Correspondence)," *IEEE Transactions on Information Theory*, vol. 29, no. 3, pp. 439–441, 1983.

[33] J. Mietzner, R. Schober, L. Lampe, W. H. Gerstacker, and P. A. Hoeher, "Multiple-antenna techniques for wireless communications-a comprehensive literature survey," *IEEE Communications Surveys & Tutorials*, vol. 11, no. 2, pp. 87–105, 2009.

[34] D. J. Love, R. W. Heath, V. K. Lau, D. Gesbert, B. D. Rao, and M. Andrews, "An overview of limited feedback in wireless communication systems," *IEEE Journal on Selected Areas in Communications*, vol. 26, no. 8, pp. 1341–1365, 2008.

[35] H. Lou, M. Ghosh, P. Xia, and R. Olesen, "A comparison of implicit and explicit channel feedback methods for MU-MIMO WLAN systems," in *PIMRC*, pp. 419–424, IEEE, 2013.

[36] M. X. Gong, E. Perahia, R. Want, and S. Mao, "Training protocols for multi-user MIMO wireless LANs," in *PIMRC*, pp. 1218–1223, IEEE, 2010.

[37] H. Jin, B. C. Jung, H. Y. Hwang, and D. K. Sung, "Performance Comparison of Uplink WLANs with Single-User and Multi-User MIMO Schemes," in *WCNC*, pp. 1854–1859, 2008.

[38] F. Babich and M. Comisso, "Theoretical Analysis of Asynchronous Multi-packet Reception in 802.11 Networks," *IEEE Transactions on Communications*, vol. 58, no. 6, pp. 1782–1794, 2010.

[39] P. X. Zheng, Y. J. Zhang, and S. C. Liew, "Multipacket Reception in Wireless Local Area Networks," in *ICC*, vol. 8, pp. 3670–3675, 2006.

[40] M. Torabzadeh and W. Ajib, "Packet scheduling and fairness for multiuser MIMO systems," *IEEE Transactions on Vehicular Technology*, vol. 59, no. 3, pp. 1330–1340, 2010.

[41] C. Wang and R. D. Murch, "Optimal downlink multi-user MIMO cross-layer scheduling using HOL packet waiting time," *IEEE Transactions on Wireless Communications*, vol. 5, no. 10, pp. 2856–2862, 2006.

[42] T. Tandai, H. Mori, and M. Takagi, "Cross-layer-optimized user grouping strategy in downlink multiuser MIMO systems," in *VTC*, pp. 1–6, IEEE, 2009.

[43] V. Valls and D. J. Leith, "Proportional Fair MU-MIMO in 802.11 WLANs," *arXiv preprint arXiv:1305.4538*, 2013.

[44] X. Zhang, S. Zhou, Z. Niu, and X. Lin, "An energy-efficient user scheduling scheme for multiuser MIMO systems with RF chain sleeping," in *WCNC*, pp. 169–174, IEEE, 2013.

[45] C. Anton-Haro, P. Svedman, M. Bengtsson, A. Alexiou, and A. Gameiro, "Cross-layer scheduling for multi-user MIMO systems," *IEEE Communications Magazine*, vol. 44, no. 9, pp. 39–45, 2006.

[46] V. Kawadia and P. Kumar, "A cautionary perspective on cross-layer design," *IEEE Wireless Communications*, vol. 12, no. 1, pp. 3–11, 2005.

[47] W. L. Huang, K. Letaief, and Y. J. Zhang, "Cross-layer multi-packet reception based medium access control and resource allocation for space-time coded MIMO/OFDM," *IEEE Transactions on Wireless Communications*, vol. 7, no. 9, pp. 3372–3384, 2008.

[48] X. Yu, P. Navaratnam, and K. Moessner, "Resource Reservation Schemes for IEEE 802.11-Based Wireless Networks: A Survey," *IEEE Communications Surveys & Tutorials*, vol. 15, no. 3, pp. 1042–1061, 2013.

[49] G. Bianchi, "Performance analysis of the IEEE 802.11 distributed coordination function," *IEEE Journal on Selected Areas in Communications*, vol. 18, no. 3, pp. 535–547, 2000.

[50] A. Mukhopadhyay, N. B. Mehta, and V. Srinivasan, "Acknowledgement-aware MPR MAC protocol for distributed WLANs: Design and analysis," in *GLOBECOM*, pp. 5087–5092, IEEE, 2012.

[51] S. Wu, W. Mao, and X. Wang, "Performance Analysis of Random Access Multi-user MIMO Wireless LANs," in *GLOBECOM*, 2013.

[52] K. Tan, H. Liu, J. Fang, W. Wang, J. Zhang, M. Chen, and G. M. Voelker, "SAM: enabling practical spatial multiple access in wireless LAN," in *INFOCOM*, pp. 49–60, ACM, 2009.

[53] Microsoft, "Research Software Radio (SORA)." http://research.microsoft.com/en-us/projects/sora. [Accessed 02 June 2014].

[54] T.-H. Lin and H. Kung, "Concurrent channel access and estimation for scalable multiuser mimo networking," in *INFOCOM*, pp. 140–144, April 2013.

[55] E. J. Candès and M. B. Wakin, "An introduction to compressive sampling," *IEEE Signal Processing Magazine*, vol. 25, no. 2, pp. 21–30, 2008.

[56] W. L. Huang, K. Ben Letaief, and Y. J. Zhang, "Joint Channel State Based Random Access and Adaptive Modulation in Wireless LANs with Multi-Packet Reception," *IEEE Transactions on Wireless Communications*, vol. 7, no. 11, pp. 4185–4197, 2008.

[57] T. Tandai, H. Mori, K. Toshimitsu, and T. Kobayashi, "An efficient uplink multiuser MIMO protocol in IEEE 802.11 WLANs," in *PIMRC*, pp. 1153–1157, IEEE, 2009.

[58] D. Jung and H. Lim, "Opportunistic MAC Protocol for Coordinating Simultaneous Transmissions in Multi-User MIMO Based WLANs," *IEEE Communications Letters*, vol. 15, no. 8, pp. 902–904, 2011.

[59] S. Barghi, H. Jafarkhani, and H. Yousefi'zadeh, "MIMO-assisted MPR-aware MAC design for asynchronous WLANs," *IEEE/ACM Transactions on Networking*, vol. 19, no. 6, pp. 1652–1665, 2011.

[60] S. Zhou and Z. Niu, "Distributed Medium Access Control with SDMA Support for WLANs," *IEICE Transactions*, vol. 93-B, no. 4, pp. 961–970, 2010.

[61] Y. J. Zhang, "Multi-round contention in wireless LANs with multipacket reception," *IEEE Transactions on Wireless Communications*, vol. 9, pp. 1503–1513, Apr. 2010.

[62] D. Jung, R. Kim, and H. Lim, "Asynchronous Medium Access Protocol for Multi-User MIMO Based Uplink WLANs," *IEEE Transactions on Communications*, vol. 60, no. 12, pp. 3745–3754, 2012.

[63] L. X. Cai, H. Shan, W. Zhuang, X. Shen, J. W. Mark, and Z. Wang, "A Distributed Multi-User MIMO MAC Protocol for Wireless Local Area Networks," in *GLOBECOM*, pp. 4976–4980, 2008.

[64] H. Li, A. Attar, and V. C. M. Leung, "Multi-User Medium Access Control in Wireless Local Area Network," in *WCNC*, pp. 1–6, 2010.

[65] M. X. Gong, E. Perahia, R. Stacey, R. Want, and S. Mao, "A CSMA/CA MAC Protocol for Multi-User MIMO Wireless LANs," in *GLOBECOM*, pp. 1–6, 2010.

[66] E. Kartsakli, N. Zorba, L. Alonso, and C. V. Verikoukis, "Multiuser MAC Protocols for 802.11n Wireless Networks," in *ICC*, pp. 1–5, 2009.

[67] Z. Zhang, S. Bronson, J. Xie, and H. Wei, "Employing the one-sender-multiple-receiver technique in wireless LANs," in *INFOCOM*, pp. 1–9, IEEE, 2010.

[68] Ettus, "Universal Software Radio Peripheral (USRP)." http://www.ettus.com. [Accessed 02 June 2014].

[69] G. Redieteab, L. Cariou, P. Christin, and J.-F. Hélard, "SU/MU-MIMO in IEEE 802.11 ac: PHY+ MAC performance comparison for single antenna stations," in *Wireless Telecommunications Symposium*, pp. 1–5, IEEE, 2012.

[70] G. Breit, et al., "IEEE P802.11 Wireless LANs TGac Channel Model Addendum." https://mentor.ieee.org/802.11/dcn/09/11-09-0308-03-00ac-tgac-channel-model-addendum-document.doc. [Accessed 02 June 2014].

[71] J. Cha, H. Jin, B. C. Jung, and D. K. Sung, "Performance Comparison of Downlink User Multiplexing Schemes in IEEE 802.11ac: Multi-user MIMO vs. Frame Aggregation," in *WCNC*, pp. 1514–1519, 2012.

[72] H. V. Balan, R. Rogalin, A. Michaloliakos, K. Psounis, and G. Caire, "Achieving high data rates in a distributed mimo system," in *MOBICOM*, pp. 41–52, ACM, 2012.

[73] Rice University, "Wireless Open-Access Research Platform (WARP)." http://warp.rice.edu/trac/wiki/about. [Accessed 02 June 2014].

[74] C. Zhu, A. Bhatt, Y. Kim, O. Aboul-magd, and C. Ngo, "MAC Enhancements for Downlink Multi-user MIMO Transmission in Next Generation WLAN," in *CCNC*, pp. 832–837, 2012.

[75] B. Ji, K. Song, Y. Hu, and H. Chen, "Cooperative Transmission Mechanisms in Next Generation WiFi: IEEE 802.11 ac," *International Journal of Distributed Sensor Networks*, vol. 2014, 2014.

[76] H. Shen, S. Lv, Y. Sun, X. Dong, X. Wang, and X. Zhou, "Concurrent Access Control Using Subcarrier Signature in Heterogeneous MIMO-Based WLAN," in *MACOM*, pp. 109–121, 2012.

[77] T. Kim and N. Vaidya, "MAC Protocol Design for Multiuser MIMO Wireless Networks," Technical Report, University of Illinois at Urbana-Champaign, 2008.

[78] S. Yun, L. Qiu, and A. Bhartia, "Multi-point to multi-point MIMO in wireless LANs," in *INFOCOM*, pp. 125–129, 2013.

[79] G. Chen and B. Szymanski, "Component-oriented Simulation Toolkit." http://www.ita.cs.rpi.edu. [Accessed 02 June 2014].

[80] R. Liao, B. Bellalta, M. Oliver, and N. Garcia, "A queueing model for sdma downlink transmissions," in *Multiple Access Communications*, pp. 74–78, Springer, 2010.

[81] M. Kihl, P. Odling, C. Lagerstedt, and A. Aurelius, "Traffic analysis and characterization of internet user behavior," in *Ultra Modern Telecommunications and Control Systems and Workshops (ICUMT), 2010 International Congress on*, pp. 224–231, IEEE, 2010.

[82] F. Wamser, R. Pries, D. Staehle, K. Heck, and P. Tran-Gia, "Traffic characterization of a residential wireless internet access," *Telecommunication Systems*, vol. 48, no. 1-2, pp. 5–17, 2011.

[83] Cisco, "Cisco Visual Networking Index: Global Mobile Data Traffic Forecast Update, 2012-2017," in *Cisco White Paper*, pp. 1–34, 2013.

[84] E. H. Ong, J. Kneckt, O. Alanen, Z. Chang, T. Huovinen, and T. Nihtila, "Ieee 802.11 ac: Enhancements for very high throughput wlans," in *Personal Indoor and Mobile Radio Communications*

(PIMRC), 2011 IEEE 22nd International Symposium on, pp. 849–853, IEEE, 2011.

[85] O. Aboul-Magd, U. Kwon, Y. Kim, and C. Zhu, "Managing downlink multi-user mimo transmission using group membership," in *Consumer Communications and Networking Conference (CCNC), 2013 IEEE*, pp. 370–375, IEEE, 2013.

[86] G. Chen, J. Branch, M. Pflug, L. Zhu, and B. Szymanski, "SENSE: a wireless sensor network simulator," in *Advances in pervasive computing and networking*, pp. 249–267, Springer, 2005.

[87] B. Bellalta, J. Barcelo, D. Staehle, A. Vinel, and M. Oliver, "On the Performance of Packet Aggregation in IEEE 802.11ac MU-MIMO WLANs," *IEEE Communications Letters*, vol. 16, no. 10, pp. 1588–1591, 2012.

[88] J. Barcelo, B. Bellalta, C. Cano, A. Faridi, and M. Oliver, "On the distributed construction of a collision-free schedule in multi-hop packet radio networks," *Springer Telecommunication Systems*, pp. 1–14, 2013.

[89] G. R. Hiertz, D. Denteneer, L. Stibor, Y. Zang, X. P. Costa, and B. Walke, "The ieee 802.11 universe," *Communications Magazine, IEEE*, vol. 48, no. 1, pp. 62–70, 2010.

[90] G. Redieteab, L. Cariou, P. Christin, and J. F. Helard, "PHY+MAC channel sounding interval analysis for IEEE 802.11ac MU-MIMO," in *ISWCS*, pp. 1054–1058, 2012.

[91] D. Nojima, L. Lanante, Y. Nagao, M. Kurosaki, and H. Ochi, "Performance evaluation for multi-user mimo ieee 802.11 ac wireless lan system," in *Advanced Communication Technology (ICACT), 2012 14th International Conference on*, pp. 804–808, IEEE, 2012.

[92] Z. Zhang, Y. Yang, and M. Zhao, "Enhancing downlink performance in wireless networks by simultaneous multiple packet

transmission," *Computers, IEEE Transactions on*, vol. 58, no. 5, pp. 706–718, 2009.

[93] J. Zhang and H.-N. Lee, "Throughput enhancement with a modified 802.11 mac protocol with multi-user detection support," *AEU-International Journal of Electronics and Communications*, vol. 62, no. 5, pp. 365–373, 2008.

[94] R. de Vegt, "IEEE 802.11ac Usage Model." https://mentor.ieee.org/802.11/dcn/09/11-09-0161-02-00ac-802-11ac-usage-model-document.ppt. [Accessed 02 June 2014].

[95] Cisco, "802.11ac: The Fifth Generation of Wi-Fi," in *Cisco White Paper*, pp. 1–25, 2012.

[96] L. Ward, "802.11ac Technology Introduction," in *Rohde & Schwarz White Paper*, 2012.

[97] E. Perahia and R. Stacey, *Next Generation Wireless LANs: 802.11 n and 802.11 ac*. Cambridge university press, 2013.

[98] A. Kumar, E. Altman, D. Miorandi, and M. Goyal, "New insights from a fixed point analysis of single cell ieee 802.11 wlans," in *INFOCOM 2005. 24th Annual Joint Conference of the IEEE Computer and Communications Societies. Proceedings IEEE*, vol. 3, pp. 1550–1561, IEEE, 2005.

[99] C.-s. Hwang and J. M. Cioffi, "Opportunistic csma/ca for achieving multi-user diversity in wireless lan," *Wireless Communications, IEEE Transactions on*, vol. 8, no. 6, pp. 2972–2982, 2009.

[100] J. Kivinen, X. Zhao, and P. Vainikainen, "Empirical characterization of wideband indoor radio channel at 5.3 ghz," *Antennas and Propagation, IEEE Transactions on*, vol. 49, no. 8, pp. 1192–1203, 2001.

[101] N. Singh, D. Gunawardena, A. Proutiere, B. Radunovic, H. V. Balan, and P. Key, "Efficient and fair mac for wireless networks with self-interference cancellation," in *2011 International Symposium on Modeling and Optimization in Mobile, Ad Hoc and Wireless Networks (WiOpt)*, pp. 94–101, IEEE, 2011.

[102] M. Duarte, A. Sabharwal, V. Aggarwal, R. Jana, K. Ramakrishnan, C. W. Rice, and N. Shankaranarayanan, "Design and characterization of a full-duplex multi-antenna system for wifi networks," vol. 63, no. 7, pp. 2592–2602, 2012.

[103] A. Sahai, G. Patel, and A. Sabharwal, "Pushing the limits of full-duplex: Design and real-time implementation," *arXiv preprint arXiv:1107.0607*, 2011.

[104] S. Goyal, P. Liu, O. Gurbuz, E. Erkip, and S. Panwar, "A distributed mac protocol for full duplex radio," in *Forty Seventh Asilomar Conference on Signals, Systems and Computers (ASILOMAR)*, 2013.

[105] W. Zhou, K. Srinivasan, and P. Sinha, "Rctc: Rapid concurrent transmission coordination in full duplex wireless networks," in *Proc. of IEEE ICNP*.

[106] H. Jin, B. C. Jung, H. Y. Hwang, and D. K. Sung, "A mimo-based collision mitigation scheme in uplink wlans," *Communications Letters, IEEE*, vol. 12, no. 6, pp. 417–419, 2008.

[107] A. Kishida, M. Iwabuchi, Y. Inoue, Y. Asai, Y. Takatori, T. Shintaku, T. Sakata and A. Yamada, "Issues of Low-Rate Transmission." https://mentor.ieee.org/802.11/dcn/13/11-13-0801-01-0hew-issues-of-low-rate-transmission.pptx. [Accessed 02 June 2014].

[108] H. Singh, J. Hsu, L. Verma, S. S. Lee, and C. Ngo, "Green operation of multi-band wireless LAN in 60 GHz and 2.4/5 GHz," in *CCNC*, pp. 787–792, IEEE, 2011.

[109] T. D. Laurent Cariou and J.-P. L. Rouzic, "Carrier-oriented WIFI for cellular offload." https://mentor.ieee.org/802.11/dcn/12/11-12-0910-00-0wng-carrier-oriented-wifi-cellular-offload.ppt. [Accessed 02 June 2014].

[110] J. Barcelo, B. Bellalta, C. Cano, A. Sfairopoulou, M. Oliver, and K. Verma, "Towards a collision-free WLAN: dynamic parameter adjustment in CSMA/E2CA," *EURASIP Journal on Wireless Communications and Networking*, vol. 2011, pp. 1–11, 2011.

[111] E. Aryafar, M. A. Khojastepour, K. Sundaresan, S. Rangarajan, and M. Chiang, "MIDU: enabling MIMO full duplex," in *MobiCom*, pp. 257–268, ACM, 2012.

[112] M. Duarte, A. Sabharwal, V. Aggarwal, R. Jana, K. Ramakrishnan, C. Rice, and N. Shankaranarayanan, "Design and Characterization of a Full-Duplex Multiantenna System for WiFi Networks," *IEEE Transactions on Vehicular Technology*, vol. 63, no. 3, pp. 1160–1177, 2014.

[113] J. I. Choi, S. Hong, M. Jain, S. Katti, P. Levis, and J. Mehlman, "Beyond full duplex wireless," in *ASILOMAR*, pp. 40–44, IEEE, 2012.

[114] A. Sahai, G. Patel, and A. Sabharwal, "Pushing the limits of full-duplex: Design and real-time implementation," *arXiv preprint arXiv:1107.0607*, 2011.

[115] W. Zhou, K. Srinivasan, and P. Sinha, "RCTC: Rapid concurrent transmission coordination in full DuplexWireless networks," in *ICNP*, pp. 1–10, 2013.

[116] W. Zhuang and M. ISMAIL, "Cooperation in wireless communication networks," *IEEE Wireless Communications*, vol. 19, no. 2, pp. 10–20, 2012.

[117] T. C. Minh, B. Bellalta, S. Oechsner, R. Liao, and M. Oliver, "Managing Heterogeneous WSNs in Smart Cities: Challenges and Requirements," *arXiv preprint arXiv:1310.6901*, 2013.

[118] E. Hossain, Z. Han, and H. V. Poor, *Smart grid communications and networking*. Cambridge University Press, 2012.

[119] E. Hossain, M. Rasti, H. Tabassum, and A. Abdelnasser, "Evolution Towards 5G Multi-tier Cellular Wireless Networks: An Interference Management Perspective," *arXiv preprint arXiv:1401.5530*, 2014.

[120] L. Le and E. Hossain, "Cross-layer optimization frameworks for multihop wireless networks using cooperative diversity," *IEEE Transactions on Wireless Communications*, vol. 7, no. 7, pp. 2592–2602, 2008.

[121] W. Lee, et al., "HEW SG PHY Considerations For Outdoor Environment." https://mentor.ieee.org/802.11/dcn/13/11-13-0536-00-0hew-hew-sg-phy-considerations-for-outdoor-environment.pptx. [Accessed 02 June 2014].

[122] R. Agarwal and A. Tomer, "Carrier Wi-Fi Offload: Charting the Road Ahead," in *Tata Consultancy Services White Paper*, pp. 1–14, 2013.